



**UNIVERSITY OF THESSALY**

**SCHOOL OF ENGINEERING**

**DEPARTMENT OF ELECTRICAL AND COMPUTER ENGINEERING**

# **Dynamic Stability Analysis of Power Systems**

Diploma Thesis

Tsantili Angeliki

Supervisor: Bargiotas Dimitrios, Associate Professor U.TH.

Volos 2020



**UNIVERSITY OF THESSALY**

**SCHOOL OF ENGINEERING**

**DEPARTMENT OF ELECTRICAL AND COMPUTER ENGINEERING**

# **Dynamic Stability Analysis of Power Systems**

Diploma Thesis

Tsantili Angeliki

Supervisor: Bargiotas Dimitrios, Associate Professor U.TH.

Volos 2020



**ΠΑΝΕΠΙΣΤΗΜΙΟ ΘΕΣΣΑΛΙΑΣ**

**ΠΟΛΥΤΕΧΝΙΚΗ ΣΧΟΛΗ**

**ΤΜΗΜΑ ΗΛΕΚΤΡΟΛΟΓΩΝ ΜΗΧΑΝΙΚΩΝ ΚΑΙ ΜΗΧΑΝΙΚΩΝ  
ΥΠΟΛΟΓΙΣΤΩΝ**

# **Δυναμική Ευστάθεια Συστημάτων Ηλεκτρικής Ενέργειας**

Διπλωματική Εργασία

Τσαντίλη Αγγελική

Επιβλέπων: Μπαργιώτας Δημήτριος, Αναπληρωτής Καθηγητής Π.Θ.

Βόλος 2020

## **ACKNOWLEDGEMENTS**

Primarily, I would like to express my gratitude to Prof. Bargiotas Dimitrios for his guidance and constant supervision along with providing essential information and directing me towards the successful completion of this thesis.

I would also like to thank my friends for their understanding and support through these years. Last but not least, I would like to express my appreciation to my family for providing me valuable support and encouragement throughout my years of study.

## ΥΠΕΥΘΥΝΗ ΔΗΛΩΣΗ ΠΕΡΙ ΑΚΑΔΗΜΑΪΚΗΣ ΔΕΟΝΤΟΛΟΓΙΑΣ ΚΑΙ ΠΝΕΥΜΑΤΙΚΩΝ ΔΙΚΑΙΩΜΑΤΩΝ

«Με πλήρη επίγνωση των συνεπειών του νόμου περί πνευματικών δικαιωμάτων, δηλώνω ρητά ότι η παρούσα διπλωματική εργασία, καθώς και τα ηλεκτρονικά αρχεία και πηγαίοι 9 κώδικες που αναπτύχθηκαν ή τροποποιήθηκαν στα πλαίσια αυτής της εργασίας, αποτελεί αποκλειστικά προϊόν προσωπικής μου εργασίας, δεν προσβάλλει κάθε μορφής δικαιώματα διανοητικής ιδιοκτησίας, προσωπικότητας και προσωπικών δεδομένων τρίτων, δεν περιέχει έργα/εισφορές τρίτων για τα οποία απαιτείται άδεια των δημιουργών/δικαιούχων και δεν είναι προϊόν μερικής ή ολικής αντιγραφής, οι πηγές δε που χρησιμοποιήθηκαν περιορίζονται στις βιβλιογραφικές αναφορές και μόνον και πληρούν τους κανόνες της επιστημονικής παράθεσης. Τα σημεία όπου έχω χρησιμοποιήσει ιδέες, κείμενο, αρχεία ή/και πηγές άλλων συγγραφέων, αναφέρονται ευδιάκριτα στο κείμενο με την κατάλληλη παραπομπή και η σχετική αναφορά περιλαμβάνεται στο τμήμα των βιβλιογραφικών αναφορών με πλήρη περιγραφή. Αναλαμβάνω πλήρως, ατομικά και προσωπικά, όλες τις νομικές και διοικητικές συνέπειες που δύναται να προκύψουν στην περίπτωση κατά την οποία αποδειχθεί, διαχρονικά, ότι η εργασία αυτή ή τμήμα της δεν μου ανήκει διότι είναι προϊόν λογοκλοπής».

Ο/Η Δηλών/ούσα

Τσαντίλη Αγγελική  
(Υπογραφή)

Φεβρουάριος 2020

## **ABSTRACT**

The last few years, an extension of power systems all over the world has been observed, causing system reliability and stability issues. For the determination of the best operation of a power system, load flow analysis methods such as Gauss-Seidel, Newton Raphson and Fast decoupled methods are used. It is true that, different types of faults appear in a power system can result to frequency, voltage and rotor angle instability. This thesis is mainly dealing with transient stability, which is one of the major stability problem linked with power systems. In this project, PSS/E software by Siemens is used to perform a load flow analysis in IEEE 9-bus system, as well as, a transient stability analysis.

## ΠΕΡΙΛΗΨΗ

Τα τελευταία χρόνια, έχει παρατηρηθεί μια επέκταση των συστημάτων ισχύος σε όλο τον κόσμο, δημιουργώντας ζητήματα αξιοπιστίας και ευστάθειας. Για τον προσδιορισμό της βέλτιστης λειτουργίας ενός συστήματος ηλεκτρικής ενέργειας, χρησιμοποιούνται μέθοδοι ανάλυσης ροής φορτίου όπως, για παράδειγμα, οι Gauss-Seidel, Newton Raphson και Fast decoupled. Είναι πραγματικό το γεγονός ότι, τα διάφορα σφάλματα που εμφανίζονται σε ένα σύστημα ισχύος, μπορεί να οδηγήσουν σε αστάθεια συχνότητας, τάσης και γωνίας δρομέα. Η παρούσα διπλωματική εργασία ασχολείται κυρίως με την μεταβατική ευστάθεια, η οποία είναι ένα από τα σημαντικότερα ζητήματα που σχετίζονται με τα συστήματα ισχύος. Σε αυτή την εργασία, για την ανάλυση ροής φορτίου καθώς και για την ανάλυση μεταβατικής ευστάθειας του συστήματος 9 ζυγών της IEEE, χρησιμοποιείται το λογισμικό PSS / E της Siemens.

# TABLE OF CONTENTS

<b>ACKNOWLEDGEMENTS</b> .....	iv
<b>ABSTRACT</b> .....	vi
<b>ΠΕΡΙΛΗΨΗ</b> .....	vii
<b>LIST OF FIGURES</b> .....	x
<b>LIST OF TABLES</b> .....	xiii
<b>1. INTRODUCTION</b> .....	<b>1</b>
<b>2. LOAD FLOW ANALYSIS</b> .....	<b>5</b>
<b>2.1 Classification of Bus Types</b> .....	<b>5</b>
<b>2.2 Power Flow Analysis Methods</b> .....	<b>6</b>
2.2.1. Gauss-Seidel Method .....	8
2.2.2. Newton-Raphson Method .....	9
2.2.3. Fast Decoupled Method .....	11
<b>3. FAULT AND STABILITY ANALYSIS</b> .....	<b>13</b>
<b>3.1 Types of Faults in Electrical Power System</b> .....	<b>13</b>
3.1.1 Symmetrical or Balanced faults .....	14
3.1.2 Asymmetrical or Unbalanced faults .....	15
3.1.3 Short-circuit Faults .....	17
3.1.4 Open-circuit Faults .....	17
3.1.5 Simultaneous Faults .....	18
<b>3.2 Consequences of Faults on Balanced Electrical Power System</b> .....	<b>18</b>
<b>4. POWER SYSTEM STABILITY</b> .....	<b>20</b>
<b>4.1. Voltage Stability</b> .....	<b>21</b>
4.1.1. Causes of Voltage Instability .....	22
4.1.2. Analysis model for voltage stability .....	23
<b>4.2. Frequency Stability</b> .....	<b>24</b>
4.2.1. Inertia .....	25
4.2.2. Primary Frequency Control .....	26



4.2.3. Secondary Frequency Control .....	26
4.2.4. Tertiary Frequency Control .....	26
4.2.5. Importance of frequency stability .....	26
<b>4.3. Rotor Angle Stability .....</b>	<b>27</b>
4.3.1. Small signal stability .....	27
4.3.2. Transient stability .....	33
<b>4.4. Concept of Transient Stability .....</b>	<b>34</b>
4.4.1 Numerical integration methods .....	36
4.4.2. Swing equation .....	40
4.4.3. Equal Area Criterion .....	42
4.4.4. Critical Clearing Time .....	46
4.4.5 Factors Influencing Transient Stability .....	48
<b>5. TRANSIENT STABILITY ANALYSIS OF IEEE 9-BUS SYSTEM ...</b>	<b>49</b>
5.1. Transient Stability and Power Flow .....	49
5.2 Dynamic simulation for transient stability analysis in PSS/E .....	50
5.2.1. Stable condition .....	51
5.2.2. Unstable condition .....	70
<b>6. CONCLUSIONS .....</b>	<b>83</b>
<b>REFERENCES .....</b>	<b>84</b>
<b>APPENDIX A .....</b>	<b>86</b>

## LIST OF FIGURES

Figure 1: Electric power system configuration and structure.....	1
Figure 2: Simple power system .....	6
Figure 3.1: 3-L fault .....	14
Figure 3.2: 3-L-G fault .....	15
Figure 3.3: SLG fault.....	15
Figure 3.4: L-L fault.....	16
Figure 3.5: L-L-G fault.....	16
Figure 3.6: Single-phase open circuit .....	17
Figure 3.7: Two-phase open circuit .....	18
Figure 4.1: Classification of Power System Stability.....	20
Figure 4.2: PSS block diagram.....	30
Figure 4.3: Block Diagram of The System with PSS .....	31
Figure 4.4: Block Diagram of The System with Excitation System .....	32
Figure 4.5: Reduced equivalent circuit of single machine infinite bus system .....	34
Figure 4.6: Application of Euler Method .....	36
Figure 4.7: Powers and torques in synchronous machines.....	40
Figure 4.8: Application of the equal area criterion .....	42
Figure 4.9: Power-angle curves .....	43
Figure 4.10: Pre-fault, During fault, Postfault Power-Angle curve .....	46
Figure 5.1: Load flow diagram of IEEE 9 Bus.....	50
Figure 5.2: Angle plot of all generators for a fault at bus 4 .....	51
Figure 5.3: Active power output variation of all generators for fault at bus 4.....	52
Figure 5.4: Reactive power output variation of all generators for fault at bus 4.....	52
Figure 5.5: Terminal voltage output variation of all generators for fault at bus 4.....	53
Figure 5.6: Frequency output variation of bus 4 for fault at bus 4.....	53
Figure 5.7: Voltage output variation of bus 4 for fault at bus 4 .....	54
Figure 5.8: Angle plot of all generators for a fault at bus 5 .....	55
Figure 5.9: Active power output variation of all generators for fault at bus 5.....	55
Figure 5.10: Reactive power output variation of all generators for fault at bus 5.....	56
Figure 5.11: Terminal voltage output variation of all generators for fault at bus 5.....	56
Figure 5.12: Frequency output variation of bus 5 for fault at bus 5.....	57

Figure 5.13: Voltage output variation of bus 5 for fault at bus 5 .....	57
Figure 5.14: Angle plot of all generators for a fault at bus 6 .....	58
Figure 5.15: Active power output variation of all generators for fault at bus 6 .....	58
Figure 5.16: Reactive power output variation of all generators for fault at bus 6.....	59
Figure 5.17: Terminal voltage output variation of all generators for fault at bus 6 .....	59
Figure 5.18 Frequency output variation of bus 6 for fault at bus 6 .....	60
Figure 5.19: Voltage output variation of bus 6 for fault at bus 6 .....	60
Figure 5.20: Angle plot of all generators for a fault at bus 7 .....	61
Figure 5.21: Active power output variation of all generators for fault at bus 7 .....	61
Figure 5.22: Reactive power output variation of all generators for fault at bus 7.....	62
Figure 5.23: Terminal voltage output variation of all generators for fault at bus 7 .....	62
Figure 5.24: Frequency output variation of bus 7 for fault at bus 7 .....	63
Figure 5.25: Voltage output variation of bus 7 for fault at bus 7 .....	63
Figure 5.26: Angle plot of all generators for a fault at bus 8 .....	64
Figure 5.27: Active power output variation of all generators for fault at bus 8 .....	64
Figure 5.28: Reactive power output variation of all generators for fault at bus 8.....	65
Figure 5.29: Terminal voltage output variation of all generators for fault at bus 8 .....	65
Figure 5.30: Frequency output variation of bus 8 for fault at bus 8 .....	66
Figure 5.31: Voltage output variation of bus 8 for fault at bus 8 .....	66
Figure 5.32: Angle plot of all generators for a fault at bus 9 .....	67
Figure 5.33: Active power output variation of all generators for fault at bus 9 .....	67
Figure 5.34: Reactive power output variation of all generators for fault at bus 9.....	68
Figure 5.35: Terminal voltage output variation of all generators for fault at bus 9 .....	68
Figure 5.36: Frequency output variation of bus 9 for fault at bus 9 .....	69
Figure 5.37: Voltage output variation of bus 9 for fault at bus 9 .....	69
Figure 5.38: Angle plot of all generators for a fault at bus 8 .....	71
Figure 5.39: Active power output variation of all generators for fault at bus 8 .....	71
Figure 5.40: Reactive power output variation of all generators for fault at bus 8.....	72
Figure 5.41: Terminal voltage output variation of all generators for fault at bus 8 .....	72
Figure 5.42: Terminal voltage output variation of bus 8 for fault at bus 8 .....	73
Figure 5.43: Frequency output variation of bus 8 for fault at bus 8.....	73
Figure 5.44: Angle plot of all generators for a fault at bus 7 .....	74
Figure 5.45: Active power output variation of all generators for fault at bus 7 .....	74
Figure 5.46: Reactive power output variation of all generators for fault at bus7 .....	75

Figure 5.47: Terminal voltage output variation of all generators for fault at bus 7 .....	75
Figure 5.48: Terminal voltage output variation of bus 7 for fault at bus 7 .....	76
Figure 5.49: Frequency output variation of bus 7 for fault at bus 7 .....	76
Figure 5.50: Angle plot of all generators for a fault at bus 9 .....	77
Figure 5.51: Active power output variation of all generators for fault at bus 9 .....	77
Figure 5.52: Reactive power output variation of all generators for fault at bus 9.....	78
Figure 5.53: Terminal voltage output variation of all generators for fault at bus 9 .....	78
Figure 5.54: Terminal voltage output variation of bus 9 for fault at bus 9 .....	79
Figure 5.55: Frequency output variation of bus 9 for fault at bus 9 .....	79
Figure 5.56: Angle plot of all generators for a fault at bus 4 .....	80
Figure 5.57: Active power output variation of all generators for fault at bus 4 .....	80
Figure 5.58: Reactive power output variation of all generators for fault at bus 4.....	81
Figure 5.59: Terminal voltage output variation of all generators for fault at bus 4 .....	81
Figure 5.60: Terminal voltage output variation of bus 4 for fault at bus 4 .....	82
Figure 5.61: Frequency output variation of bus 4 for fault at bus 4.....	82

## LIST OF TABLES

Table 1 - Standard load flow data of IEEE 9bus .....	50
Table 2 - CCT and maximum angle deviation of generator rotor angles for six case studies in PSS/E.....	70

# CHAPTER 1

## 1. INTRODUCTION

It is well known that, modeling and simulation of generation, transmission and distribution subsystems are crucial for the development and operation of a power system. The increased electricity consumption along with the need of preserving system's reliability, has led to extension of power systems all over the world. This extension includes a greater number of lines and as a result an enhanced fault and contingency simulation of the system is required [10],[11],[12],[13].

An electric power system is a network of electrical components (generators, transformers, transmission lines, compensation devices, switches, etc.) installed to supply, transfer, and use electric power. The electric power system's configuration and structure is shown in Figure 1.

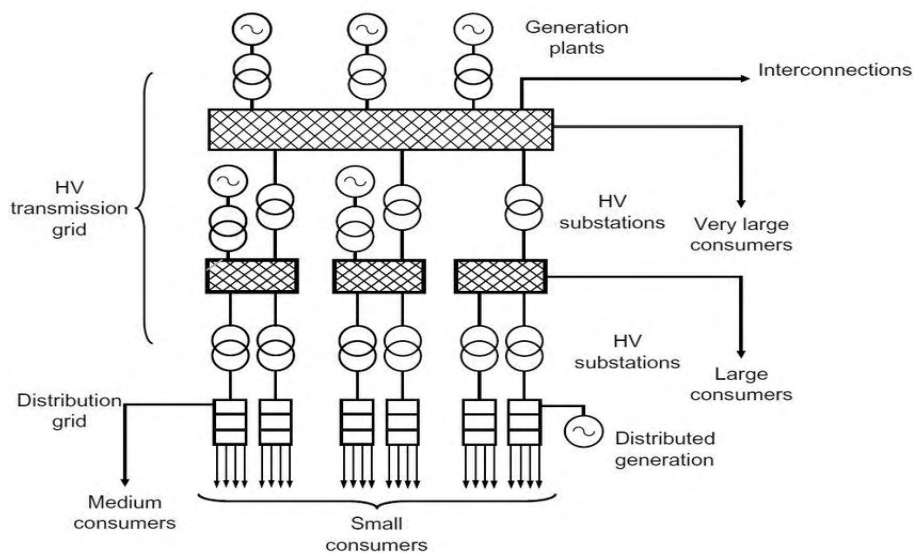


Figure 1 Electric power system configuration and structure [24]

More specifically, the electric power systems consist of [11]:

- Power generation

Power plants are mainly located in areas where their fuel is available in large quantities (for example, lignite stations are located near lignite mines). This is due to the high cost of transporting fuel in large quantities over long distances, as opposed

to the low cost of transporting electricity over similar distances. All electricity is generated at power plants and then transported to loads [11].

- Transmission system

Transmission lines are important parts of a power system. They are used to transport large amounts of electricity, with as little loss as possible, from power stations to consumption centers, where faults are most likely to happen. Faults on the transmission system can lead to severe economic losses. Sometimes, economic and environmental conditions of an area may affect the updating of a transmission system (e.g. by constructing new transmission lines) [11].

- Distribution system

The distribution network undertakes the distribution of electricity to individual consumers so that they can be exploited by converting them to heat, light, motion etc. [11],[13]

A modern power system should be designed and operated in such a way as to be safe, reliable and environmentally friendly. The size of a power system is the factor that most defines its structure. The way a small power system is designed to supply a small area is different from a large system, which serves an extended geographical area. Also, the particularities that each system is called to serve, affect the way it is built. A common feature of all systems, however, is the fact that they work at different voltage levels, which are separated by transformers. Starting from the highest voltage level, we can distinguish the following subsystems [13]:

- Transmission system

The transmission system interconnects all production stations and all high consumption points. It manages larger amounts of power than substation and distribution systems. It is possible for very large consumers to be served directly by the transmission system. Also, through interconnections, the transmission system can exchange amounts of energy with other neighboring systems [11],[12].

- Subtransmission system

The subtransmission system distributes electricity to the distribution substations of a geographical area, at a voltage level between 23kV and 150kV. Power is supplied either directly from power stations or from the transmission system through substations. It can directly feed certain large consumers, such as large industries [11],[12].

- Distribution system

In the distribution system we encounter two levels of voltages [11],[12]:

A. Primary distribution voltages:

Primary distribution voltages range from 4 kV to 35 kV phase-to-phase (2.4 kV to 20 kV phase-to-neutral). Only large consumers (such as some factories and small industries) are fed directly from distribution voltages. The majority of utility customers are connected to a transformer, which decreases the distribution voltage to the low voltage used by lighting and interior wiring systems. The primary voltage is also known as supply voltage or mains voltage.

B. Secondary distribution voltages:

A secondary or low-voltage network is a part of electric power distribution which carries electric energy from distribution transformers to electricity meters of end customers. Secondary networks are operated at a low voltage level that is equal to the mains voltage of electric appliances. Most secondary networks are operated at AC rated voltage of 100–120 or 230–240 volts, at the frequency of 50 or 60 hertz .

Distribution networks in urban areas are usually underground, while in other areas they are aerial.



It is a fact that, the constantly rising electricity demand and the effort of electricity companies to handle it while remain competitive in the liberalized electricity market, has led the power systems operating close to their stability limits. As a result, power systems face the danger of serious, unexpected situations, which often leads to system overheating. In particular, the power system becomes temporarily unstable when it is incapable to maintain synchronization of electrical machinery after a serious disturbance. In a case like that, the synchronization between a synchronous generator or a group of generators with the rest of the power system is lost, leading to partial or complete power failure, unless appropriate protection and control measures are taken [13].

It true that the loss of stability can cause severe damage to a power system. In order to avoid situations like that, it is important for electricity system operators to evaluate the stability status of the power system by studying several scenarios. Transient stability analysis during a major emergency provides an overview of the generator rotor angles, bus voltages and system frequency so that power systems' operators can devise a series of remedies to preserve system stability. In general, a transient state stability analysis requires both the type and the parameters of the dynamic model for the power system components to be known [13].

## CHAPTER 2

### 2. LOAD FLOW ANALYSIS

Load flow analysis is used for the establishment of the best operation for a power system and power exchange between utility companies. In order to have an effective operating power system, it is essential to find which load flow analysis method is more suitable for each case. Load flow analysis solves the steady state operation with bus voltages and branch power flow in the power system, while providing a balanced steady operation, without considering system transient processes. Consequently, the mathematical model of load flow problem is a nonlinear algebraic equation system without differential equations [15],[17].

#### 2.1 Classification of Bus Types

The buses in power systems can be classified into three types [15]:

- Load bus or PQ bus:

For load or PQ buses, the active power  $P$  and reactive power  $Q$  are determined as known parameters. Via the load flow solution, it is required to find out the voltage magnitude  $V$  and the phase angle  $\delta$ . Most of the times, substation buses are taken as PQ buses where the load powers are known constants. As far as load flow calculation is concerned, most buses in power systems are PQ.

- Generator bus or PV bus:

For generator or PV buses, active power  $P$  and voltage magnitude  $V$  corresponding to the generation voltage are specified as known variables, while it is required to find out the reactive power  $Q$  and voltage angle  $\delta$ . Normally, PV buses should have some manageable reactive power resources and be able to maintain bus voltage magnitude at a suitable value. In general, the buses of power plants can be considered as PV buses, because voltages at these buses can be controlled with reactive power capacity

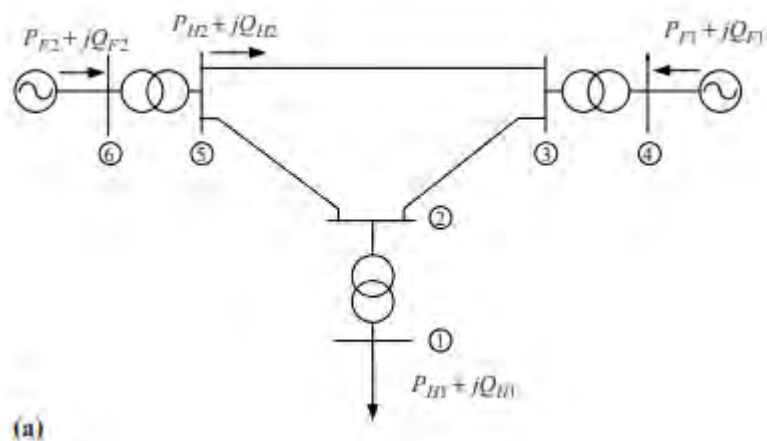
of their generators. Substations that have enough reactive power compensation devices to control the voltage, can also be considered as generator buses.

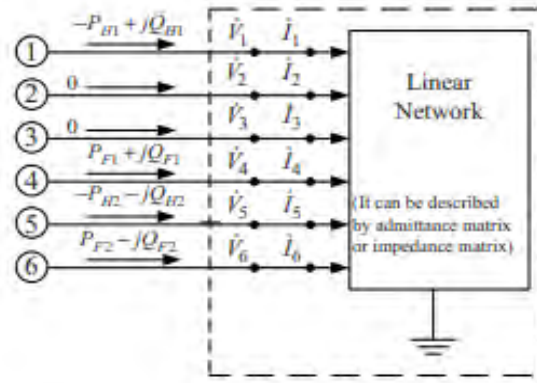
- Slack bus or reference bus:

In load flow analysis, there is only one slack bus specified in the power system. At reference buses, the voltage magnitude  $V$  and the phase angle  $\delta$  are known, while active  $P$  and reactive  $Q$  power are obtained through the load flow solution. The effective generator at this bus supplies the losses to the network, which losses are computed when the load flow solution is complete. The location of the reference bus can affect the complexity of the calculations and thus it is important to use a bus that approaches a large power station.

## 2.2 Power Flow Analysis Methods

An electric power system is composed of generators, transformers, transmission lines and loads, etc. In power system analysis, the static components like transformers, transmission lines, shunt capacitors and reactors, are represented by their equivalent circuits consisting of  $R$ ,  $L$ ,  $C$  elements. [15],[17] At Figure 2, a simple power system with its components is shown.





(b)

Figure 2 Simple power system [15]

The network formed by these static components can be considered as a linear network and be represented by the corresponding admittance matrix or impedance matrix. In load flow analysis, the generators and loads are considered as nonlinear components and they cannot be embodied in the linear network, whereas the connecting buses with zero injected power also represent boundary conditions on the network.

The solution of algebraic simultaneous equations is the key for solution of the performance equations in power system analyses. First of all, it is important to form the Y-bus admittance using the transmission line and transformer input data. The nodal equation for a power system network using Y-bus can be expressed as [17]:

$$I = Y_{Bus}V \quad (2.1)$$

For a n bus system, the nodal equation can be written as:

$$I_i = \sum_{j=1}^n Y_{ij} V_j \quad , \text{ for } i=1, 2, 3, \dots, n \quad (2.2)$$

The complex power delivered to bus i is:

$$P_i + jQ_i = V_i I_i^* \quad , \text{ for } i = 1, 2, 3, \dots, n \quad (2.3)$$

$$I_i = \frac{P_i - jQ_i}{V_i^*} \quad , \text{ for } i=1, 2, 3, \dots, n \quad (2.4)$$

Replacing  $I_i$  in terms of  $P_i$  &  $Q_i$  ,we have:

$$\frac{P_i - jQ_i}{V_i^*} = V_i \sum_{j=1}^n y_{ij} - \sum_{j=1}^n y_{ij} V_j, \text{ for } i=1, 2, 3, \dots, n, j \neq i \quad (2.5)$$

To solve the above equation, iterative techniques are needed. Solution methods that use iterative techniques and will be analyzed in this thesis are Gauss-Seidel, Newton Raphson and Fast decoupled methods.

### 2.2.1. Gauss-Seidel Method

Gauss–Seidel method is an improved form of Jacobi method, also known as the successive displacement method. This method is named after Carl Friedrich Gauss (Apr. 1777–Feb. 1855) and Philipp Ludwig von Seidel (Oct. 1821–Aug. 1896).

Gauss–Seidel method is an iterative method that solves nonlinear algebraic equations. The method uses an initial guess for the value of voltage, to obtain a computed value of a specific variable. The initial guess value is then replaced by a computed value and the process is repeated until the iteration solution converges. Gauss–Seidel method can be applied to any matrix with non-zero elements on the diagonals, but convergence is only guaranteed if the matrix is either diagonally dominant, or symmetric and positive definite[15],[17].

Solving the equation (2.5) for the value of  $V_i$ , the iterative sequence becomes [17]:

$$V_i^{(k+1)} = \frac{P_i - jQ_i + \sum y_{ij} V_j^{(k)}}{\sum y_{ij}}, \text{ for } i=1, 2, 3, \dots, n, j \neq i \quad (2.6)$$

After applying Kirchhoff's current law, it is clear that the current injected into bus  $i$  is positive and that the active powers  $P_i$  and the reactive powers  $Q_i$  supply into the buses, such as generator buses, have positive values too. The active powers  $P_i$  and the reactive powers  $Q_i$  flowing away from the buses, such as load buses, have negative values.

$P_i$  and  $Q_i$  are computed from equation (2.5) which leads to:

$$P_i^{(k+1)} = \text{Real} \left[ V_i^{*(k)} \left\{ \sum_{i=0}^n y_{ij} - \sum_{ji}^n V_i^{(k)} \right\} \right], \text{ for } i = 1, 2, 3, \dots, n, j \neq i \quad (2.7)$$

$$Q_i^{(k+1)} = \text{Imaginary} \left[ V_i^{*(k)} \left\{ \sum_{j=1}^n y_{ij} - \sum_{ji}^n V_i^{(k)} \right\} \right], \text{ for } i = 1, 2, 3, \dots, n, j \neq i \quad (2.8)$$

The power flow equation is typically expressed in terms of the bus admittance matrix, using the diagonal elements of the bus admittance and the non-diagonal elements of the matrix, hence the equation (2.6) becomes:

$$V_i^{(k+1)} = \frac{\frac{P_i - jQ_i}{V_i^{*(k)}} - \sum y_{ij} V_j^{(k)}}{Y_{ii}} \quad (2.9)$$

And

$$P_i^{(k+1)} = \text{Real} \left[ V_i^{*(k)} \left\{ V_i^{*(k)} Y_{ii} + \sum_{i=1, j=1}^n y_{ij} V_j^{(k)} \right\} \right], \text{ for } i = 1, 2, 3, \dots, n, j \neq i \quad (2.10)$$

$$Q_i^{(k+1)} = \text{Imaginary} \left[ V_i^{*(k)} \left\{ V_i^{*(k)} Y_{ii} + \sum_{i=1, j=1}^n y_{ij} V_j^{(k)} \right\} \right], \text{ for } i = 1, 2, 3, \dots, n, j \neq i \quad (2.11)$$

### 2.2.2. Newton-Raphson Method

Newton-Raphson method was named after Isaac Newton and Joseph Raphson and its origin and formulation was dated back to late 1960s. It is an iterative method which approximates a set of non-linear simultaneous equations to a set of linear simultaneous equations using Taylor's series expansion and the terms are limited to the first approximation. The fact that its convergence characteristics and reliability are better than other methods, make Newton-Raphson method the most used iterative method for load flow analysis. Specifically, if the assumed value is near the solution, the method converges very quickly. On the contrary, if the assumed value is not near the solution, the method might take longer to converge. The equations for currents entering a power system are written to the admittance matrix [15],[17].

Power balance equations can be also expressed as:

$$P_i = \sum_{j=1}^n |V_i| |V_j| |Y_{ij}| \cos(\theta_{ij} - \delta_i + \delta_j), \text{ for } i = 1, 2, 3, \dots, n, j \neq i \quad (2.12)$$

$$Q_i = \sum_{j=1}^n |V_i| |V_j| |Y_{ij}| \sin(\theta_{ij} - \delta_i + \delta_j), \text{ for } i = 1, 2, 3, \dots, n, j \neq i \quad (2.13)$$

Power flow solutions by Newton-Raphson are based on the nonlinear power-flow equations given by (2.12) and (2.13). Equations (2.12) and (2.13) are analogous to the nonlinear equation of the form  $y = f(x)$ , we define  $x$ ,  $y$  and  $f$  are vectors for the power flow problem as:

$$x = \begin{bmatrix} \delta \\ |V| \end{bmatrix} \quad (2.14), \quad y = \begin{bmatrix} P \\ Q \end{bmatrix} = \begin{bmatrix} P_2 \\ \vdots \\ P_n \\ Q_2 \\ \vdots \\ Q_n \end{bmatrix} \quad (2.15), \quad f(x) = y = \begin{bmatrix} P(x) \\ Q(x) \end{bmatrix} \quad (2.16).$$

$$\text{Let the composite vector of } \delta \text{ and } |V| \text{ as } \delta = \begin{bmatrix} \delta_2 \\ \delta_3 \\ \vdots \\ \delta_n \end{bmatrix} \quad (2.17) \text{ and } |V| = \begin{bmatrix} |V_2| \\ |V_3| \\ \vdots \\ |V_n| \end{bmatrix} \quad (2.18)$$

where all  $V$ ,  $P$  and  $Q$  terms are in per-unit and  $\delta$  terms are in radians.

Newton-Raphson method is a complex calculation involving derivative of active and reactive power with respect to  $V$  and  $\delta$ . Jacobian matrix is the matrix formed out of the derivatives of power with  $V$  and  $\delta$  and is indicated by  $J$ , where

$$J = \begin{bmatrix} J_{11} & J_{12} \\ J_{21} & J_{22} \end{bmatrix} = \begin{bmatrix} \frac{\partial P_i(x)}{\partial \delta_j} & \frac{\partial P_i(x)}{\partial |V_j|} \\ \frac{\partial Q_i(x)}{\partial \delta_j} & \frac{\partial Q_i(x)}{\partial |V_j|} \end{bmatrix} \quad (2.19), \quad i = 1, 2, 3 \dots n \text{ and } j = 1, 2, 3 \dots n$$

The iterative process for Newton-Raphson method:

$$J^k \Delta x^k = -f(x^k) \quad (2.20)$$

$$\Delta P(x) = \begin{bmatrix} P_2 - P_2(x) \\ \vdots \\ P_n - P_n(x) \end{bmatrix} \quad (2.21)$$

$$\Delta Q(x) = \begin{bmatrix} Q_2 - Q_2(x) \\ \vdots \\ Q_n - Q_n(x) \end{bmatrix} \quad (2.22)$$

where  $\Delta P(x)$  and  $\Delta Q(x)$  are the mismatch vectors.

It is true that the flow of reactive power cannot be affected a lot by a small change in phase angle, while it changes the flow of active power. Likewise, a small change in nodal voltage

does not affect active power practically, whereas it changes the flow of reactive power. The set of linear load flow equations using the polar coordinates can be expressed in matrix form as follows:

$$\begin{bmatrix} J_{11}^k & J_{12}^k \\ J_{21}^k & J_{22}^k \end{bmatrix} \begin{bmatrix} \Delta\delta^k \\ \Delta|V|^k \end{bmatrix} = -f(x) = \begin{bmatrix} \Delta P(x^k) \\ \Delta Q(x^k) \end{bmatrix} \quad (2.23)$$

The new estimates for bus voltage are:

$$\delta^{(k+1)} = \delta_i^k + \Delta\delta_i^k \quad (2.24)$$

$$|V^{(k+1)}| = |V_i^k| + \Delta|V_i^k| \quad (2.25)$$

### 2.2.3. Fast-Decoupled Method

The fast-decoupled power flow method is a very fast and effective method of obtaining power flow problem solution. This method is an extension of Newton-Raphson method formulated in polar coordinates with certain approximations. This method exploits the capacity of the power system where in MW flow-voltage angle and MVAR flow-voltage magnitude are loosely coupled. That means that, a small change in the magnitude of the bus voltage does not alter the real power flow at the bus. Likewise, a small change in phase angle of the bus voltage has hardly any effect on reactive power flow [15],[17].

Nevertheless, fast decoupled method in cases of high resistance-to-reactance ( $R/X$ ) ratios or heavy loading (low voltage) at some buses, does not converge well. This is mainly because it is an approximation method and make some assumption to simplify Jacobian matrix. For cases like that, in order to overcome these convergence obstacles, many efforts and developments have been made. Ignoring the element of  $J_2$  and  $J_3$  has reduced the Jacobian matrix of equation (2.23) to half. [17] [18]

Equation (2.23) is simplified as[17]:

$$\begin{bmatrix} \Delta P \\ \Delta Q \end{bmatrix} = \begin{bmatrix} J_1 & 0 \\ 0 & J_4 \end{bmatrix} \begin{bmatrix} \Delta\delta \\ \Delta|V| \end{bmatrix} \quad (2.26)$$

Expanding Equation (26) gives two separate matrices,



$$\Delta P = J_1 \Delta \delta = \left[ \frac{\partial P}{\partial \delta} \right] \Delta \delta \quad (2.27)$$

$$\Delta Q = J_4 \Delta |V| = \left[ \frac{\partial Q}{\partial |V|} \right] \Delta |V| \quad (2.28)$$

$$\frac{\Delta P}{V_i} = -B' \delta \quad (2.29)$$

$$\frac{\Delta Q}{V_i} = -B'' \Delta |V| \quad (2.30)$$

where  $B'$  and  $B''$  are the imaginary parts of the bus admittance. In order to make the formation of  $J_1$  and  $J_4$  simpler, it is nicer to ignore all the shunt connected elements. The successive and voltage magnitude and phase angle changes are:

$$\Delta \delta = -[B']^{-1} \frac{\Delta P}{|V|} \quad (2.31)$$

$$\Delta |V| = -[B'']^{-1} \frac{\Delta Q}{|V|} \quad (2.32)$$

## **CHAPTER 3**

### **3. FAULT AND STABILITY ANALYSIS**

#### **3.1 Types of Faults in Electrical Power System**

Electrical components of a power system are frequently exposed to several types of faults during their operation. During a fault, the characteristic values (e.g. impedance) of the machines might alter to different values than the normal ones, until the fault is cleared. Lightning, wind, tree falling on lines etc. are possible to cause faults in a power system. As a fault can be defined any unusual condition of the system that entails the electrical failure of its equipment (transformers, generators, busbars) as long as insulation failures and conducting path failures which leads to short circuit and open circuit of conductors [18],[19].

Under normal circumstances, the electric equipment of a power system operates at regular voltage and current ratings. Every time a fault occurs in a circuit or device, the values of voltage and current become different from their nominal ranges. It is a fact that faults may cause overcurrent, undervoltage, unbalance of the phases, reversed power and high voltage in a power system. Devastating effects of these faults might be the interruption of the normal operation of the network, a possible failure of equipment or either electrical fires, etc. For these reasons, it becomes obvious that power system networks should be protected. That becomes possible with the use of switchgear protection equipment (circuit breakers, relays) in a way to reduce the losses [18],[19].

Different types of faults in the interconnected electrical power system can be categorized according to types of their nature and severity as follows [18].

There are two types of faults which can occur on power system's electric equipment:

- Symmetrical or Balanced faults
- Asymmetrical faults or Unbalanced faults

It is true that unbalanced faults are more likely to occur on a power system than the balanced three-phase faults. In addition to the previous categorization, faults can be classified as:

- Series faults or Open circuit faults
- Short circuit faults
- Simultaneous faults

### 3.1.1 Symmetrical or Balanced faults

Symmetrical or Balanced faults involve all the three phases and remain balanced even after the fault occurs. They are more likely to happen at the terminal of the generators and the reason they appear is owing to the resistance of the arc between the conductors or to the lower footing resistance. Symmetric faults that we can discern are [18],[19]:

a. Line to Line to Line fault:

The 3– L fault is the most dangerous kind of fault because it involves the largest current, even though it doesn't happen often. The value of this large current is used for the determination of the rating of the circuit breaker. Figure 3.1 shows a 3-L fault.

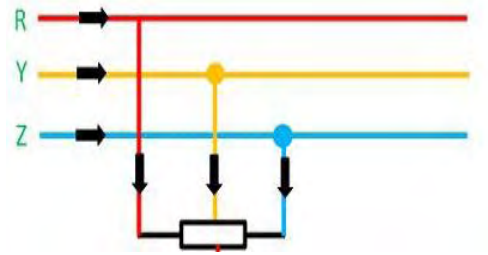


Figure 3.1 3-L fault [25]

b. Line to Line to Line to Ground fault

The 3 – L – G fault occurs between the three phases and the ground of the system and the probability of this kind of fault to occur is approximately 2-3% of the fault cases. A 3-L-G fault is shown in Figure 3.2.

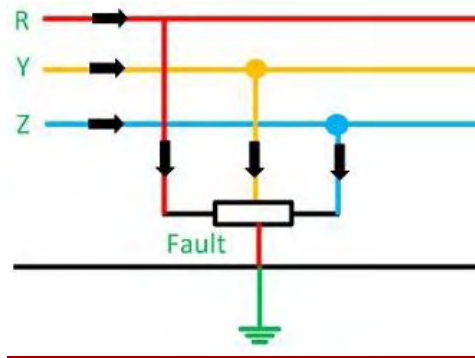


Figure 3.2 3-L-G fault [25]

### 3.1.2 Asymmetrical or Unbalanced faults

Asymmetrical fault is the fault that produces asymmetrical current which is the current differing in magnitude and phases in all the three phases of the power system. In this category of faults belong the L- G, L – L, L – L – G faults. The asymmetrical fault is the most ordinary type of fault occur in the power system and makes the system unbalanced [18],[19].

#### a. Single Line to ground (L – G) Fault

When one phase of any transmission lines establishes a connection with the ground either by falling tree, ice, wind etc., a single line to ground fault occurs. The 70 – 80 % of the faults in the power system belongs to this type of faults. A single line to ground fault is shown in Figure 3.3.

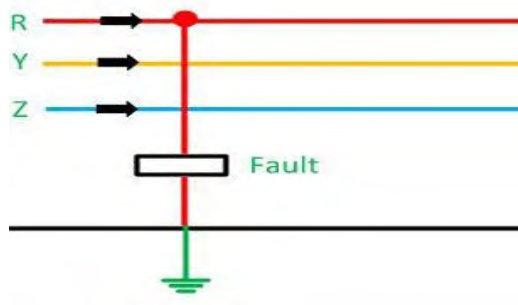


Figure 3.3 SLG fault [25]

b. Line-to-Line Fault (L – L)

A line to line fault occurs when two conductors are short circuited. Heavy wind is the main cause of this type of fault because swinging the line conductors may result to the touch of one phase to another causing short-circuit. This type of faults forms the 15 – 20% of the faults in the power system. A line to line fault is shown in Figure 3.4.

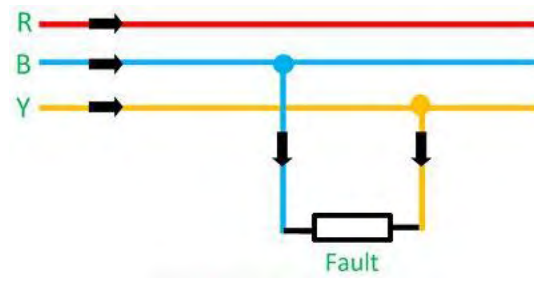


Figure 3.4 L-L fault [25]

c. Double Line-to-ground (L – L – G) Fault

When two phases come in contact with each other along with the ground because of a falling tree, a L-L-G fault occurs. The probability of this kind of faults to happen is nearly 10 %. A double line to ground fault is shown in Figure 3.5.

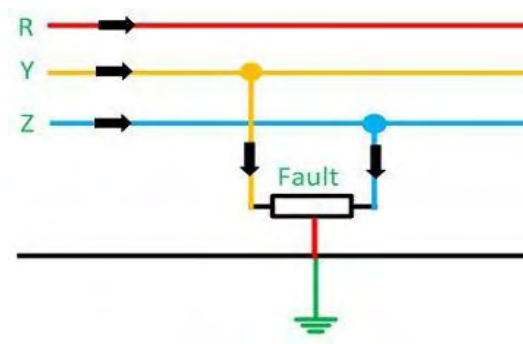


Figure 3.5 L-L-G fault [25]

### 3.1.3 Short-circuit Faults

A short circuit can be defined as an abnormal connection of very low impedance between two points of different potential. These are the most popular and dangerous kind of faults because they are responsible for abnormal elevated currents through the equipment or transmission lines. These faults should be cleared in a short period of time otherwise they may cause extensive damage to the equipment.

This category of faults involves the three phases to earth faults, the three phase clear of earth faults, phase to phase, the single phase to earth faults, the two phase to earth faults, the phase to phase faults and also the single phase to earth faults [18],[19].

### 3.1.4 Open-circuit Faults

The open-circuit fault is one of the common faults in power three-phase rectifiers. This kind of faults occurs due to the failure of one or more conductors. Figures 3.6 and 3.7 show the single-phase and two-phase open-circuit faults respectively [19].

Single-phase open circuit involves a break in one of the three conductors. This condition is mathematically identical to the condition in the L-L-G fault, except that the voltages are measured in a different manner. A single-phase open circuit is shown in Figure 3.6.

Two-phase open circuit involves a break in two of the three conductors. This condition is mathematically identical to the condition in the L-G fault. A two-phase open circuit is shown in Figure 3.7.



Figure 3.6 Single-phase open circuit [25]



Figure 3.7 Two-phase open circuit [25]

Typical causes of these faults may be joint failures of cables and overhead lines, failure of one or more phase of circuit breaker or even the melting of a fuse or conductor in one or more phases. Open circuit faults are also known as **series faults**. When one of the phases gets melted, the actual loading of the alternator is reduced, and this provokes the rise of the acceleration of the alternator. As a result, this over speed causes over voltages in other transmission lines.

Single-phase and two-phase open circuit can produce the unbalance of the power system voltages and currents that causes great damage to the equipment [18],[19].

### 3.1.5 Simultaneous Faults

It is possible that, more than one type of fault take place simultaneously, such as single-line-to-ground fault on one phase, and a line-to-line fault between other two phases. Short-circuiting faults coupled with open circuit faults are also possible to happen at the same time [18],[19].

## 3.2 Consequences of Faults on Balanced Electrical Power System

The effects of these faults on transmission system, connected generators and loads depends on types of faults, location of fault, severity of fault, duration of fault, fault level and stability of the zone of protection. The consequences of these faults can be reduced by proper coordination of relays and circuit breakers for fault clearing.

In order to maintain the stability of the system and to protect it from further damage, the faults are supposed to be cleared within specific time Once fault is initialized and during its

clearing process, the response of inertial energy comes into effect in the form of transient stability.

The faults in the electrical systems cause abnormally high currents (sometimes in terms of thousands of ampere) resulting in excess amount of power consumption and heat generation temporarily. The high amount of power consumption and heat dissipation due to fault event for extended time (often in terms of several seconds) can lead to equipment damage and unbalance in grid frequency and bus voltage. As a result, faults are meant to be isolated from the healthy operating power system within specified time. Unbalance in active and reactive power demand-supply causes frequency and bus voltage deviations from nominal values respectively. Major unbalance in the frequency and bus voltage causes sequential tripping in power system considering severity of fault and contingency ranking. Additionally, due to mismatch between input mechanical power and connected electrical power output, the faults in the electrically balanced system cause transient unbalance. The faults cause momentary shortfall of electrical power supply as high amount of current is fed to fault and turbine's mechanical controllers are not able to match with the speed of response.

Transient instability causes generators' rotor angles to be shifted from their positions magnetically due to turbine's mechanical controllers' comparatively slow response. The response of unbalancing of mechanical input and electrical output power of the system results in either accelerating or de-accelerating of generator's rotor [18],[19].



## CHAPTER 4

### 4. POWER SYSTEM STABILITY

Power system stability relates with the ability of a power system to preserve its normal operating condition as long as maintaining a stable equilibrium or being able to regain a state of normal operating conditions after a small or large disturbance [1]. Conventionally, the instability problem is relevant to the ability of machines to maintain synchronism within the power system. Even though instability may also happen without the loss of synchronism in cases of a sudden voltage drop due to load change, that lead the transmission line to unstable state. In general, relative and absolute rotor angle and power angle between the machines are parameters important for the stability.

There are small and large disturbances. Small disturbances, such as load change, happens really often in the system and that's why the system adapts to these changes by maintaining an acceptable voltage and frequency level for normal state of power system. Large disturbances, such as fault in transmission lines or a generator trip, provokes a high change in voltage and frequency of system and activate the generation controls which try to bring the system's stability back. Power system stability is a challenging matter for the engineers who use mathematical simulations for solving stability issues. That's why it is important to understand the size of disturbance and model it. The complexity power system's stability has led to the classification of power system stability in different sub-categories as seen at Figure 4.1 [1],[2].

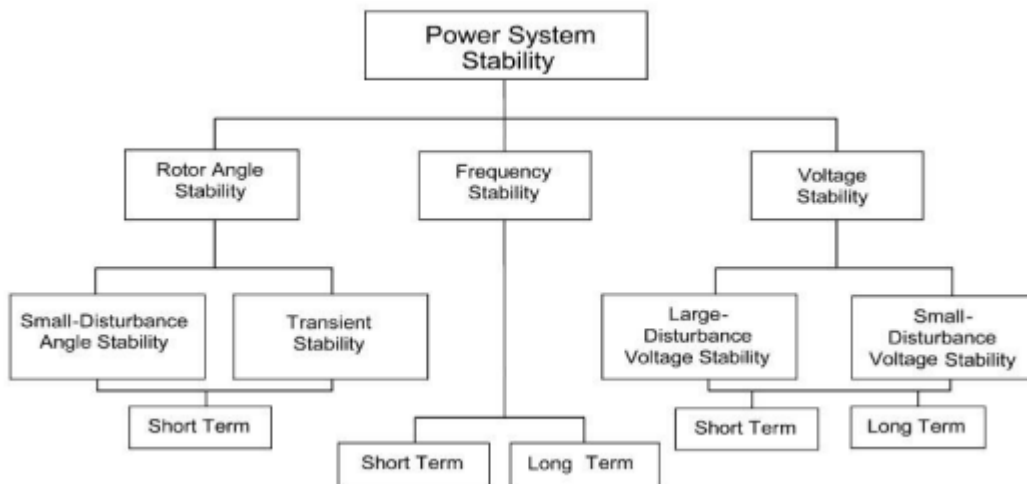


Figure 4.1 Classification of Power System Stability [2]

## 4.1. Voltage Stability

Voltage stability describes the ability of a system to maintain its voltage stable at each bus of the system, after the appearance of a disturbance. The increase or drop of voltage happens when the system is incapable to cope with the load demand. Possible effect of the voltage instability is the tripping of an area which can cause a transient stability phenomenon and loss of synchronism. Vice versa, a transient stability phenomenon can cause voltage instability. During a voltage instability situation, a blackout or unusually low voltage may appear in a large part of the power system. Voltage stability is distinguished in [1],[2]:

- *Small-disturbance voltage stability*

The term small-disturbance voltage stability describes the ability of the system to maintain its voltage stable when exposed to small perturbations (e.g. incremental changes in system load). Loads' characteristics, constant and discrete controls may affect this kind of stability.

- *Large-disturbance voltage stability*

The term large-disturbance voltage stability describes the ability of the system to maintain its voltage stable when exposed to large disturbances (e.g. system faults, loss of generation, circuit contingencies). This ability is defined by the system and load characteristics, constant and discrete controls and protections. To determine large-disturbance voltage stability it is required to examine the nonlinear response of the power system over time to capture the performance and interactions of devices like thermostat controllers, under load transformer tap changers, and generator field-current limiters.

#### 4.1.1. Causes of Voltage Instability

We can discern three main causes of voltage instability [16]:

1. Dynamics of loads: Loads are the driving force of voltage instability. Loads that may affect the voltage stability of power system are:

- Load tap changing (LTC) transformers: LTC transformer's role is to maintain the load side voltage in a range close to the rated voltage by changing the ratio of transformer. Any disturbance causing a voltage drop at a load bus will cause a decrease in the power consumption, since most of the loads are voltage reliant, fact that tends to favor stability. Though, in such a case, the load tap changing transformers will try to restore the voltage by changing the ratio. The increase in voltage will cause an increase in the power demand that will eventually weaken the power system stability.
- Thermostat controllers: Thermostat control the electrical heating by frequently switching the heating resistance on and off. In the case of a voltage drop, the power consumption, meaning the heating power, will be decreased and the thermostat will continue to supply the load for a longer period of time.
- Induction motors: Induction motors have dynamic characteristics with short time constants. In the case of a voltage drop, the motor must continue to supply a mechanical load with a torque more or less constant.

2. Transmission system: Transmission components like lines or transformers have a restricted transfer capability that depends on several factors such as the power factor of the load, the impedance of the transmission component, the existence of voltage controlled sources (e.g. generators or Static Var Compensator-SVC) and the presence of reactive compensation devices (e.g. mechanically switched capacitors or reactors) [1].

3. Generation system: Once the power system flows increase, the transmission system consumes more reactive power. Therefore, the generators must increase their reactive power output. Though, due to the presence of over-excitation limiter (OEL) and stator current limiter (SCL), voltage isn't controllable after the limiters are activated [1].

#### 4.1.2. Analysis model for voltage stability

The typical steady state model of a power system considered in voltage stability analysis is generally given by the differential and algebraic equations as follows [6]:

$$\begin{aligned} \dot{x} &= f(x, y, \lambda) \\ 0 &= g(x, y, \lambda) \end{aligned} \tag{4.1}$$

where  $\mathbf{x}$  is the vector of state variables and  $\mathbf{y}$  is the vector of algebraic variables. The variable  $\lambda$  is a parameter or a set of parameters that slowly changes over time so that the power system moves from an equilibrium point to another until reaching the collapse point. To simplify the power system description, a new vector  $z = [x, y]^T$  is defined so that equation (4.1) can be rewritten as:

$$\begin{bmatrix} \dot{x} \\ 0 \end{bmatrix} = F(z, \lambda) \tag{4.2}$$

In static voltage stability analysis, we are interested in the operating condition reaching an equilibrium point given by  $(z_0, \lambda_0)$ . The system equation as shown in equation (4.2) becomes  $F(z_0, \lambda_0) = 0$ . Based on the singularity assumption, an equilibrium point  $(z_0, \lambda_0)$  which makes  $\frac{\partial F(z_0, \lambda_0)}{\partial z}$  singular is mathematically defined as the saddle bus bifurcation point. Such a bifurcation point is directly associated with the voltage collapse problems. It is a fact that that different control parameters of system components in generation and load sides sway the location of collapse points.

Under the consideration that slow variation of active and reactive power demand is the key driving force of the system to the collapse point, the power flow model produces enough results. The power flow model used to get different voltage stability indices is represented

by the typical nonlinear equation of active and reactive power mismatches at the system buses such as [1],[6]:

$$\begin{bmatrix} \Delta P(u, \lambda) \\ \Delta Q(u, \lambda) \end{bmatrix} = F(u, \lambda) = 0 \quad (4.3)$$

where  $\mathbf{u}$  represents a vector of system variables such as voltage magnitudes  $U$  and voltage angles  $\delta$ . Reactive power generation  $Q$  can be as well swapped with  $U$  in  $\mathbf{u}$  when a reactive power limit is reached. The variable is a scalar parameter used to simulate the system load changes that drive the system to voltage collapse as follows:

$$\begin{aligned} P_{D,i} &= P_{D0,i}(1 + k_{P,i}\lambda) \\ Q_{D,i} &= Q_{D0,i}(1 + k_{Q,i}\lambda) = P_{D0,i} \tan(\varphi_i)(1 + k_{Q,i}\lambda) \end{aligned} \quad (4.4)$$

where  $P_{D,i}$  is the active power demand and  $Q_{D,i}$  is the reactive power demand at bus  $i$ .  $P_{D0,i}$  is the initial active power demand and  $Q_{D0,i}$  is the initial reactive power demand before the load changes.  $k_{P,i}$  and  $k_{Q,i}$  are constants representing alterations (increase or decrease) in active and reactive power demand at bus  $i$ , and  $\varphi_i$  is the power factor angle at bus  $i$ . For a generator, the active power output of generator  $i$  should be altered to adapt the changed power demand according to:

$$P_{G,i} = P_{G0,i}(1 + \lambda k_{Gi}) \quad (4.5)$$

where  $P_{G0,i}$  is the initial active power generation of bus  $i$ .  $k_{Gi}$  is the constant specifying the rate of change in generation when  $\lambda$  is varied [1],[6].

## 4.2. Frequency Stability

Frequency stability describes the ability of a power system to maintain its frequency stable after a severe system upset, resulting in a significant imbalance between generation and load. The power system must maintain or restore the balance between system generation and load, with the least possible loss of load. Frequency instability may sometimes lead to tripping of generating units or loads [1].

#### 4.2.1. Inertia

The inertia of a power system is the ability of a system to oppose to shifts in frequency due to the resistance provided by kinetic energy of the rotating masses in synchronous machines. In case of major operational disturbances, low inertia in the system causes an increased risk of disconnection of consumption due to low frequency. The system inertia is very important for reducing the frequency drop and stabilizing the system for the first few seconds after a disturbance, before the primary control responds. Too low inertia can cause the frequency drop to such a low level that consumption is eliminated, and at worst case, a larger area becomes darkened [3]. The inertia constant states how much time it would take to bring the machine from synchronous speed to standstill if rated power is extracted from it while no mechanical power is fed into it. [3]:

$$H = \frac{1}{2} \frac{J\omega_m^2}{S_n} \quad (4.6)$$

Where

***H***: Inertia constant [s]

***J***: Moment of inertia [kgm<sup>2</sup>]

***ω<sub>m</sub>***: Mechanical angular frequency [rad/s]

***S<sub>n</sub>***: Rated apparent power [VA]

The inertia constant varies for different types of production units. Nuclear and thermal power plants have the largest inertia constants. The units are rotating fast because of the low mass, while hydropower units are rotating slowly because of relative large mass. The inertia constant for HVDC and wind power is zero and do not provide inertia to the power system [14].

The way that the mathematical formula of inertia arises, is analyzed in the section of swing equation.

#### 4.2.2. Primary Frequency Control

The purpose of the primary frequency control is to preserve the balance between production and consumption. A change in the power balance changes the kinetic energy of the rotation mass of the unit and alters the system frequency. The primary control stabilizes the system frequency at a stationary value by using a so-called turbine governor when an imbalance in the power system occurs. The governor sets with a frequency-power characteristic called droop [1],[4].

#### 4.2.3. Secondary Frequency Control

The aim of the secondary control is to restore the system frequency back to the nominal value and releasing the primary control. The secondary control activates when the Transmission System Operator (TSO) send a control signal to the power supplier's control system, which automatically changes the power production or consumption of the unit. The secondary control is handled by the Automatic Generation Controller (AGC). AGC transfers the set-point to the generator automatically when the controller receives control orders from the TSO. The response time for the secondary control is approximately 120-210 seconds after the AGC received the signal from the TSO [4].

#### 4.2.4. Tertiary Frequency Control

The tertiary control (Manual Frequency Restoration Reserve) is used to regulate the imbalances in the power systems and release the primary- and secondary control, but also to handle regional bottlenecks. Tertiary control is a common denomination of manual reserves that have an activation time of up to 15 minutes [4].

#### 4.2.5. Importance of frequency stability

There are several factors that need to be considered to maintain the system frequency stability [1],[4].

Firstly, the performance of the generators is usually reliant on the performance of the supplementary electric motor drives. The supplementary electric motor drives deliver air and fuel to the boiler, oil bearings and cooling services for the entire systems. When a situation

of low speed occurs due to low frequency, the supplementary motors will be affected, the output for the power stations will reduce, and this phenomenon will lead to shutdowns of the power stations.

In addition, power transformers are sensitive to system frequency variations and might be overloaded if the frequency deviates from the normal value.

Last but not least, in order to ensure that AC electric motors operates at a steady speed, a fixed speed is necessary. This is possible with the use of an AC motor to drive the equipment at an approximately fixed rate.

### **4.3. Rotor Angle Stability**

Rotor angle stability describes the ability of the synchronous machines to maintain synchronism even after a fault occurs [2]. To understand rotor angle stability and successfully plot the power output variations is important to study the rotor angle alteration of each machine relative to one another, as well as to comprehend the synchronous machine. Rotor angle is the relative angle between fixed references on rotating magnetic field of the stator to the rotating shaft. It is a fact that the power output of generator depends on the rotor angle. When disturbance appears, one machine will decelerate or accelerate with respect to its rotor angle perturbation. The resulting angular difference between the machines will result in reforming load between the machines (from slow to fast machine). This will damp the fast machine and eventually the system becomes stable at another equilibrium point. But sometimes the speed difference is so high that the power transfer gradually decreases, and the machine loses synchronism. Rotor angle stability is divided into small signal stability and transient stability.

#### **4.3.1. Small signal stability**

Small signal stability is relevant to the ability of system to maintain synchronism after small disturbance, such as variation of loads and generation [2]. Commonly, the disturbances are considered so low that it allows to use a linear model of system for analyzing such stability issues. Eigenvalue analysis is used to examine small signal stability of a power system.

There is local and global small signal stability. Local stability concerns a minor part of the power system where a single generator swinging against it, whereas global stability concerns



a larger part of the power system where a group of generators of a region swing with another group of generators in another region [2].

For the confrontation of such oscillations in power systems, stabilizers and automatic voltage regulators in combination with series and shunt compensators are used [2].

### Eigenvalue Analysis

Assume a nonlinear and dynamic system such as power system, when the system is at equilibrium point,  $\dot{x}$  is zero. Therefore, the system is described as follows [8],[9]:

$$\dot{x}_0 = f(x_0, u_0) = 0 \quad (4.7)$$

$$y_0 = g(x_0, u_0) \quad (4.8)$$

Where  $x_0$  and  $u_0$  refer to the state and input at the equilibrium point,  $y_0$  indicates the output at the equilibrium point. The value of  $x$  could be assumed as the change at the state  $x_0$ . The relation is described as below:

$$\dot{x} = \dot{x}_0 + \Delta \dot{x} \quad (4.9)$$

$\Delta x$  is the change at the state of  $x_0$  when disturbance happens. Equation (4.9) is expressed in this way:

$$\dot{x} = f[(x_0 + \Delta x), (u_0 + \Delta u)] \quad (4.10)$$

Then Taylor's series expansion can be used if the disturbance is small such as small signal stability. Equation (4.10) is expanded as:

$$\begin{aligned} \dot{x}_n &= \dot{x}_{n-0} + \Delta \dot{x}_n = f_n[(x_0 + \Delta x), (u_0 + \Delta u)] \\ &= f_n(x_0, u_0) + \frac{\partial f_n}{\partial x_1} \Delta x_1 + \dots + \frac{\partial f_n}{\partial x_m} \Delta x_m + \dots + \frac{\partial f_n}{\partial u_1} \Delta u_1 + \dots + \frac{\partial f_n}{\partial u_q} \Delta u_q \quad (4.11) \end{aligned}$$

$\dot{x}_{n-0}$  in Equation (4.11) is the derivation state at  $n$ -th time, which is zero, so

$$\dot{x}_n = \Delta \dot{x}_n = \frac{\partial f_n}{\partial x_1} \Delta x_1 + \dots + \frac{\partial f_n}{\partial x_m} \Delta x_m + \dots + \frac{\partial f_n}{\partial u_1} \Delta u_1 + \dots + \frac{\partial f_n}{\partial u_q} \Delta u_q \quad (4.12)$$

Similarly, the output can be obtained in the same way:

$$\Delta y_m = \frac{\partial g_m}{\partial x_1} \Delta x_1 + \dots + \frac{\partial g_m}{\partial x_m} \Delta x_m + \dots + \frac{\partial g_m}{\partial u_1} \Delta u_1 + \dots + \frac{\partial g_m}{\partial u_q} \Delta u_q \quad (4.13)$$

To summarize the structures of equation (4.12) and (4.13), they are expressed as:

$$\dot{\Delta x} = A\Delta x + B\Delta u \quad (4.14)$$

$$\dot{\Delta y} = C\Delta x + D\Delta u \quad (4.15)$$

Where

$$A = \begin{bmatrix} \frac{\partial f_1}{\partial x_1} & \dots & \frac{\partial f_1}{\partial x_m} \\ \vdots & \ddots & \vdots \\ \frac{\partial f_m}{\partial x_1} & \dots & \frac{\partial f_m}{\partial x_m} \end{bmatrix}, B = \begin{bmatrix} \frac{\partial f_1}{\partial u_1} & \dots & \frac{\partial f_1}{\partial u_q} \\ \vdots & \ddots & \vdots \\ \frac{\partial f_m}{\partial u_1} & \dots & \frac{\partial f_m}{\partial u_q} \end{bmatrix}, C = \begin{bmatrix} \frac{\partial g_1}{\partial x_1} & \dots & \frac{\partial g_1}{\partial x_m} \\ \vdots & \ddots & \vdots \\ \frac{\partial g_m}{\partial x_1} & \dots & \frac{\partial g_m}{\partial x_m} \end{bmatrix} \text{ and}$$

$$D = \begin{bmatrix} \frac{\partial g_1}{\partial u_1} & \dots & \frac{\partial g_1}{\partial u_q} \\ \vdots & \ddots & \vdots \\ \frac{\partial g_m}{\partial u_1} & \dots & \frac{\partial g_m}{\partial u_q} \end{bmatrix}$$

The whole process of calculation is called linearization around small disturbance of power system. In order to get eigenvalues, the process of linearization is necessary. The characteristic equation can be obtained from Equation (4.14):

$$\det(A - \lambda I) = 0 \quad (4.16)$$

Where  $\lambda$  is the eigenvalues of matrix A. The value of  $\lambda$  usually represents the stability of a system. Based on the knowledge in control system [1],[8], when

- $\lambda < 0$ , the system is stable.
- $\lambda = 0$ , the system is at critical position.
- $\lambda > 0$ , the system is unstable.

However, in power system, the eigenvalues are usually not real, they contain imaginary part. When eigenvalues are real, the negative value stands for descent oscillation which is the stable state, when the positive value means the instability of the system. In case that

eigenvalues are conjugate, the real part of eigenvalue represents damping magnitude, when it is positive, the system is stable. The imaginary part provides the frequency of oscillations [1],[9].

Power System Stabilizers

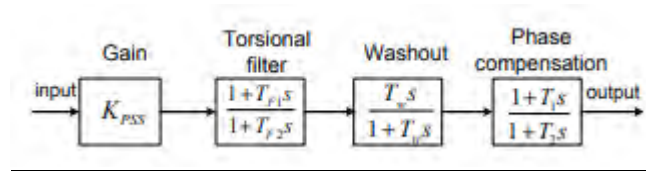


Figure 4.2: PSS block diagram [14]

In order power systems to enhance stability, they use Power System Stabilizers that are additional control devices installed at generator excitation systems. Power System Stabilizers add an extra stabilizing signal to compensate for undamped oscillations [20]. A Power System Stabilizer has a gain block, a washout block and a phase compensation block and sometimes an additional torsional filter [21] as shown in Figure 4.2. Power System Stabilizers can use single or multiple inputs considering the availability of input signals. Modern designs of controllers typically use multi-objective control [23], adaptive coordinated multi-controllers [9], and a hierarchical approach [5]. The decentralized hierarchical approach is more trustworthy and more adaptable than the centralized approach because it becomes possible to operate under challenging circumstances such as loss of wide-area signal [5]. Additionally, centralized controllers need much smaller gain than in the decentralized approach to accomplish an analogous damping effect, but their ability to discard disturbances is lower. An alternative method is to use both centralized and decentralized control to successfully generate both wide-area and local damping [23].

The system becomes quite different when adding PSS to the diagram as the oscillation is damped during the small disturbance as shown at Figure 4.3.

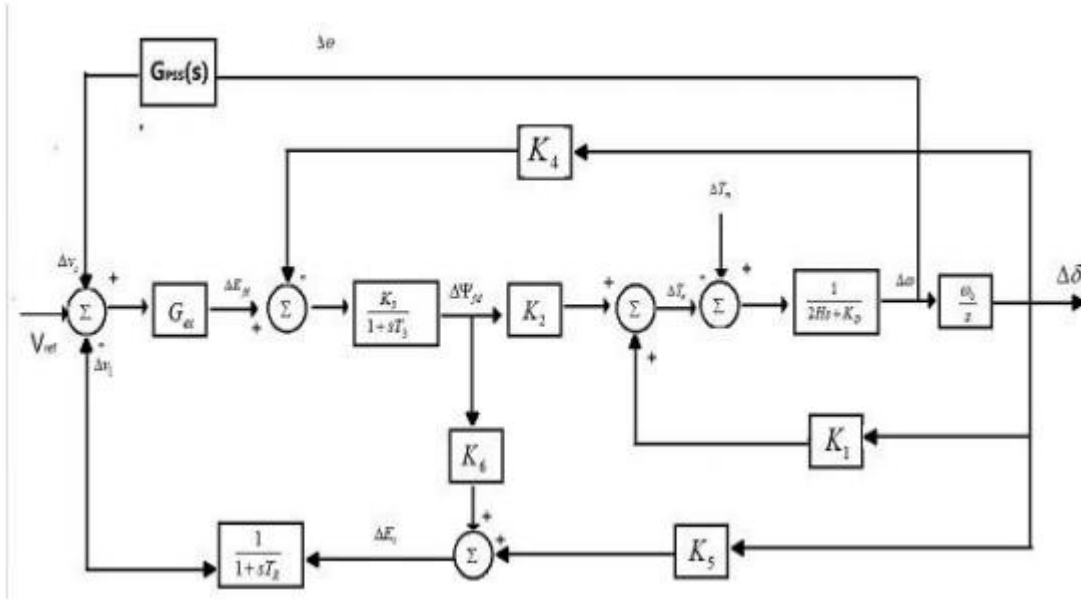


Figure 4.3 Block Diagram of The System with PSS [3]

The state matrix after installing PSS in the system should add the relation about the variable  $v_5$ . Assume the gain for power system stabilizer is  $G_S$  instead of the filter block. The voltage after the wash-out block is  $v_2$ .

When use rotor speed to be the input for PSS, then the following equation is obtained [1]:

$$\Delta v_2 = \frac{pT_w}{1+pT_w} (G_S \Delta \omega_r) \quad (4.17)$$

Where  $T_w$  is the time constant for wash-out block. In order to make derivation of  $\Delta v_2$ , the following expression is shown based upon Equation (4.17):

$$p\Delta v_2 = a_{51}\Delta \omega_r + a_{52}\Delta \delta + a_{53}\Delta \psi_{fd} + a_{55}\Delta v_2 + \frac{G_S}{2H} \Delta T_m \quad (4.18)$$

Where  $a_{51}, a_{52}, a_{53}, a_{55}$  are the coefficients when calculating the state matrix. Therefore, the derivation of output of the change for  $v_5$  is obtained as below [1]:

$$pv_5 = a_{61}\Delta \omega_r + a_{62}\Delta \delta + a_{63}\Delta \psi_{fd} + a_{64}\Delta v_1 + a_{65}\Delta v_2 + a_{66}\Delta v_5 + \frac{T_1 G_S}{2HT_2} \Delta T_m \quad (4.19)$$

Where  $a_{61}, \dots, a_{65}$  are the coefficients,  $T_1, T_2$  are the time constants in phase compensate block when assuming only one phase compensate block exists.

State matrix can be obtained in the following form with specified coefficients that relate to different state variables [1]:

$$\begin{bmatrix} \Delta \dot{\omega}_r \\ \Delta \dot{\delta} \\ \Delta \dot{\psi}_{fd} \\ \Delta \dot{v}_1 \\ \Delta \dot{v}_2 \\ \Delta \dot{v}_s \end{bmatrix} = \begin{bmatrix} \alpha_{11} & \alpha_{12} & \alpha_{13} & 0 & 0 & 0 \\ \alpha_{21} & 0 & 0 & 0 & 0 & 0 \\ 0 & \alpha_{32} & \alpha_{33} & \alpha_{34} & 0 & \alpha_{36} \\ 0 & \alpha_{42} & \alpha_{43} & \alpha_{44} & 0 & 0 \\ \alpha_{51} & \alpha_{52} & \alpha_{53} & 0 & \alpha_{55} & 0 \\ \alpha_{61} & \alpha_{62} & \alpha_{63} & 0 & \alpha_{65} & \alpha_{66} \end{bmatrix} \begin{bmatrix} \Delta \omega_r \\ \Delta \delta \\ \Delta \psi_{fd} \\ \Delta v_1 \\ \Delta v_2 \\ \Delta v_s \end{bmatrix} \quad (4.20)$$

All the coefficients can be calculated using the system model [3]. The eigenvalues can be then determined based on the system matrix.

### Automatic Voltage Regulator

Automatic Voltage Regulator (AVR) uses the generator's terminal voltage to adjust the field voltage in order to control the system's stability. The synchronizing torque coefficient, which is caused by the state variable, flux linkages will increase. Consequently, the total synchronizing torque coefficient is enhanced after applying any types of exciters. The value of damping torque component which also caused by flux linkages will become negative if the gain of exciter is high enough [3]. The oscillations which is caused by the disturbances in the system will become damped but with elevated synchronizing torque coefficient. The block diagram of the power system is the best way to see the principle of the system and components that will change during the disturbances happens.

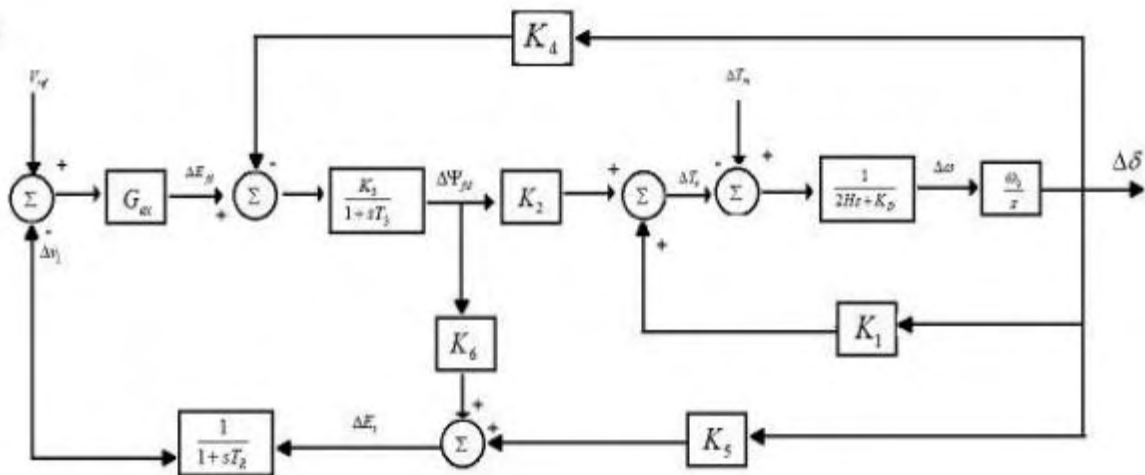


Figure 4.4 Block Diagram of The System with Excitation System [3]

In the above Figure (Figure 4.4),  $G_{ex}$  refers to the gain of the exciter,  $\frac{1}{1+ST_R}$  is the transfer function of the terminal voltage transducer in the excitation system. In this diagram, the excitation system is chosen to be the thyristor excitation system.

If one of the state variables changes, the state matrix will become a new matrix. Therefore, the eigenvalues and participation factors are different with the old ones.

In Figure 4.4,  $K_1, K_2, K_3, K_4, K_5, K_6$  are the constants described like below:

$$K_1 = \frac{V_b E_{q0}}{c} [(X'_d + X_e) \cos \delta_0 + R_e \sin \delta_0] + \frac{V_b I_{q0}}{c} \{ (X_q - X'_d) [(X_q + X_e) \sin \delta_0 - R_e \cos \delta_0] \} \quad (4.21)$$

$$K_2 = \frac{R_e E_{q0}}{c} + I_{q0} \left[ 1 + \frac{(X_q - X'_d)(X_q + X_e)}{c} \right] \quad (4.22)$$

$$K_3 = \left[ 1 + \frac{(X_d - X'_d)(X_q + X_e)}{c} \right]^{-1} \quad (4.23)$$

$$K_4 = \frac{V_b}{c} (X_q + X'_d) [(X_q + X_e) \sin \delta_0 - R_e \cos \delta_0] \quad (4.24)$$

$$K_5 = \frac{V_{d0}}{V_i} X_q \left[ \frac{R_e V_b \sin \delta_0 (X_e + X'_d) V_b \sin \delta_0}{c} \right] + \frac{V_{q0}}{V_i} X'_d \left[ \frac{R_e V_b \cos \delta_0 - (X_e + X_q) V_b \sin \delta_0}{c} \right] \quad (4.25)$$

$$K_6 = \frac{V_{q0}}{V_i} \left[ 1 - \frac{X'_d (X_q + X_e)}{c} \right] + \frac{V_{d0} X_q R_e}{V_i c} \quad (4.26)$$

Where  $C = R_e^2 + (X_q + X_e)(X_d + X_e)$ ,  $X'_d$  is transient reactance,  $R_e$  is line reactance,  $V_{d0}, V_{q0}$  are the initial values of the generator's terminal voltage on q-axis and d-axis respectively [8]. The participation factors of the state matrix will show the location and reasons that cause the unstable situation.

#### 4.3.2. Transient stability

Transient stability is relevant to the ability of a system to maintain synchronism within the machines after high transient disturbance occurs [2]. During severe disturbances, depending upon the initial operating point, significant variations of rotor angle can be detected [1]. The duration of transient stability analysis varies depending on the study, but it usually lasts a few seconds [2].

#### 4.4. Concept of Transient Stability

The model to analyze power system's stability refers to a single machine connected to the infinite bus system. Furthermore, all the resistances are neglected to simplify the analysis [1],[2]. In Figure 4.5 is shown a reduced equivalent circuit of single machine infinite bus system.

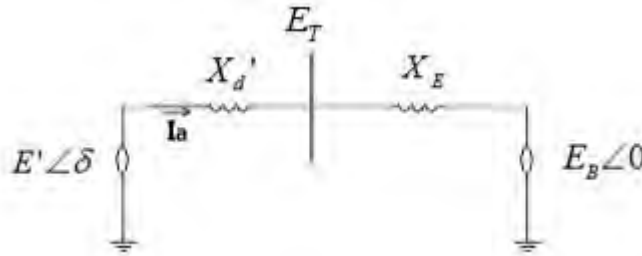


Figure 4.5 Reduced equivalent circuit of single machine infinite bus system [1]

Since all the resistances are neglected,  $E' \angle \delta$  represents the voltage before the transient reactance  $X'_d$ . The system at receiving end is connected through the reactance of  $X_E$  and the voltage at the receiving end is  $E_B \angle 0$ .

$E_T$  is the terminal voltage of the stator,  $I_a$  is the current of this system. The relationships are presented as follows [1],[2]:

$$I_a = \frac{E' \angle 0 - E_B \angle \delta}{j(X'_d + X_E)} \quad (4.27)$$

Assume  $X'_d + X_E = X_T$  in Equation (4.27), then the power generated from sending end is expressed as below,  $I_a^*$  is the conjugate form of  $I_a$ .

$$S_S = E' I_a^* = \frac{E' E_B \sin \delta}{X_T} + j \frac{E'(E' - E_B \cos \delta)}{X_T} \quad (4.28)$$

Since all the resistance are neglected, then we have [1],[2]:

$$T_e = \frac{E'E_B}{X_T} \sin\delta \quad (4.29)$$

$T_e$  is the air gap torque of the generator. In order to perform small change of the system. The change of air gap torque is noted as  $\Delta T_e$ , the initial state of rotor angle is  $\delta_0$ . The relation is represented as follow [1],[2]:

$$\Delta T_e = \frac{\partial T_e}{\partial \delta} \Delta\delta = \frac{E'E_B}{X_T} \cos\delta_0 (\Delta\delta) \quad (4.30)$$

Where  $\Delta\delta$  is the change of rotor angle. In order to linearize the system around the initial point, the motion equation is used here to analyze.

$$\frac{d\Delta\omega_r}{dt} = \frac{1}{2H} (T_m - T_e - K_D \Delta\omega_r) \quad (4.31)$$

$H$  is inertia constant,  $K_D$  is the damping coefficient which is important when detect the system,  $\omega_r$  refers to angular velocity of the rotor in electrical rad/s and  $\omega_0$  is the rated value of  $\omega_r$ . Substitute Equation (4.30) when linearize Equation (4.31), the expression should be like follows:

$$\frac{d\Delta\omega_r}{dt} = \frac{1}{2H} (\Delta T_m - K_S \Delta\delta - K_D \Delta\omega_r) \quad (4.32)$$

In Equation (4.32),  $K_S = \frac{E'E_B}{X_T} \cos\delta_0$  because of previous derivation. The angle's position has the relation as below:

$$\frac{d\delta}{dt} = \omega_0 \Delta\omega_r \quad (4.33)$$

Express the Equation (4.32) and (4.33) in matrix form,

$$\begin{bmatrix} \Delta\dot{\omega} \\ \Delta\dot{\delta} \end{bmatrix} = \begin{bmatrix} -\frac{K_D}{2H} & -\frac{K_S}{2H} \\ \omega_0 & 0 \end{bmatrix} \begin{bmatrix} \Delta\omega_r \\ \Delta\delta \end{bmatrix} + \begin{bmatrix} \frac{1}{2H} \\ 0 \end{bmatrix} \Delta T_m \quad (4.34)$$



Equation (4.34) is also expressed as the form of  $\dot{x} = Ax + bu$ . Where  $x$  is the state of system and  $u$  is the input of system. According to the matrix, damping relates to the speed deviation, synchronism corresponds with rotor angle deviation. When analyzing stability problems, the damping ratio and synchronism are the indices to evaluate the behavior of power system. [1],[2].

#### 4.4.1 Numerical integration methods

To analyze power system's stability, nonlinear ordinary differential equations with known initial values need to be solved:

$$\frac{dx}{dt} = f(x, t) \quad (4.35)$$

In this equation  $x$  is the state vector of  $n$  dependent variables and  $t$  is the independent variable(time).It is a necessity to solve  $x$  as a function of  $t$ , with the initial values of  $x$  equal to  $x_0$  and  $t$  equal to  $t_0$  [1].

#### Euler Method

Consider the first-order differential equation

$$\frac{dx}{dt} = f(x, t)$$

With  $x = x_0$  at  $t = t_0$ .Figure (4.6) shows an application of Euler Method.

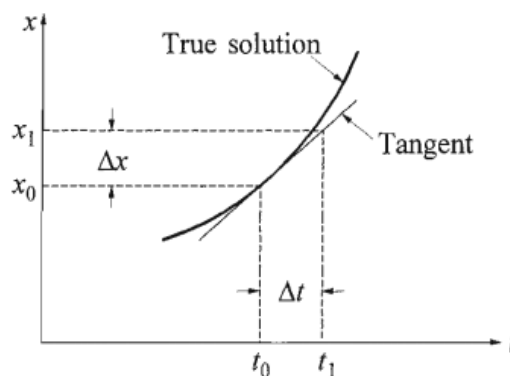


Figure 4.6 Application of Euler Method [1]

At  $x = x_0$ ,  $t = t_0$  the true solution of the problem can be approximated by the tangent on the curve having a slope [1].

$$\left. \frac{dx}{dt} \right|_{x=x_0} = f(x_0, t_0) \quad (4.36)$$

Thus,

$$\Delta x = \left. \frac{dx}{dt} \right|_{x=x_0} \cdot \Delta t \quad (4.37)$$

The value of  $x$  at  $t = t_1 = t_0 + \Delta t$  is given by

$$x_1 = x_0 + \Delta x = x_0 + \left. \frac{dx}{dt} \right|_{x=x_0} \cdot \Delta t \quad (4.38)$$

The first two terms of the Taylor series expansion for  $x$  around the point  $(x_0, t_0)$  are equivalent to Euler Method:

$$x_1 = x_0 + \Delta t(\dot{x}_0) + \frac{\Delta t^2}{2!}(\ddot{x}_0) + \frac{\Delta t^3}{3!}(\dddot{x}_0) + \dots \quad (4.39)$$

After the determination of  $x = x_1$  corresponding to  $t = t_1$ , another short time step  $\Delta t$  is taken to find out  $x_2$  corresponding to  $t_2 = t_1 + \Delta t$ :

$$x_2 = x_1 + \left. \frac{dx}{dt} \right|_{x=x_1} \cdot \Delta t \quad (4.40)$$

Likewise, other values of  $x$  corresponding to different values of  $t$ , can be determined.

Euler method is a first-order method and to provide accurate results in every stage,  $\Delta t$  must be small.

Generally, when using numerical integration methods, the propagation of error must be taken under consideration. That might cause minor errors made early in the process to be enlarged later. The method is said to be numerically stable when early errors carry through but cause no significant further errors later [1].

### Modified Euler Method

Due to the use of the derivative at the beginning of the interval, the standard Euler method often results in inaccuracies. On the other hand, the modified Euler method tries to overcome this problem by using the average of the derivatives at the two ends [1].

More specifically, the modified Euler method follows the below steps [1]:

1. Predictor step: By using the derivative at the beginning of the step, the value at the end of the step is predicted:

$$x_1^P = x_0 + \left. \frac{dx}{dt} \right|_{x=x_0} \cdot \Delta t \quad (4.41)$$

2. Corrector step: By using the predicted value of  $x_1^P$ , the derivative at the end of the step is computed and the average of this derivative and the derivative at the beginning of the step is used to find the correct value:

$$x_1^C = x_0 + \frac{1}{2} \left( \left. \frac{dx}{dt} \right|_{x=x_0} + \left. \frac{dx}{dt} \right|_{x=x_1^P} \right) \cdot \Delta t \quad (4.42)$$

By using  $x = x_1^C$ , a more accurate value of the derivative at the end of the step can be computed. This derivative can be used to calculate a more accurate value of the average derivative and then apply the corrector step again. This process can be used over and over again until successive converge with the desired accuracy is achieved [1].

### Runge-Kutta Method

The Runge-Kutta methods approximate the Taylor series solution. Nevertheless, Runge-Kutta methods do not necessitate specific evaluation of derivatives higher than the first. The effects of higher derivatives are included by several evaluations of the first derivative. Depending on the number of terms effectively retained in the Taylor series, there is second order and fourth order Runge-Kutta methods [1].

- Second order Runge-Kutta method [1]

The second order Runge-Kutta formula for the value of  $x$  at  $t = t_0 + \Delta t$  is:

$$x_1 = x_0 + \Delta x = x_0 + \frac{k_1+k_2}{2} \Delta t \quad (4.43)$$

Where

$$k_1=f(x_0 ,t_0) \Delta t \quad (4.44)$$

$$k_2=f(x_0 + k_1 ,t_0 + \Delta t) \Delta t \quad (4.45)$$

This method is equivalent to considering first and second derivative terms in the Taylor series, while error is on the order of  $\Delta t^3$ .

Finding the value of x for the  $(n + 1)^{st}$  step:

$$x_{n+1}= x_n + \frac{k_1+k_2}{2} \Delta t \quad (4.46)$$

Where

$$k_1=f(x_n ,t_n) \Delta t \quad (4.47)$$

$$k_2=f(x_n + k_1 ,t_n + \Delta t) \Delta t \quad (4.48)$$

- Fourth order Runge-Kutta method [1]

Finding the value of x for the  $(n + 1)^{st}$  step:

$$x_{n+1}= x_n + \frac{1}{6}(k_1 + 2k_2 + 2k_3 + k_4) \Delta t \quad (4.49)$$

Where

$$k_1=f(x_n ,t_n) \Delta t \quad (4.50)$$

$$k_2=f(x_n + \frac{k_1}{2} ,t_n + \frac{\Delta t}{2}) \Delta t \quad (4.51)$$

$$k_3=f(x_n + \frac{k_2}{2} ,t_n + \frac{\Delta t}{2}) \Delta t \quad (4.52)$$

$$k_4=f(x_n + k_3 ,t_n + \Delta t) \Delta t \quad (4.53)$$

$k_1$ : slope at the beginning of the time step  $\Delta t$

$k_2$ : first approximation to slope at midstep  $\Delta t$

$k_3$ : second approximation to slope at midstep  $\Delta t$

$k_4$ :slope at the end of step  $\Delta t$

$$\Delta x = \frac{1}{6}(k_1 + 2k_2 + 2k_3 + k_4) \Delta t \quad (4.54)$$

Therefore,  $\Delta x$  is the incremental value of x given by the weighted average of estimates based on slopes at the beginning, midpoint, and end of the time step.

This method is equivalent to considering up to fourth derivative terms in the Taylor series expansion. The error is on the order of  $\Delta t^5$ [1].

#### 4.4.2. Swing equation

Swing equation is called the electromechanical equation that connects the rotor angle to the stator rotating magnetic field as a function of time [1].

Swing equation is used for the study of electromechanical oscillations in power systems. In steady state operation, all synchronous machines of a power system have the same electrical angular velocity. Though, due to different disturbances, one or more generators could accelerate or decelerate and lose synchronism. This fact influences system's stability since generators that lost synchronism must be disconnected, otherwise they could be permanently harmed. Swing equation is used to find the energy stored during swing from one operating point to another and then to perform the transient stability analysis [14].

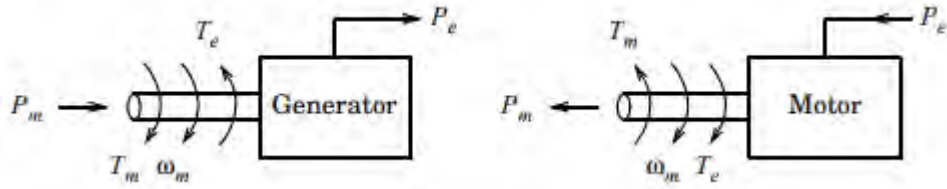


Figure 4.7 Powers and torques in synchronous machines [14]

The synchronous machine models are the basis for the derivation of the swing equation describing the electro-mechanical oscillations in a power system. Figure 4.7 is a scheme of the different torques and powers of a synchronous machine with their mechanical  $m$  and electrical  $e$  quantities. The differential equation describing the rotor dynamics is [14]:

$$J \frac{d^2 \theta_m}{dt^2} = T_m - T_e \quad (4.55)$$

where

$J$ : The total moment of inertia of the synchronous machine ( $\text{kg} \cdot \text{m}^2$ )

$\theta_m$ : The mechanical angle of the rotor (rad)

$T_m$ : Mechanical torque from turbine or load ( $\text{N} \cdot \text{m}$ ). Positive  $T_m$  corresponds to mechanical power fed into the machine, i.e. normal generator operation in steady state.

$T_e$ : Electrical torque on the rotor (N·m). Positive  $T_e$  in normal generator operation.

If equation (4.55) is multiplied with the mechanical angular velocity  $\omega_m$  one gets

$$\omega_m J \frac{d^2 \theta_m}{dt^2} = P_m - P_e \quad (4.56)$$

where

$P_m = T_m \omega_m$  : mechanical power acting on the rotor (W)

$P_e = T_e \omega_m$  : electrical power acting on the rotor (W)

If the angular acceleration should be expressed in electrical angle, we have

$$\frac{2}{p} \omega_m J \frac{d^2 \theta_e}{dt^2} = P_m - P_e \quad (4.57)$$

where the left-hand side can be re-arranged:

$$2 \frac{2}{p \omega_m} \left( \frac{1}{2} \omega_m^2 J \right) \frac{d^2 \theta_e}{dt^2} = P_m - P_e \quad (4.58)$$

If equation (4.58) is divided by the rating of the machine  $S$ , the result is

$$\frac{2}{\omega_e} \frac{\left( \frac{1}{2} \omega_m^2 J \right)}{S} \frac{d^2 \theta_e}{dt^2} = \frac{P_m - P_e}{S} \quad (4.59)$$

During disturbances, the angular velocity of the rotor will not differ significantly from the nominal values, i.e. from  $\omega_{m0}$  and  $\omega_{e0}$ , respectively. That means that equation (4.59) can be written as

$$\frac{2H}{\omega_{e0}} \frac{d^2 \theta_e}{dt^2} = P_m^{pu} - P_e^{pu} \quad (4.60)$$

where  $pu$  suggests that the mechanical and electrical powers should be expressed in p.u. of the rating of the synchronous machine. A more general form of the swing equation is [14]:

$$\frac{2H}{\omega_0} \frac{d^2 \theta}{dt^2} = P_m - P_e \quad (4.61)$$

#### 4.4.3. Equal Area Criterion

One method of investigating the transient stability behavior of a single machine/infinite bus system is to apply the Equal Area Criterion. The method does not solve for the rotor angle, rather it tells us the maximum angle which the machine can advance to before the fault is cleared in order to preserve transient stability [1],[14].

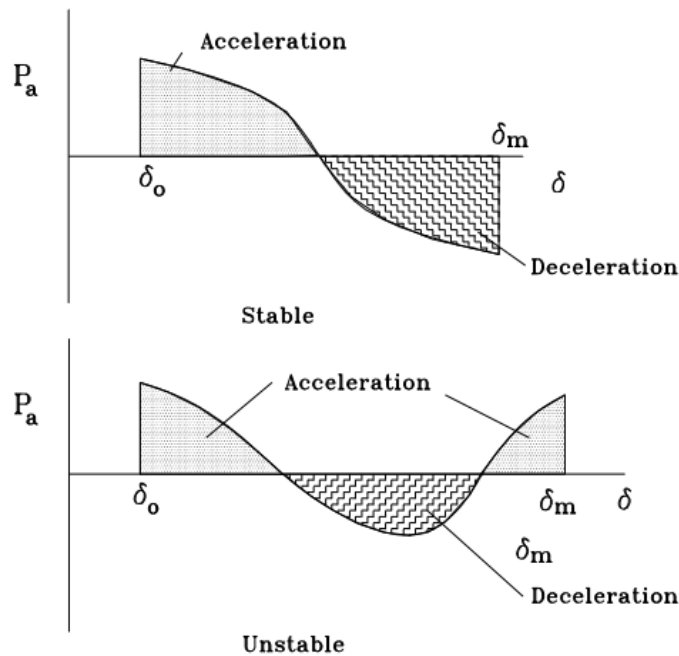


Figure 4.8 Application of the equal area criterion [14]

The application of the equal area criterion is shown in Figure 4.8. In the first case, the fault occurs at an angle  $\delta_o$  and the machine begins to accelerate. The fault is cleared at some subsequent time (and angle) and the machine begins to decelerate and reaches a maximum angle  $\delta_m$  when the acceleration area and deceleration area are equal. In this case the machine is stable as the fault was cleared at a time which allowed the machine a sufficient interval to decelerate. In the second case, the acceleration area exceeds the deceleration area and the machine is unstable. This is because the time taken to clear the fault was excessive. The acceleration area can be determined from the power angle curve. Figure 4.9 shows the power-angle curves for the system described earlier. The pre-fault, fault and post-fault power curves are shown together with the constant mechanical power. The accelerating power is

equal to the difference between the electrical power curve and the mechanical power input [1],[14].

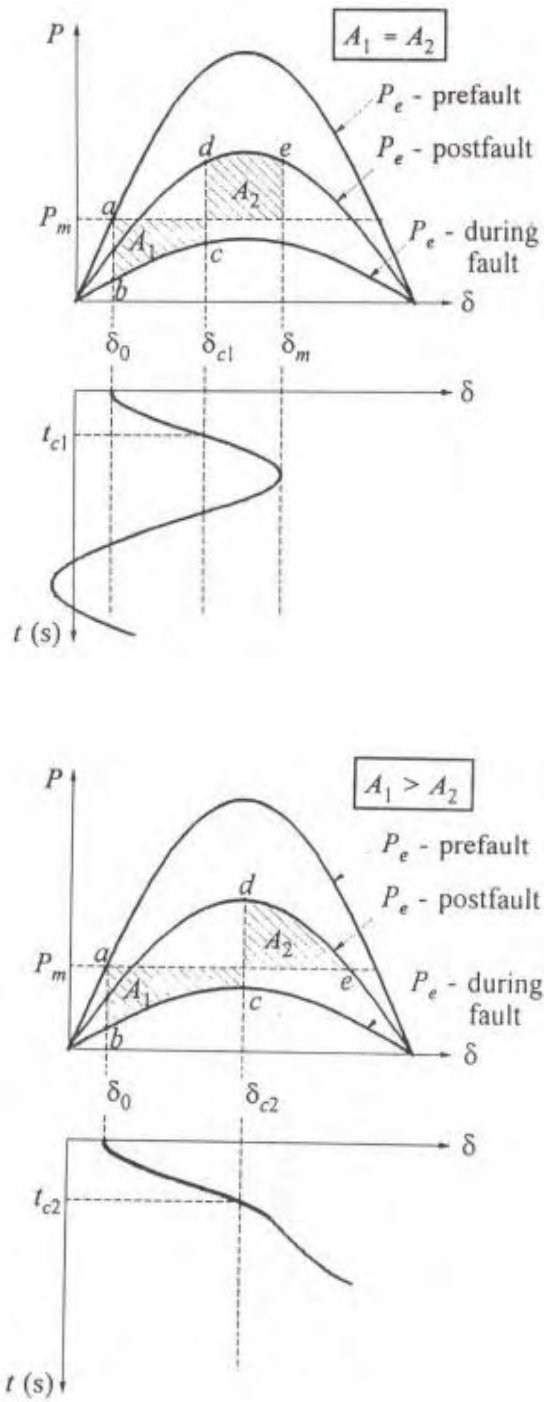


Figure 4.9 Power-angle curves [26]

The swing equation of the system be expressed as [14]:



$$\frac{d^2\delta}{dt^2} = \frac{\omega_0}{2H}(P_m - P_{e,max}\sin\delta) \quad (4.62)$$

or

$$\frac{d^2\delta}{dt^2} = \frac{\omega_0}{2H} P_a \quad (4.63)$$

with the accelerating power  $P_a$  described by

$$P_a = P_m - P_{e,max}\sin\delta \quad (4.64)$$

An essential condition for stability is that there is a moment  $t_m$  during the swing where  $\dot{\delta}(t_m) = 0$ . The corresponding angle is  $\delta_m$ . Equation (4.63) combined with the condition  $\dot{\delta}(t_m) = 0$  give a stability criterion. If equation (4.63) is multiplied with  $\dot{\delta}$  gives [14]:

$$\dot{\delta} \frac{d^2\delta}{dt^2} = \frac{\omega_0}{2H} P_a \dot{\delta} \quad (4.65)$$

which can be written as:

$$\frac{1}{2} \frac{d}{dt} \left( \frac{d\delta}{dt} \right)^2 = \frac{d}{dt} \left( \frac{\omega_0}{2H} \int_{\delta_i}^{\delta} P_a d\delta' \right) \quad (4.66)$$

that can be integrated to give

$$\frac{d\delta}{dt} = \sqrt{\frac{\omega_0}{2H} \int_{\delta_i}^{\delta} P_a d\delta' + C} \quad (4.67)$$

with  $C$  is a constant of integration equal to 0, since  $\dot{\delta} = 0$  when  $\delta = \delta_i$ . ( $\delta_i$  is the pre-fault rotor angle).

Therefore, a necessary condition for stability is that there is an angle  $\delta_m$  such that [14]:

$$\frac{\omega_0}{H} \int_{\delta_i}^{\delta_m} P_a d\delta' = 0 \quad (4.68)$$

or

$$\int_{\delta_i}^{\delta_m} P_a d\delta' = 0 \quad (4.69)$$

The system is stable when there is an angle  $\delta_m$  such that the area below the accelerating power  $P_a$  in the  $\delta$ - $P(\delta)$  diagram between  $\delta_i$  and  $\delta_m$  disappears [14].

We can distinguish two different phases in this criterion. In the first place, the rotor is accelerated up to  $\delta = \delta_c$  and then it is decelerated, where  $\delta_c \leq \delta \leq \delta_m$ . The two different areas in the  $\delta$ - $P(\delta)$  plane can be defined as [14]:

$$A_1 = \int_{\delta_i}^{\delta_c} (P_m - P_e(\delta')) d\delta' \quad (4.70)$$

$$A_2 = \int_{\delta_c}^{\delta_m} (P_e(\delta') - P_m) d\delta' \quad (4.71)$$

The angle  $\delta_c$  is the angle when the fault is cleared. The system is stable when  $A_1 = A_2$ .

During the fault, the electrical power  $P_e$  is reduced to zero. Even though the equal area criterion investigates the stability of a system without any unnecessary computational efforts, the time  $t$  is eliminated from the equations. That's why actions to enhance the stability must be made in the angle space. Using equal area criterion becomes possible to find critical fault clearing angles and then critical fault clearing times [14].

The angle  $\delta_c$  defines the positive and negative values of  $P_a$ . When applying the equal area criterion, we prefer to choose as  $\delta_c$  the angle when the fault is cleared. At this angle we have different expressions for  $P_e$ , and so, differences in computation of  $A_1$  and  $A_2$ . Different stability related problems can be solved by using the equal area criterion.

By applying equal area criterion, it is possible to find out how fast a fault must be cleared to ensure the system's stability. Also, it can be used to calculate the maximum power that can be transmitted in a specific fault case, as well as to determine if a system is stable [14].

#### 4.4.4. Critical Clearing Time

The maximum allowable value of the clearing angle and clearing time for the system to remain stable are known as critical clearing angle and critical clearing time respectively. The equal area criterion allows the calculation of the critical clearing angle but not the critical clearing time. Since the swing equation is a non-linear second order differential equation, a numerical method is needed to solve it. It is useful to use the Euler or Modified Euler, the Runge-Kutta or any other appropriate method. The result of the application of such a technique is the variation in rotor angle with time [1],[14].

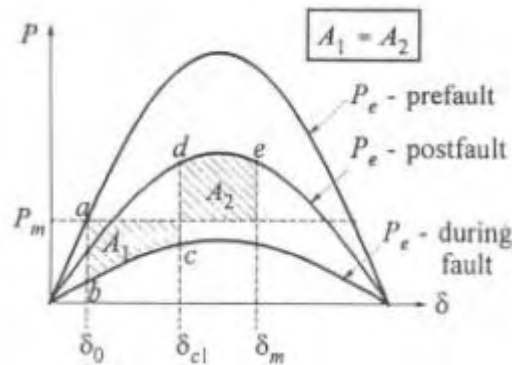


Figure 4.10 Pre-fault, During fault, Postfault Power-Angle curve [26]

Considering a three-phase short circuit occurs at the point  $F$  of the outgoing radial line, the power angle curve relation jump from initial operating condition during pre-fault state 'a' to operating point on persisting fault curve 'b'. The machine accelerates until the fault is cleared and reaches an operating point 'c' with a corresponding increase in load angle. After the fault has cleared, power-angle relation jump from operating point 'c' on persisting fault curve to operating point 'd' on post fault power-angle curve as shown in Figure 4.10. The transmitted power is  $P_e = P_{max} \cdot \sin \delta$ . Even though the output power is greater than input power of the machine at this point, the machine will continue accelerating until point 'e' due to inertia. During this period, the kinetic energy gained by the synchronous machine is given back to the system and then the machine trace back to operating point 'd' after oscillating about it.

The critical clearing angle is the maximum angle before which the fault must be cleared to ensure that the system remains stable.

The critical clearing angle can be calculated by applying the equal area criterion. Graphically, it means that the area A1 which represent energy gained and A2 which represent energy lost as shown in Figure 4.10 should be equal to have a stable condition in the system. Expressing  $area A1 = area A2$  mathematically, we have [1],[14]:

$$\int_{\delta_0}^{\delta_c} (P_m - P_{fault}) d\delta = \int_{\delta_c}^{\delta_m} (P_{postfault} - P_m) d\delta \quad (4.72)$$

where  $\delta_0$  is the initial rotor angle,  $\delta_c$  is the critical clearing angle and  $\delta_m$  is the maximum angle to which the machine can swing to and remain stable. The above equation can be written as [1],[14]:

$$P_m(\delta_c - \delta_0) = \int_{\delta_c}^{\delta_m} (P_e - P_m) d\delta \quad (4.73)$$

$$P_m(\delta_c - \delta_0) = \int_{\delta_c}^{\delta_m} P_{max} \sin\delta d\delta - P_m(\delta_m - \delta_c) \quad (4.74)$$

$$P_m\delta_c - P_m\delta_0 = P_{max}(-\cos\delta_m + \cos\delta_c) - P_m\delta_m + P_m\delta_c \quad (4.75)$$

$$P_{max}(\cos\delta_c - \cos\delta_m) = P_m(\delta_m - \delta_0) \quad (4.76)$$

Also,

$$P_m = P_{max} \sin\delta_0 \quad (4.77)$$

Using equation (4.76) and (4.77):

$$(\cos\delta_c - \cos\delta_m) = P_{max}(\delta_m - \delta_0) \sin\delta_0 \quad (4.78)$$

$$\cos\delta_c = \cos\delta_m + (\delta_m - \delta_0) \sin\delta_0 \quad (4.79)$$

In order to determine the clearing time, we rewrite the swing equation, with  $P_e=0$ , since we have a three-phase fault,

$$\frac{d^2\delta}{dt^2} = \frac{\pi f}{H} P_m \quad (4.80)$$

Integrating equation (4.80) twice and utilizing the fact that when  $t=0$ ,  $d\delta/dt=0$  yields

$$\delta = \frac{\pi f P_m}{2H} t^2 + \delta_0 \quad (4.81)$$

If  $t_c$  is a clearing time corresponding to a clearing angle  $\delta_c$ , then we obtain from equation (4.81):

$$\delta_c = \frac{\pi f P_m}{2H} t_c^2 + \delta_0 \quad (4.82)$$

and so,

$$t_c = \sqrt{\frac{2H(\delta_c - \delta_0)}{\pi f P_m}} \quad (4.83)$$

#### 4.4.5. Factors Influencing Transient Stability

Some of the factors that influence system's transient stability are fault clearing time and the inertia of the generator, as well as, the load on it. Additionally, any change in system's reactance between generation and load centers, the internal voltage magnitude of the generator and the output of the generator during fault are able to lead to transient instability [1],[14]:

## **CHAPTER 5**

### **5. TRANSIENT STABILITY ANALYSIS OF IEEE 9-BUS SYSTEM**

Power System Simulator for Engineering (PSS/E) is a software tool used by engineers to simulate electrical power transmission networks in steady-state conditions. PSS/E, launched in 1976, is nowadays an integrated, interactive program for simulating, analyzing, and optimizing power system's performance. Using PSS/E becomes possible to perform power flow, optimal power flow and fault analysis, as well as, dynamic simulation, open access and pricing of a system etc.

#### **5.1 Transient Stability and Power Flow**

Power flow analysis is used for real time system analysis as well as planning studies. With PSS/E the user can analyze the performance of a power system in both normal and under fault operating conditions. The study in normal steady-state operating conditions is called a power-flow or load-flow study and it focuses on determining the voltages, currents, and real and reactive power flows in a system under known load conditions.

Methods that have been developed to solve the nonlinear load flow problem and can be found in PSS/E are Gauss-Seidel and Newton-Raphson methods. After finding the load flow, we can proceed to dynamic simulation by inserting the dynamic model of the system into the static load flow model. PSSE model of IEEE 9 bus is given in Appendix A. Figure 5.1 shows the load flow of IEEE 9 bus system and load flow data are given in Table 1.

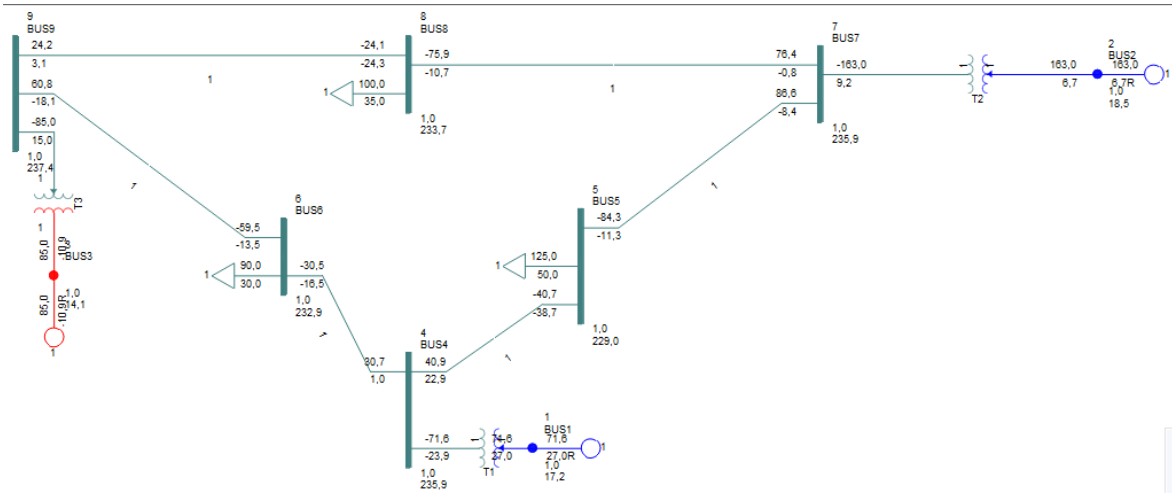


Figure 5.1– Load flow diagram of IEEE 9 Bus

Table 1 - Standard load flow data of IEEE 9bus

Bus No	Bus type	Voltage (pu)	Angle (deg)	PGen (MW)	QGen (Mvar)	Pload (MW)	Qload (Mvar)
1	Swing Bus	1,04	0	71,641	27,046	0	0
2	PV	1,025	9,28	163	6,654	0	0
3	PV	1,025	4,66	85	-10,86	0	0
4	PQ	1,0258	-2,22	0	0	0	0
5	PQ	0,9956	-3,99	0	0	125	50
6	PQ	1,0127	-3,69	0	0	90	30
7	PQ	1,0258	3,72	0	0	0	0
8	PQ	1,0159	0,73	0	0	100	35
9	PQ	1,0324	1,97	0	0	0	0

## 5.2 Dynamic simulation for transient stability analysis in PSS/E

IEEE 9 bus system is often used by engineers to perform steady state and dynamic simulation studies. The following study was simulated using PSSE software. Figure 4.1 shows the active generation, impedance and load data of IEEE 9 bus system. This test case consists of 9 buses, 3 machines, 6 transmission lines, 3 two-winding power transformers and 3 loads. This network is generating a total of 319.6 MW and supplying a total load of 315 MW, 115MVAR and transmission losses of 4.6 MW. All impedances are on 100 MVA base.

### 5.2.1 Stable condition

The steps followed for the dynamic simulation are:

- 1) The system is initialized.
- 2) One second after the initiation of the system, a bus fault occurs.
- 3) With a step of 100 msec, the fault duration increases gradually until the system is unstable.
- 4) The fault is cleared and a line from the faulted bus is tripped.
- 5) The simulation continues for a few seconds and then the tripped line closes. The total simulation time is 10 seconds.

#### Stable Case A: 3-L-G Fault at Bus 4

In this case, the critical clearing time is evaluated to 300 ms (18 cycles). Figure 5.2 illustrates the relative angle plot of generator 2 and 3 with regard to generator 1. Figure 5.3 illustrates the active power output of all the 3 generators. The maximum swing angle of generator 2 is 45 while generator's 3 is 35. Figure 5.4 illustrates the reactive power output of all the 3 generators and Figure 5.5 demonstrates the terminal voltage output variation of all generators for a fault at bus 4. Figure 5.6 illustrates the frequency output variation of bus 4 and Figure 5.7 shows the voltage output variation of bus 4 for fault at bus 4.

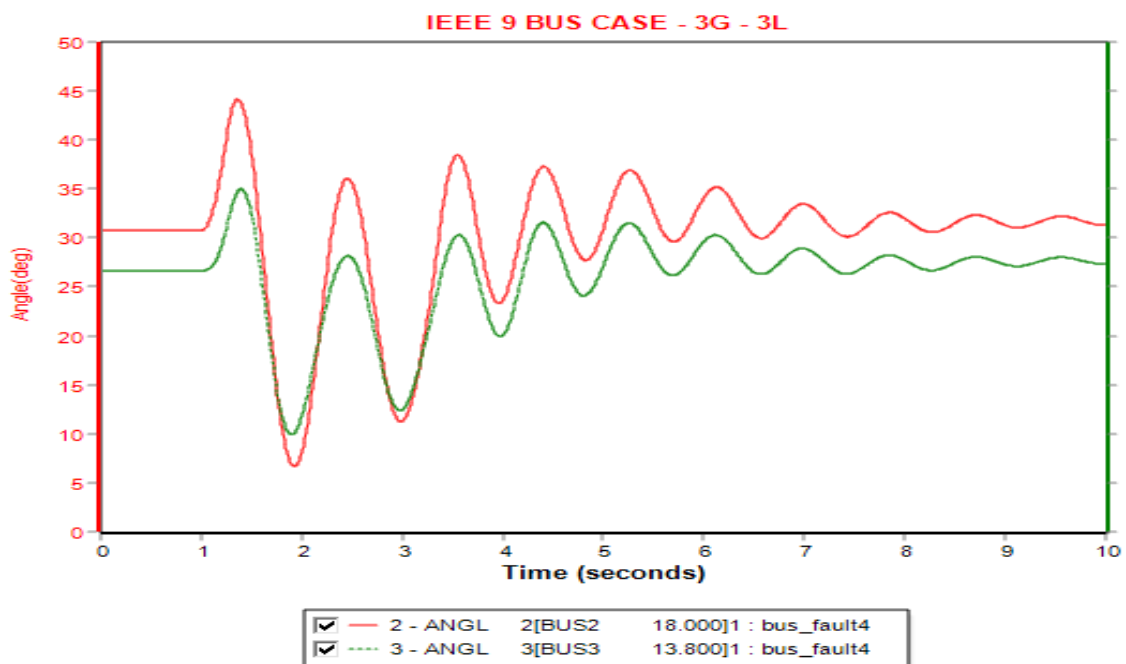


Figure 5.2- Angle plot of all generators for a fault at bus 4



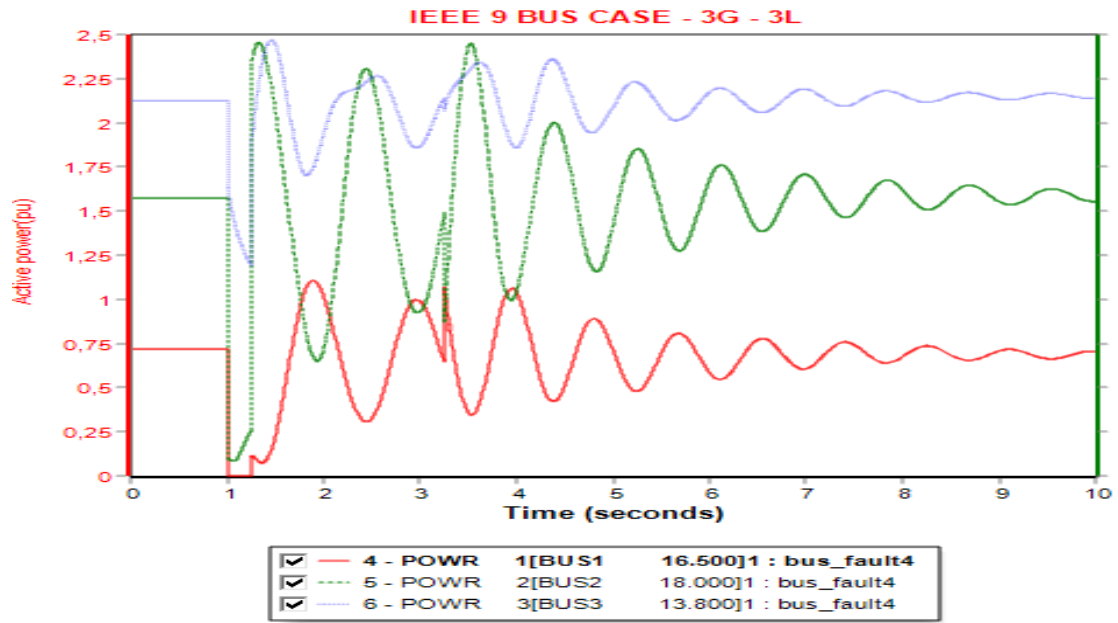


Figure 5.3 - Active power output variation of all generators for fault at bus 4

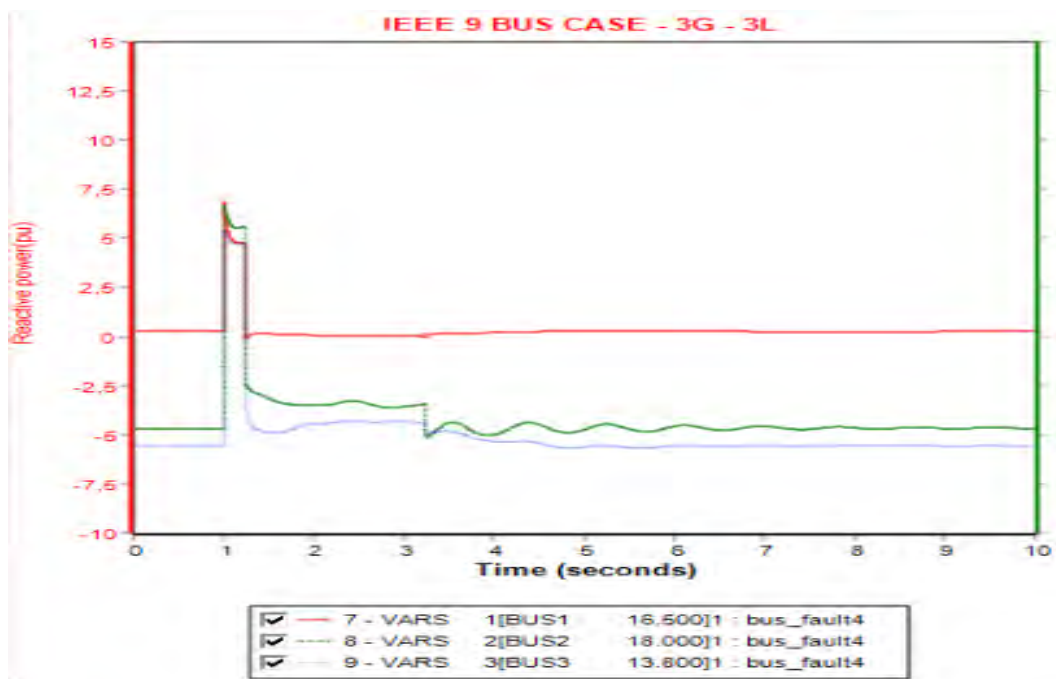


Figure 5.4 - Reactive power output variation of all generators for fault at bus 4

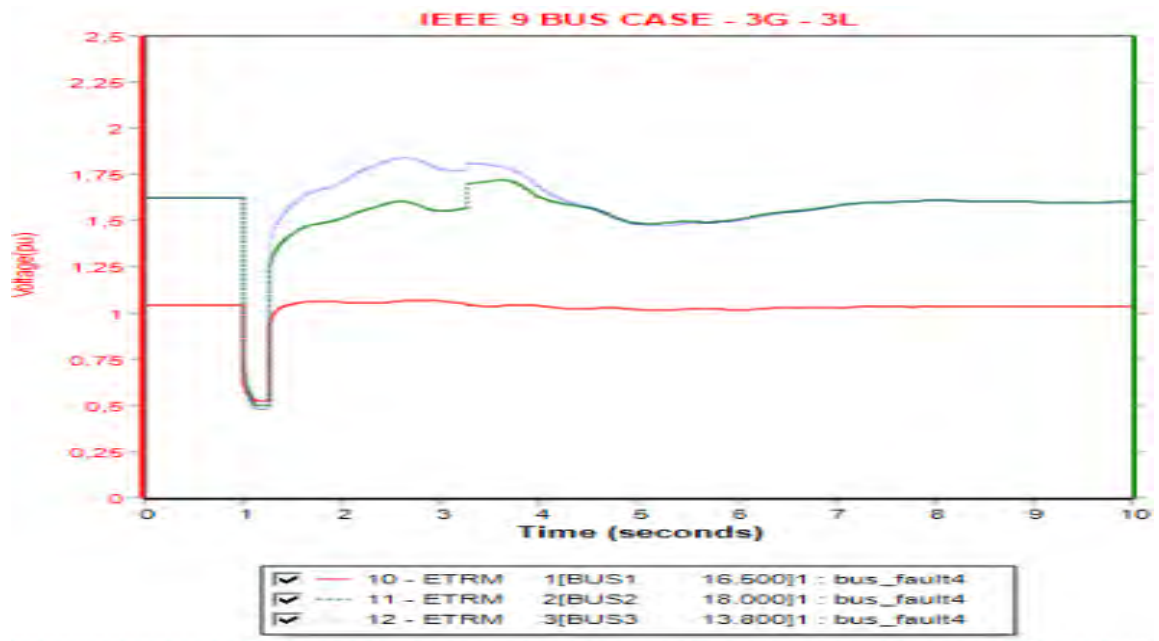


Figure 5.5 - Terminal voltage output variation of all generators for fault at bus 4

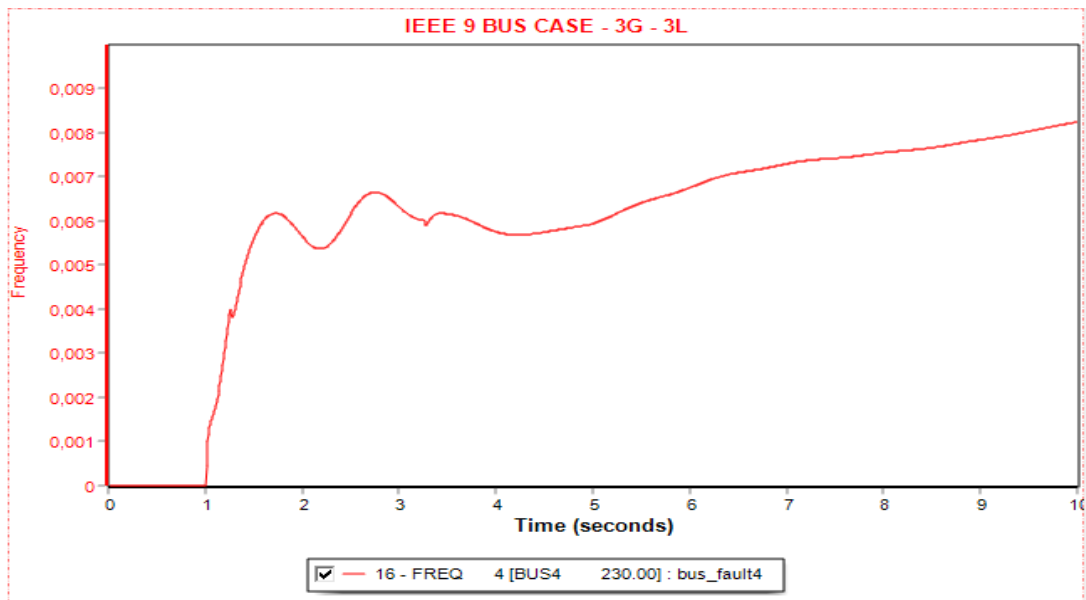


Figure 5.6 - Frequency output variation of bus 4 for fault at bus 4

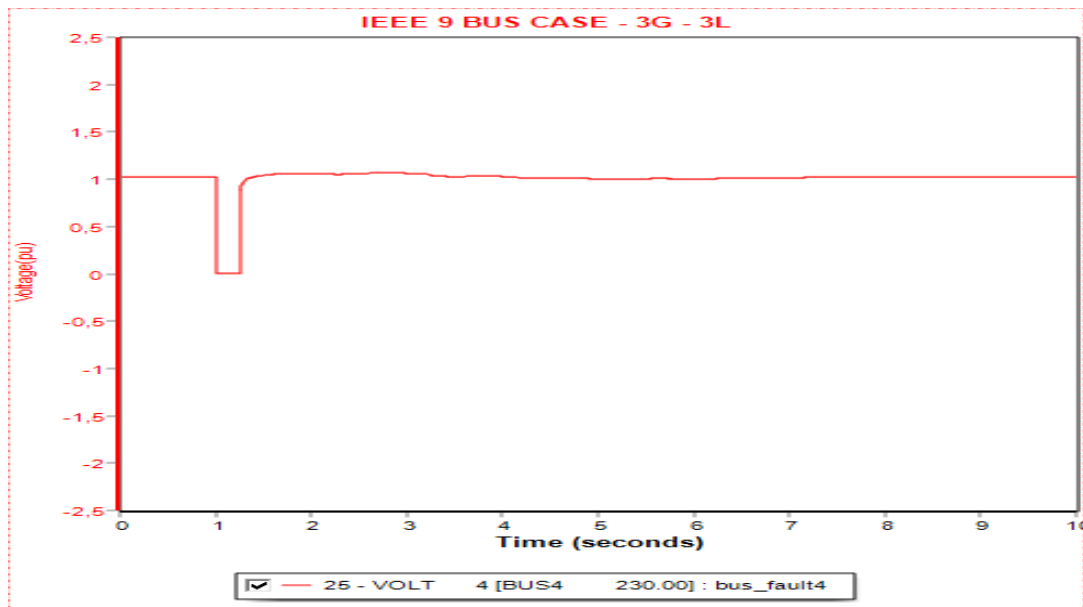


Figure 5.7 – Voltage output variation of bus 4 for fault at bus 4

#### Stable Case B: 3-L-G Fault at Bus 5

In this case, the critical clearing time is evaluated to 200 ms (12 cycles). Figure 5.8 illustrates the relative angle plot of generator 2 and 3 with regard to generator 1. Figure 5.9 illustrates the active power output of all the 3 generators. The maximum swing angle of generator 2 is 37 while generator's 3 is 42. Figure 5.10 demonstrates the reactive power output of all the 3 generators and Figure 5.11 demonstrates the terminal voltage output variation of all generators for a fault at bus 5. Figure 5.12 illustrates the frequency output variation of bus 5 and Figure 5.13 shows the voltage output variation of bus 5 for fault at bus 5.

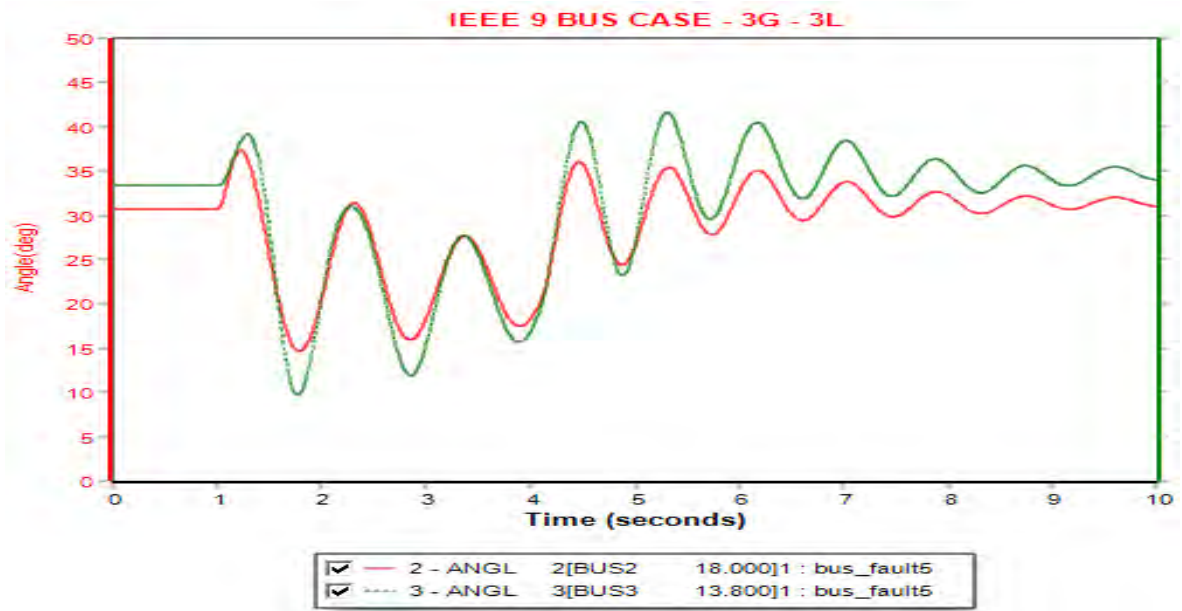


Figure 5.8 - Angle plot of all generators for a fault at bus 5

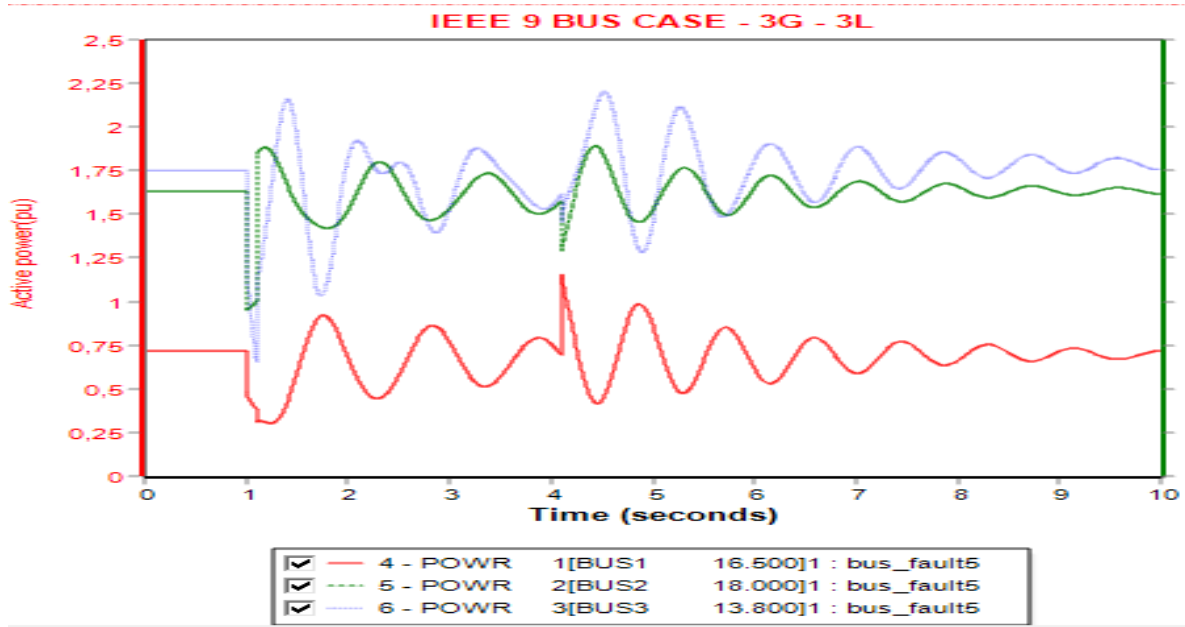


Figure 5.9 - Active power output variation of all generators for fault at bus 5

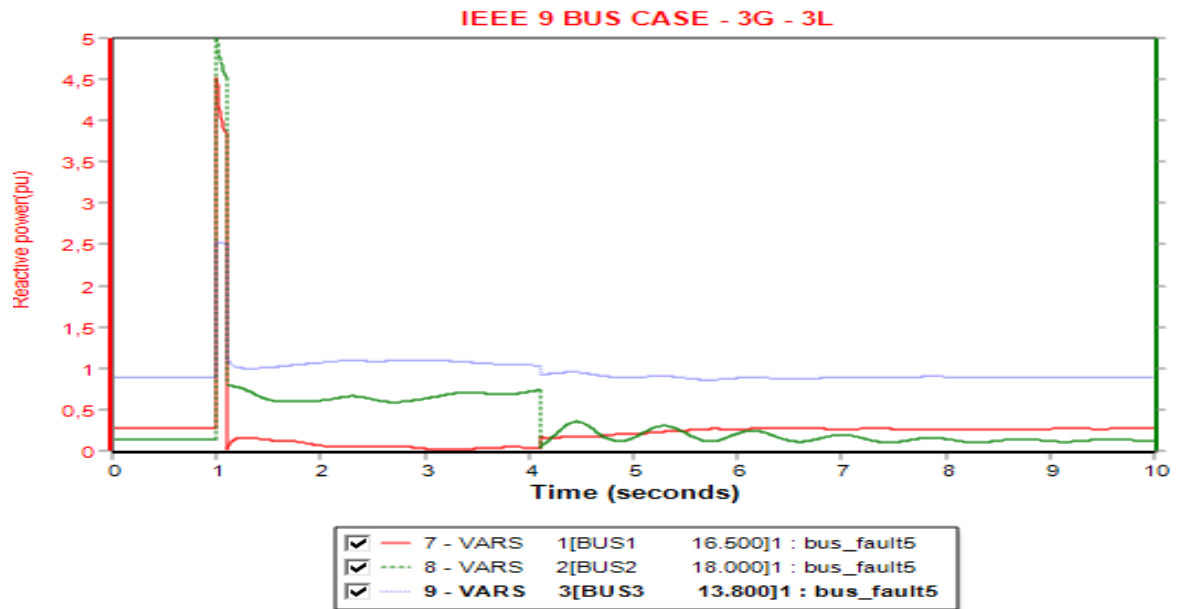


Figure 5.10- Reactive power output variation of all generators for fault at bus 5

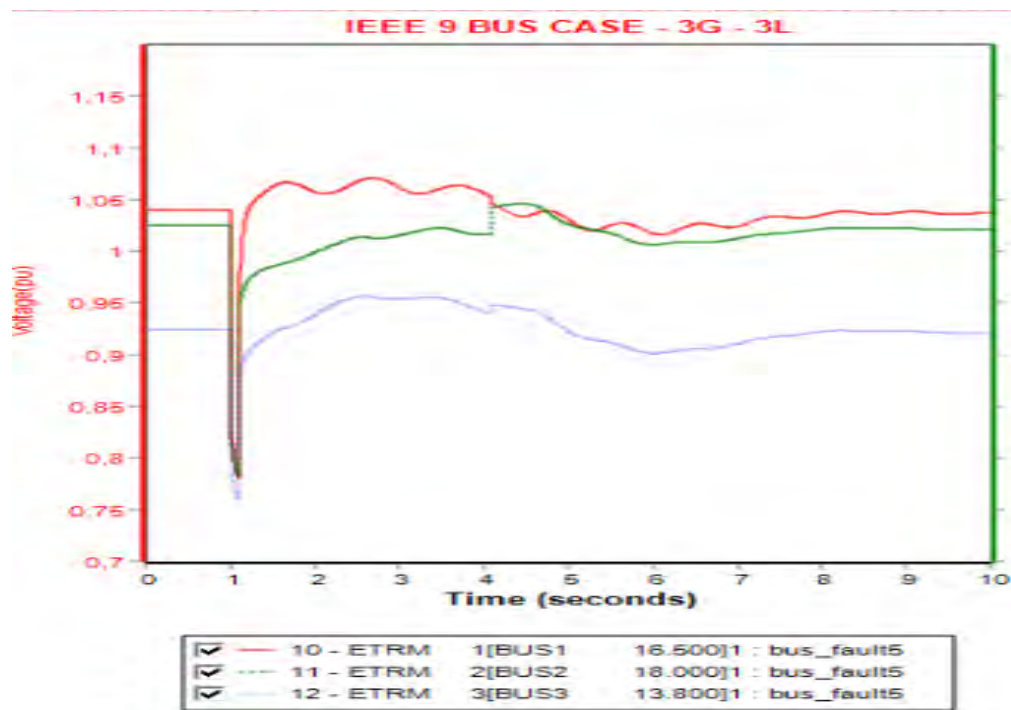


Figure 5.11 - Terminal voltage output variation of all generators for fault at bus 5

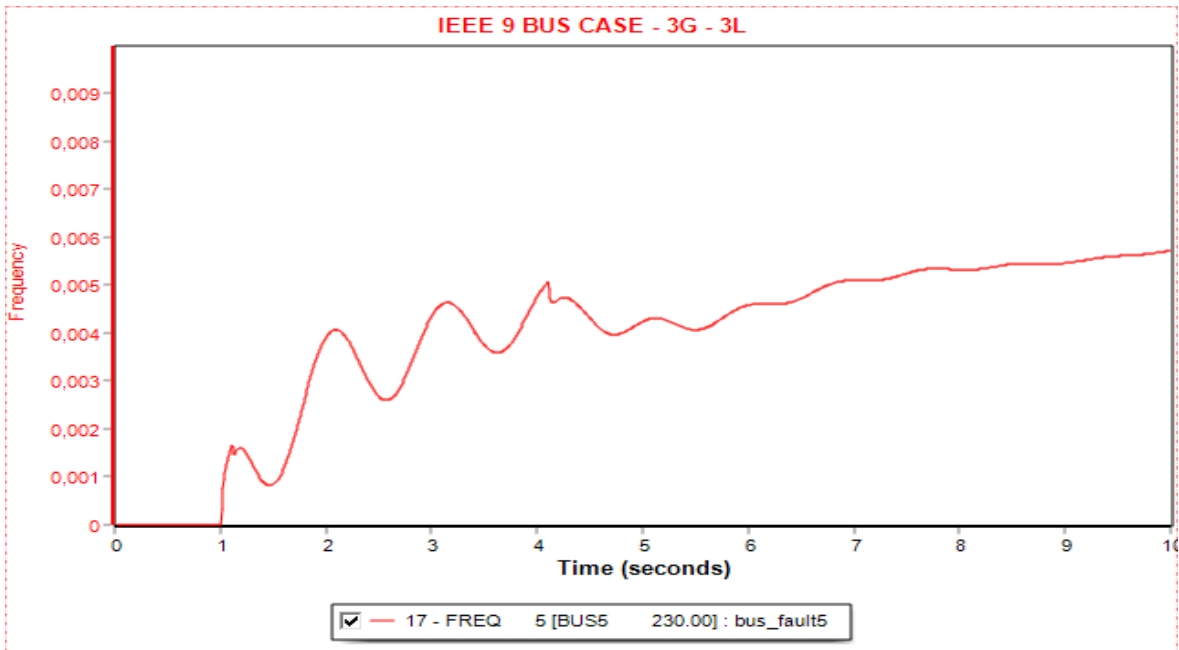


Figure 5.12 - Frequency output variation of bus 5 for fault at bus 5

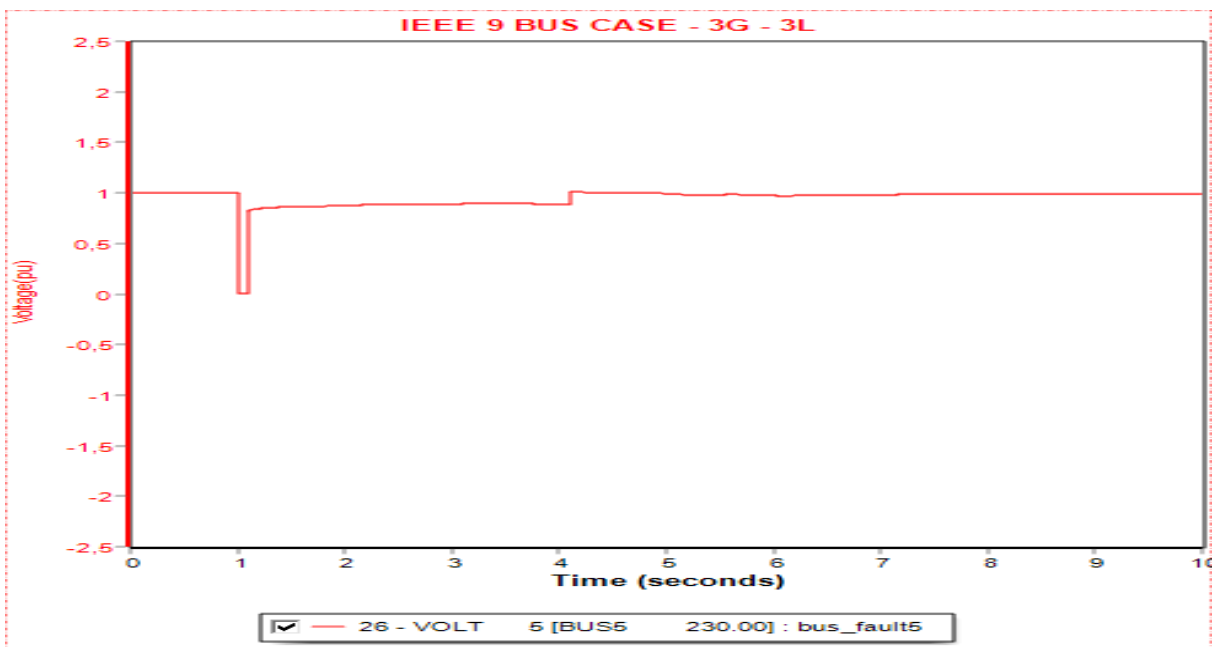


Figure 5.13 – Voltage output variation of bus 5 for fault at bus 5

Stable Case C: 3-L-G Fault at Bus 6

In this case, the critical clearing time is evaluated to 450 ms (27 cycles). Figure 5.14 illustrates the relative angle plot of generator 2 and 3 with regard to generator 1. Figure 5.15

illustrates the active power output of all the 3 generators. The maximum swing angle of generator 2 is 53 while generator's 3 is 57. Figure 5.16 illustrates the reactive power output of all the 3 generators and Figure 5.17 illustrates the terminal voltage output variation of all generators for a fault at bus 6. Figure 5.18 illustrates the frequency output variation of bus 6 and Figure 5.19 shows the voltage output variation of bus 6 for fault at bus 6.

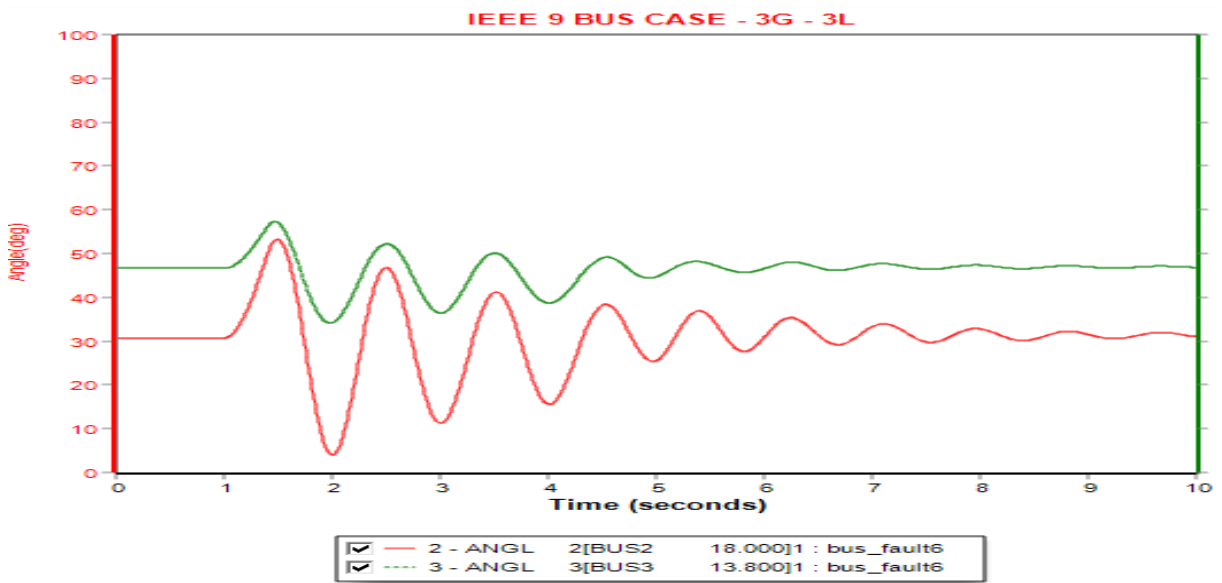


Figure 5.14 - Angle plot of all generators for a fault at bus 6

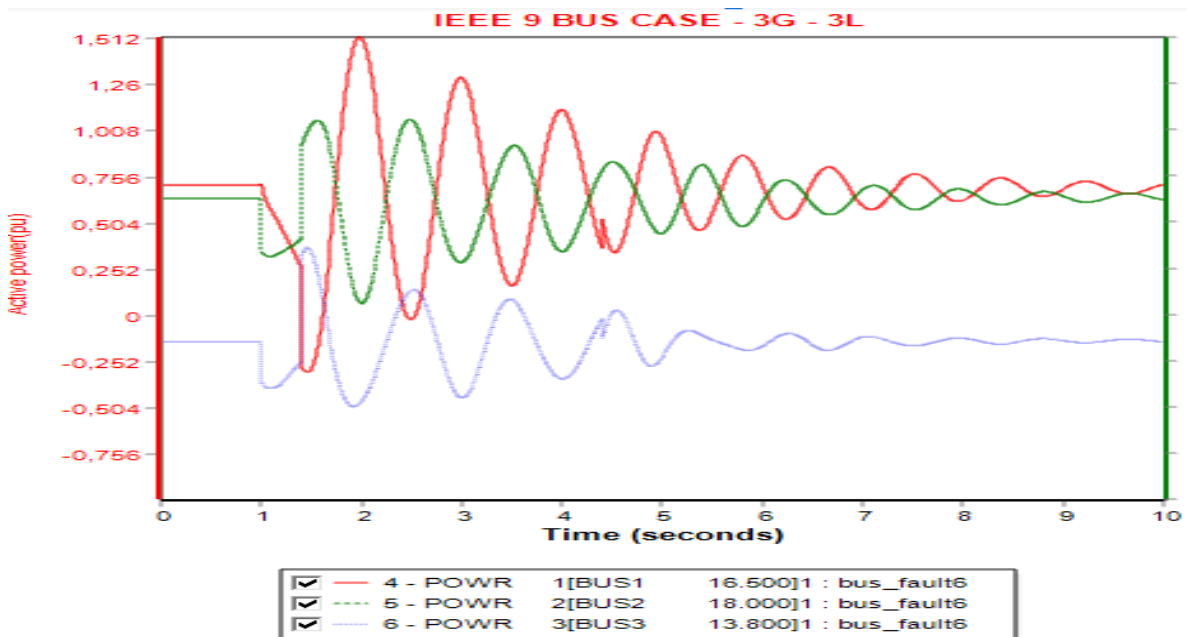


Figure 5.15 - Active power output variation of all generators for fault at bus 6

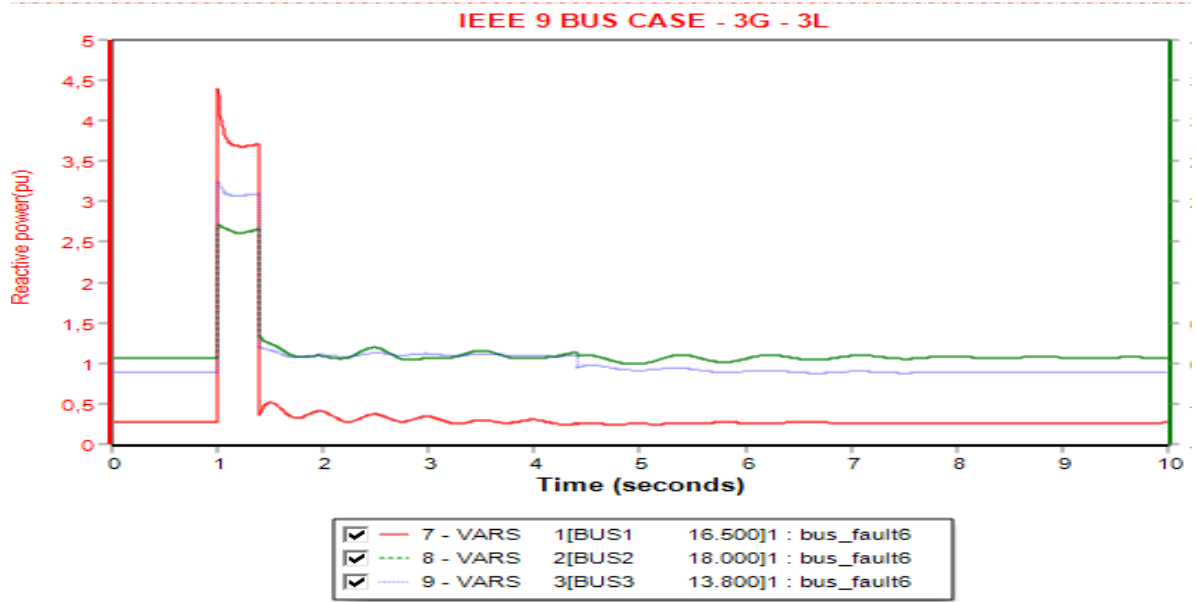


Figure 5.16 - Reactive power output variation of all generators for fault at bus 6

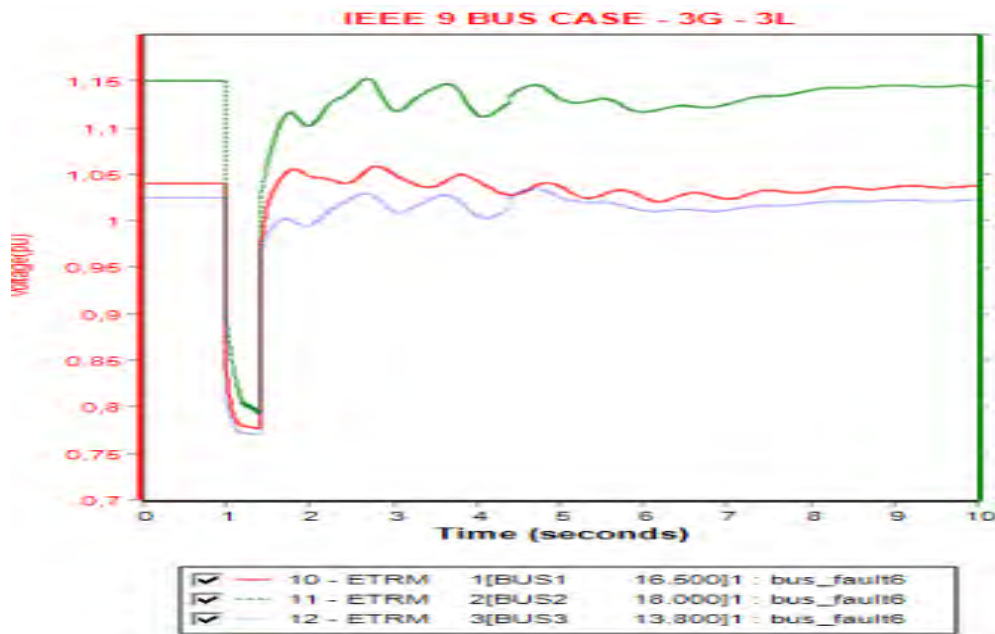


Figure 5.17 - Terminal voltage output variation of all generators for fault at bus 6



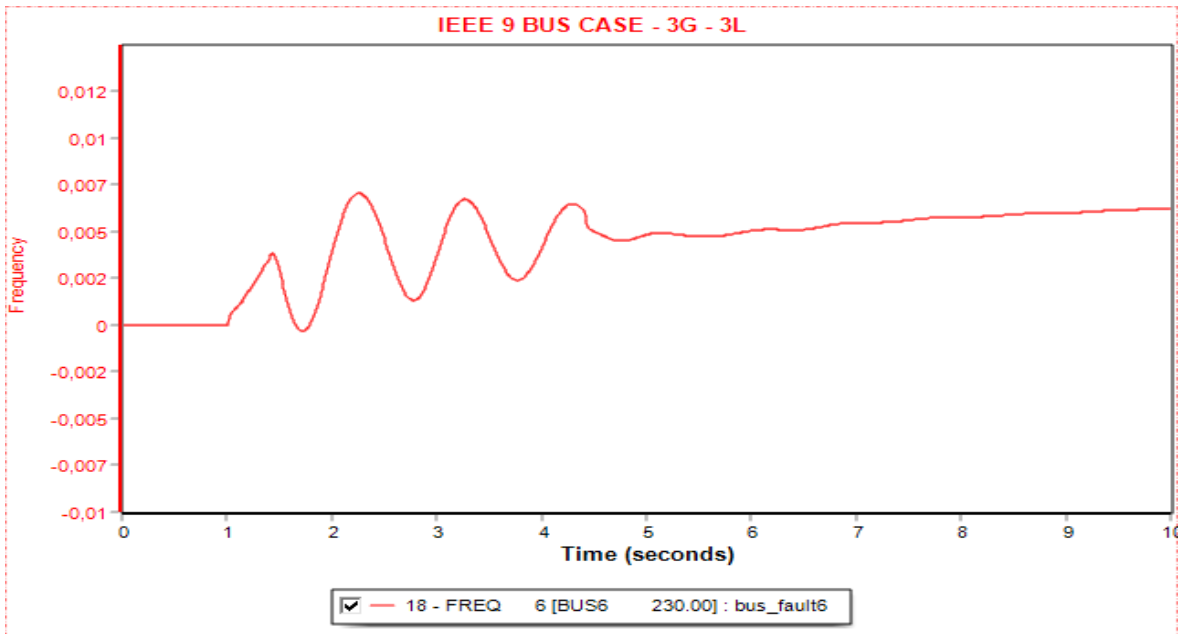


Figure 5.18 - Frequency output variation of bus 6 for fault at bus 6

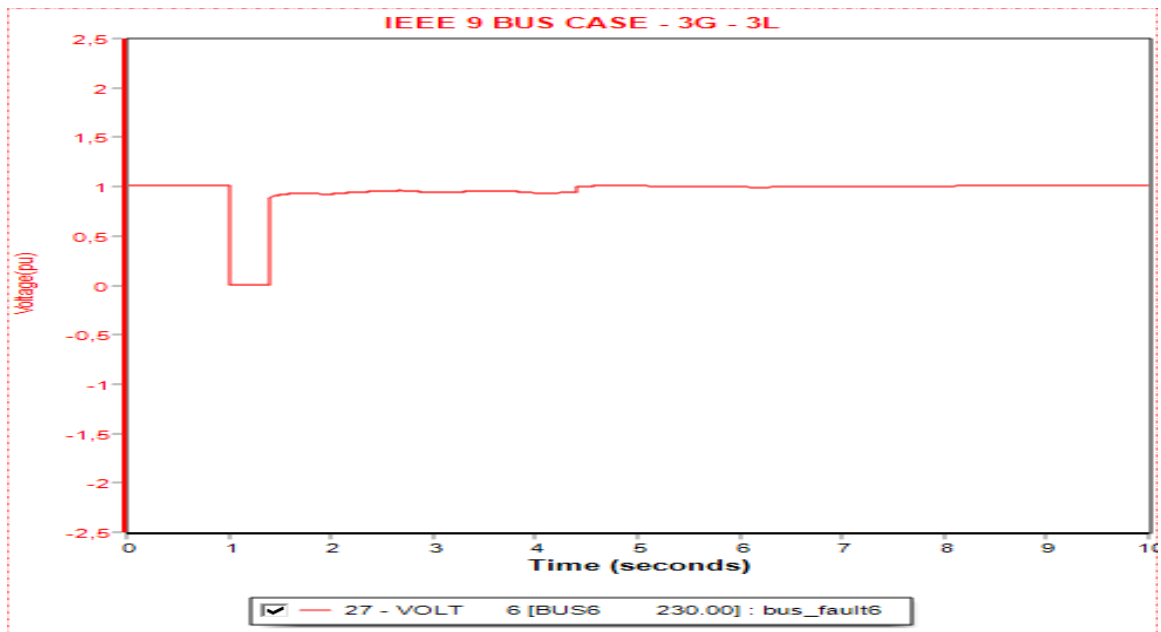


Figure 5.19 - Voltage output variation of bus 6 for fault at bus 6

Stable Case D: 3-L-G Fault at Bus 7

In this case, the critical clearing time is evaluated to 100 ms (6 cycles). Figure 5.20 illustrates the relative angle plot of generator 2 and 3 with regard to generator 1. Figure 5.21 illustrates the active power output of the all 3 machines. The maximum swing angle of generator 2 is

64 while generator's is 55. Figure 5.22 demonstrates the reactive power output of all the 3 generators and Figure 5.23 demonstrates the terminal voltage output variation of all generators for a fault at bus 7. Figure 5.24 illustrates the frequency output variation of bus 7 and Figure 5.25 shows the voltage output variation of bus 7 for fault at bus 7.

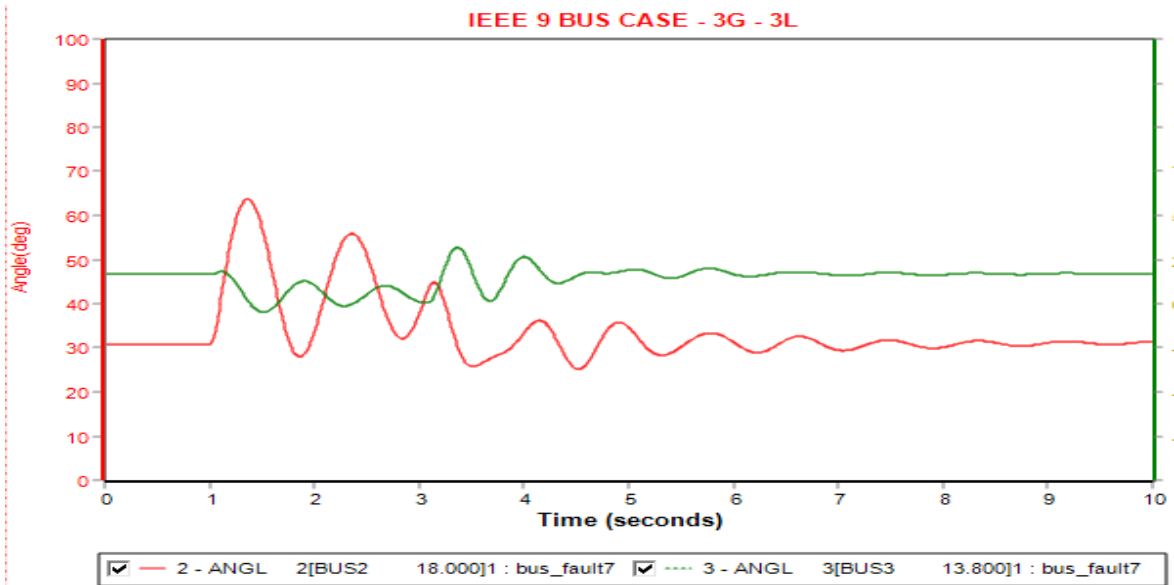


Figure 5.20 - Angle plot of all generators for a fault at bus 7

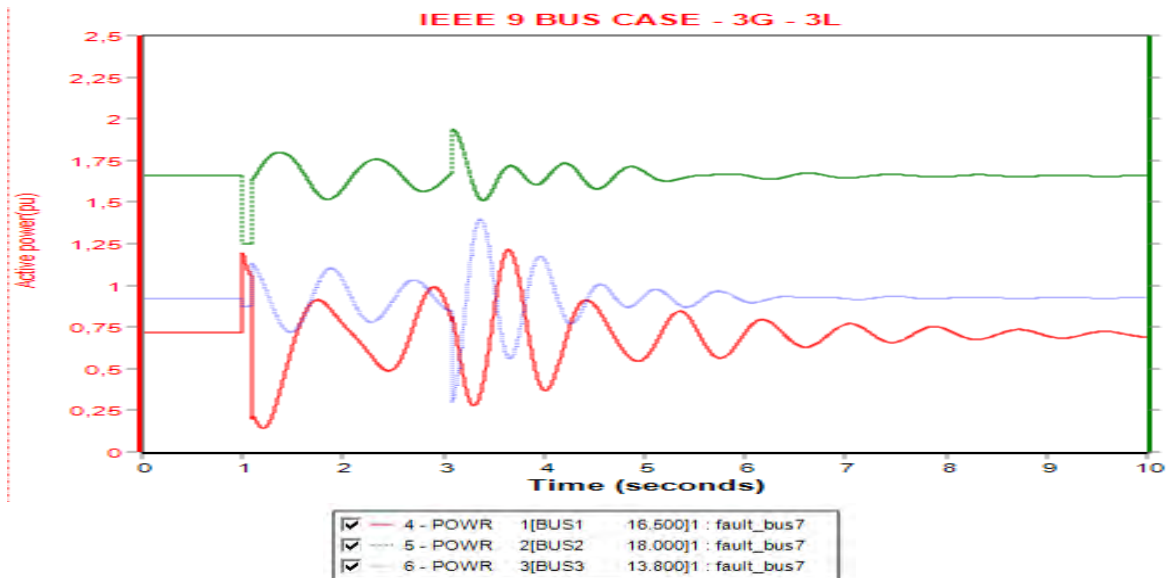


Figure 5.21 - Active power output variation of all generators for fault at bus 7

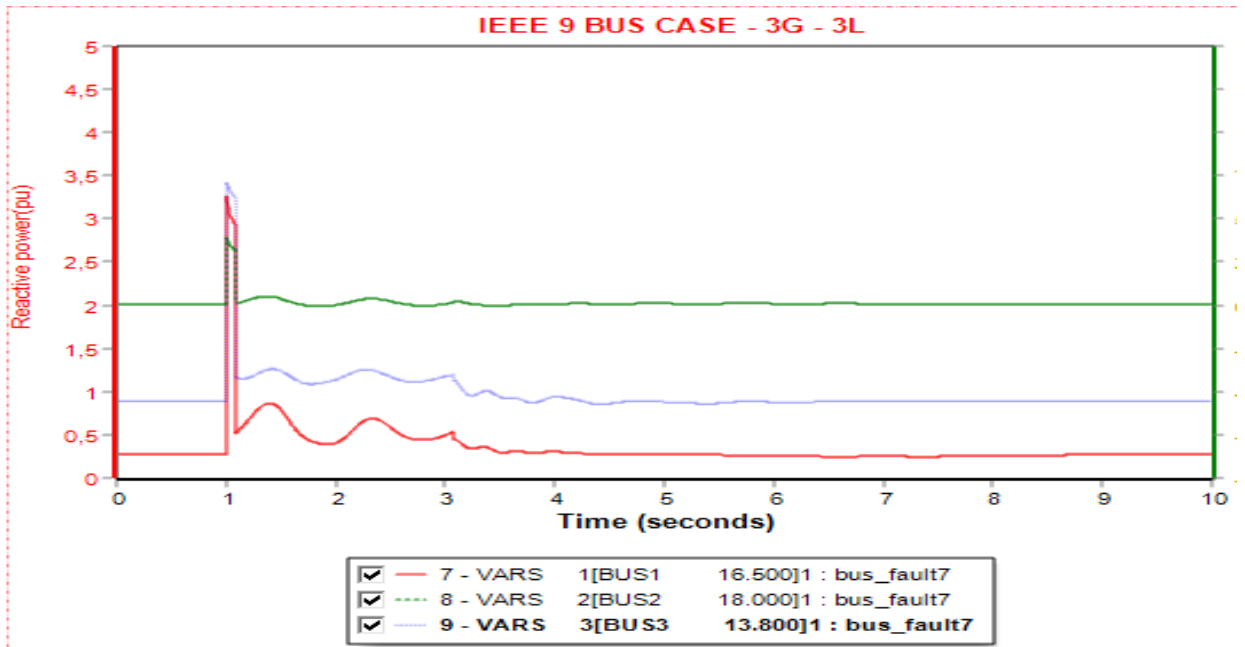


Figure 5.22 - Reactive power output variation of all generators for fault at bus 7

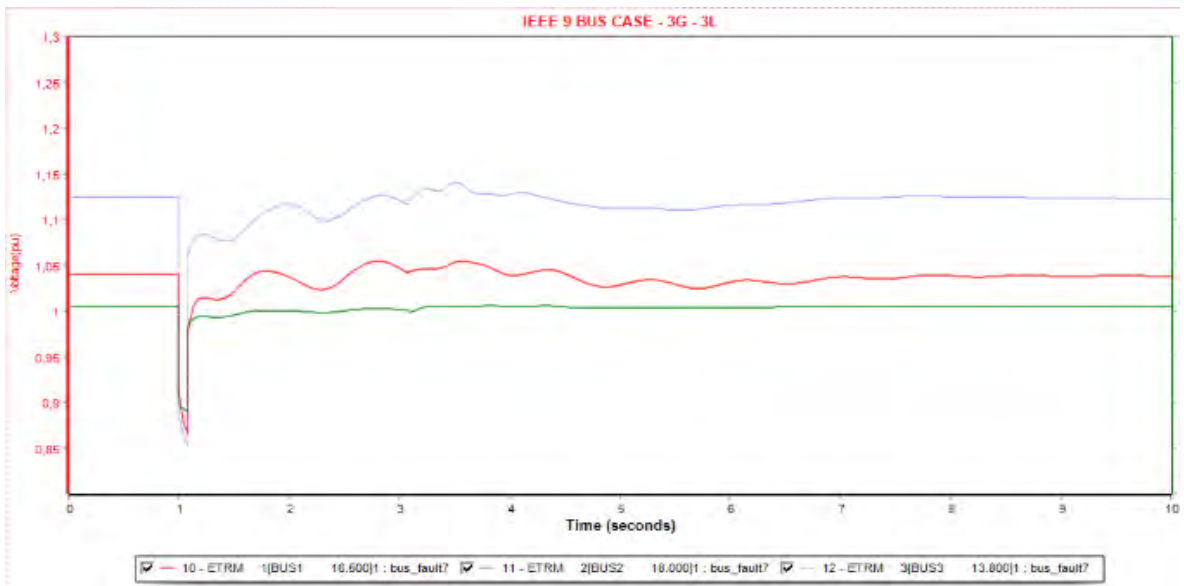


Figure 5.23 - Terminal voltage output variation of all generators for fault at bus 7

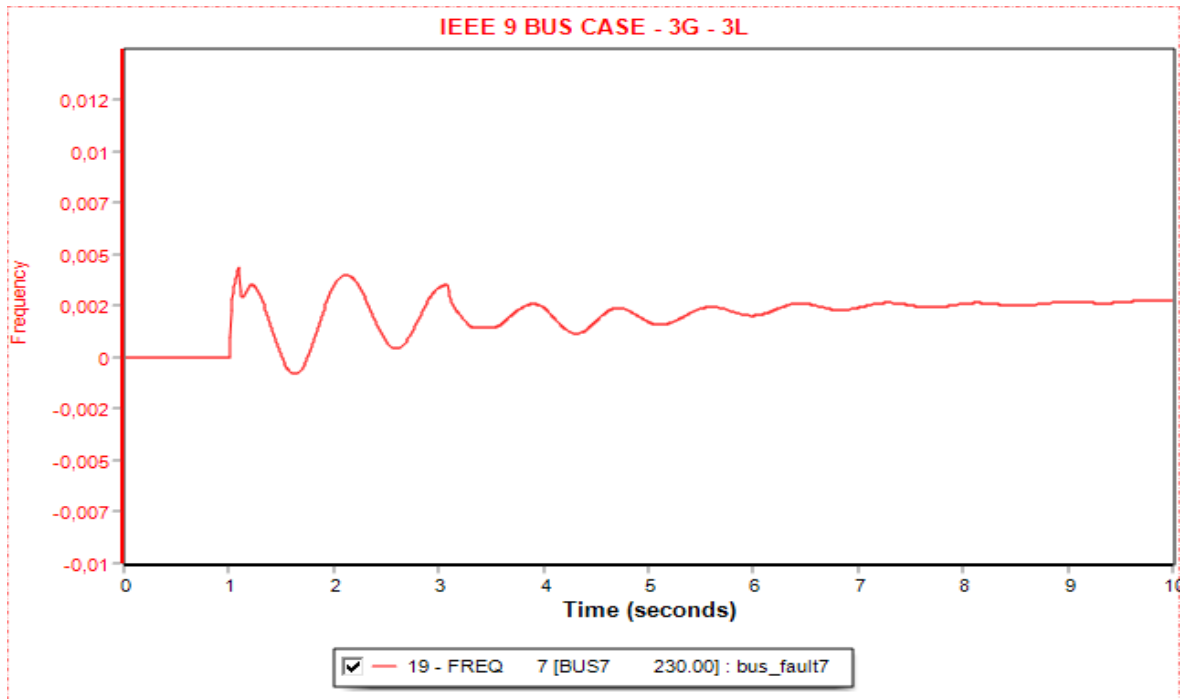


Figure 5.24 - Frequency output variation of bus 7 for fault at bus 7

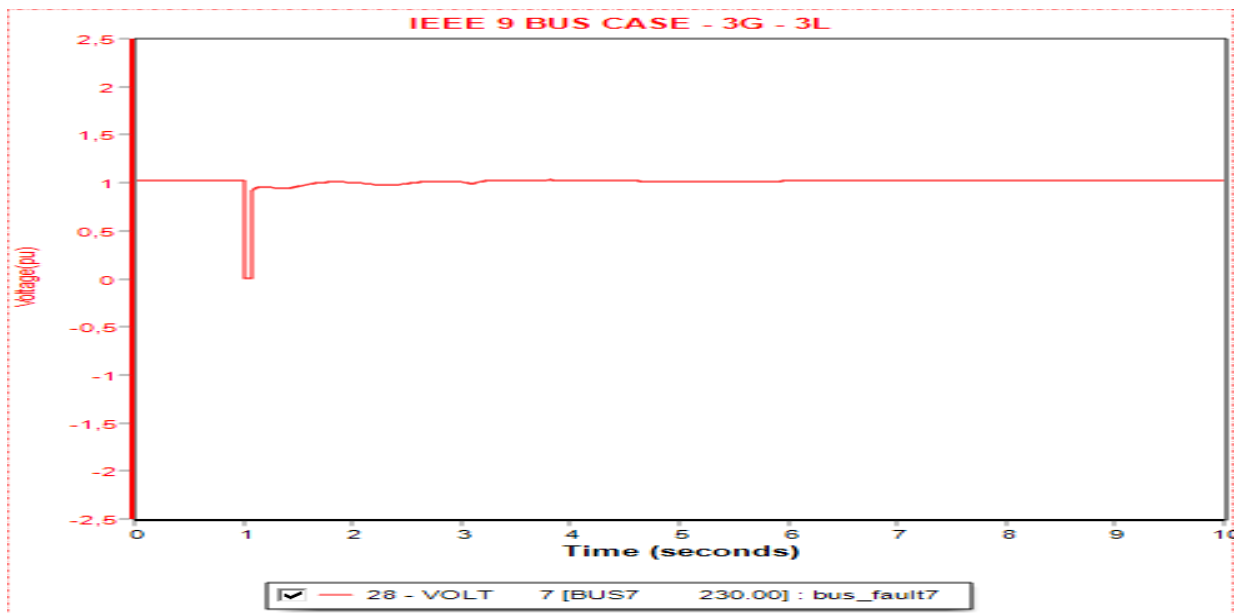


Figure 5.25 – Voltage output variation of bus 7 for fault at bus 7

Stable Case E: 3-L-G Fault at Bus 8

In this case, the critical clearing time is evaluated to 250 ms (15 cycles). Figure 5.26 illustrates the relative angle plot of generator 2 and 3 with regard to generator 1. Figure 5.27 demonstrates the active power output of all 3 generators. The maximum swing angle of

generator 2 is 68 while generator's 3 is 71 degrees. Figure 5.28 illustrates the reactive power output of all the 3 generators and Figure 5.29 demonstrates the terminal voltage output variation of all generators for a fault at bus 8. Figure 5.30 illustrates the frequency output variation of bus 8 and Figure 5.31 shows the voltage output variation of bus 8 for fault at bus 8.

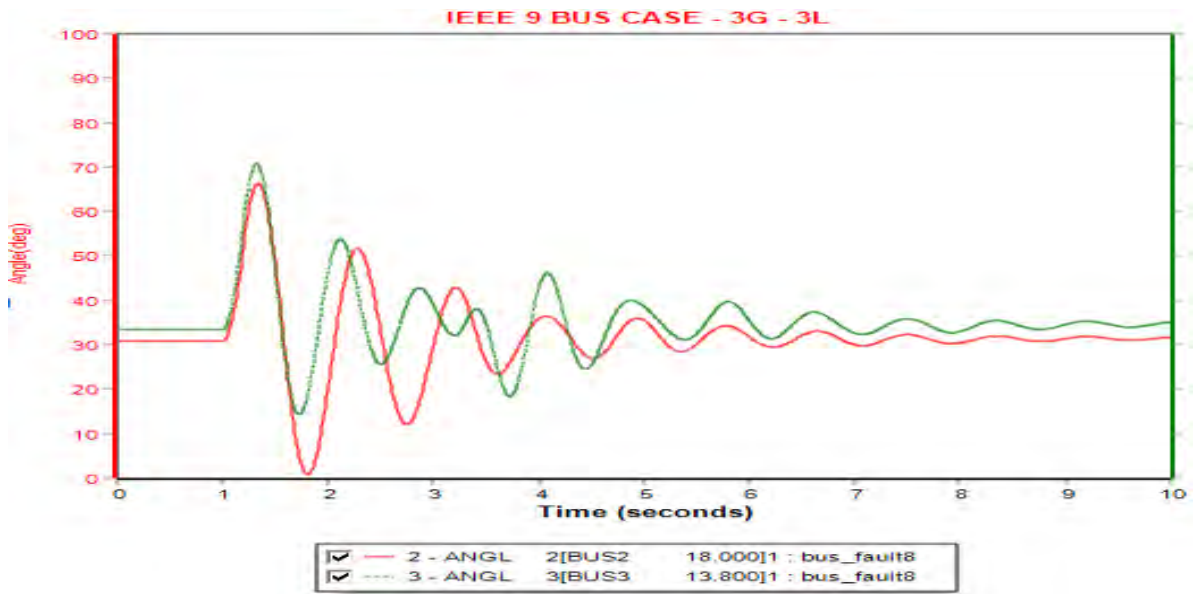


Figure 5.26 - Angle plot of all generators for a fault at bus 8

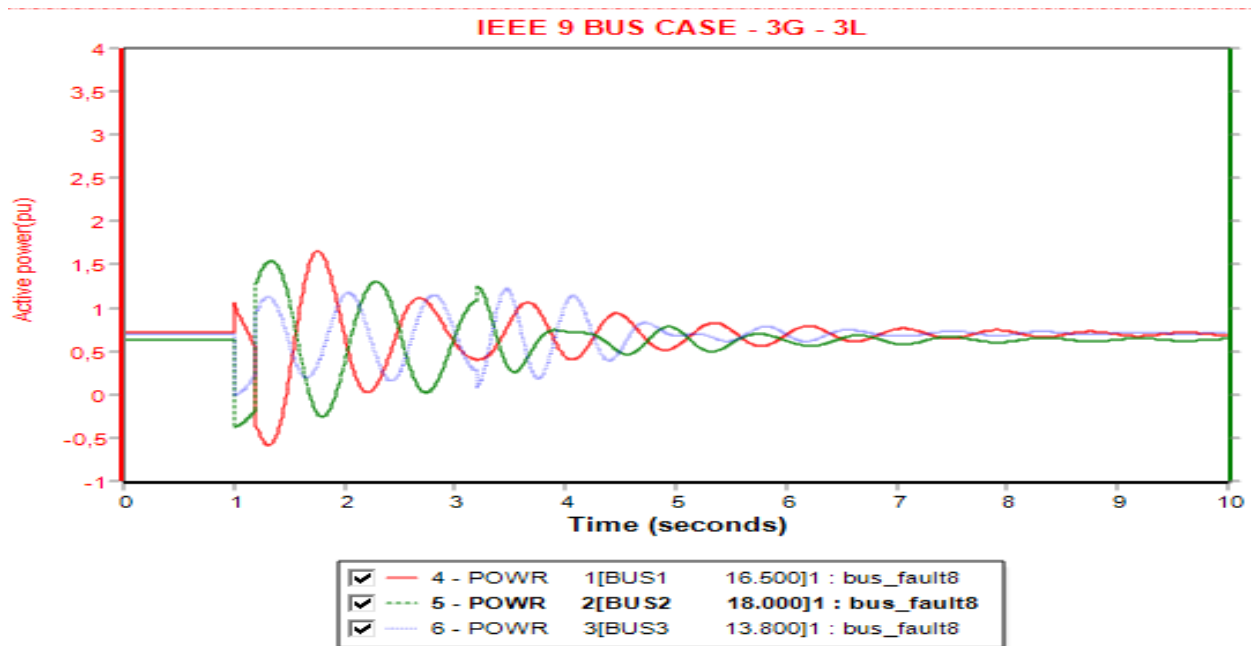


Figure 5.27 - Active power output variation of all generators for fault at bus 8

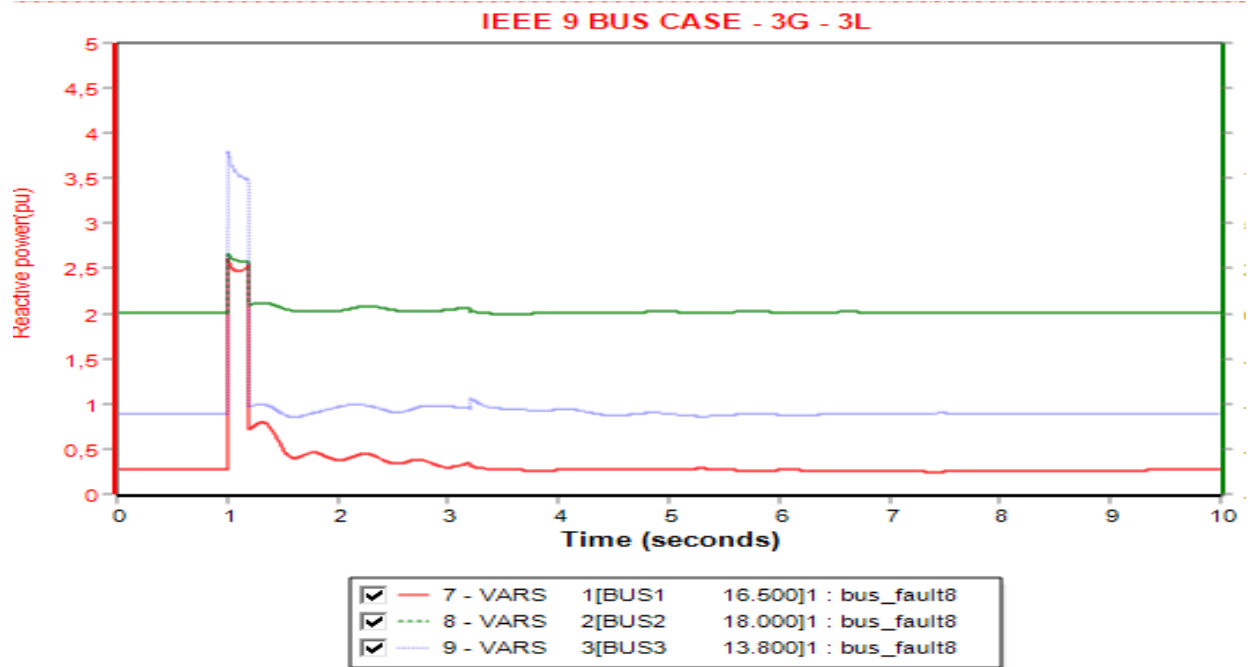


Figure 5.28 - Reactive power output variation of all generators for fault at bus 8

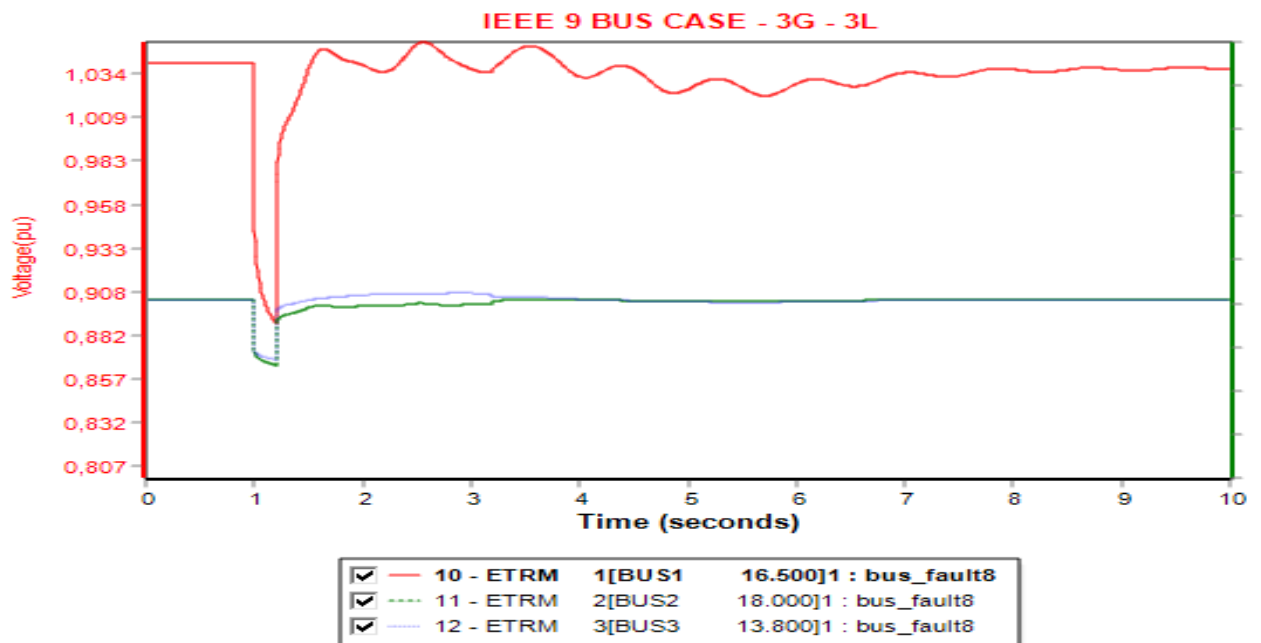


Figure 5.29 - Terminal voltage output variation of all generators for fault at bus 8

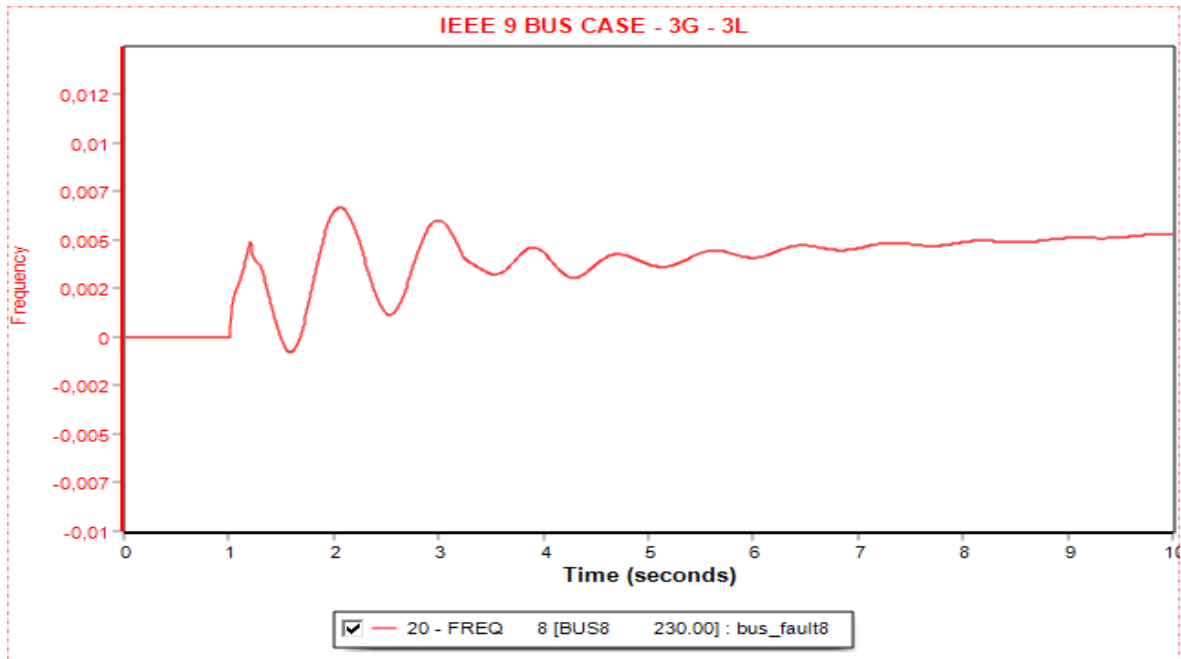


Figure 5.30 - Frequency output variation of bus 8 for fault at bus 8

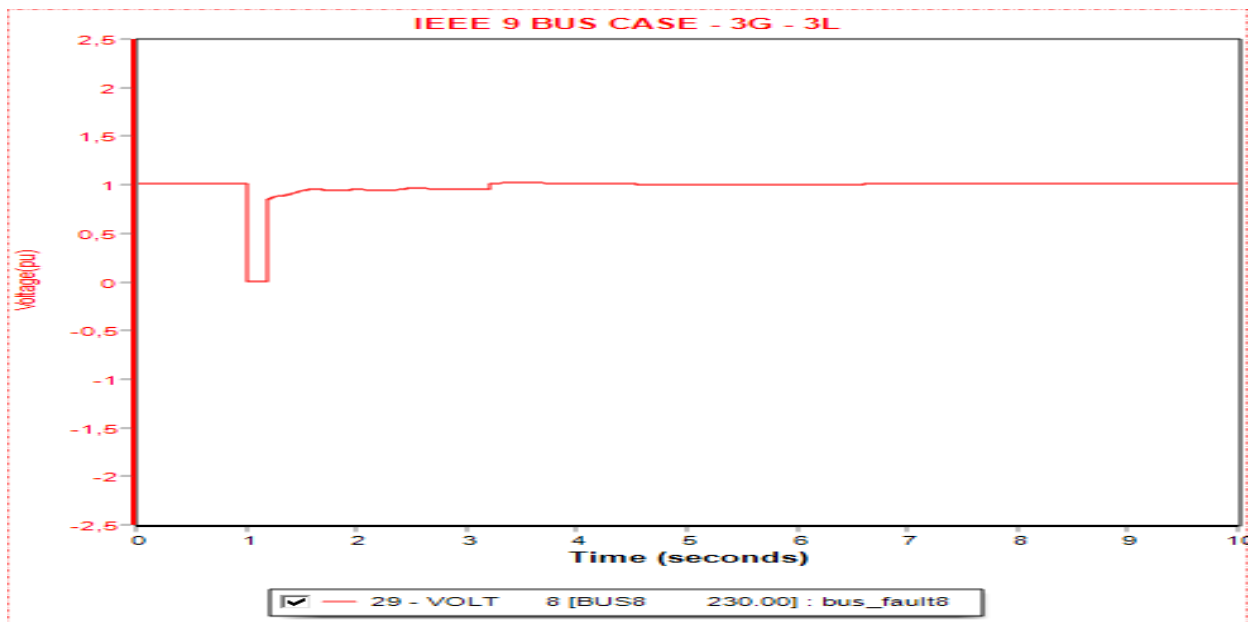


Figure 5.31 – Voltage output variation of bus 8 for fault at bus 8

#### Stable Case F: 3-L-G Fault at Bus 9

In this case, the critical clearing time is evaluated to 200 ms (12 cycles). Figure 5.32 illustrates the relative angle plot of generator 2 and 3 with regard to generator 1. Figure 5.33 illustrates the active power output of all 3 machines. The maximum swing angle of generator

2 is 71 and the maximum swing angle of generator 3 is 72 degrees. Figure 5.34 demonstrates the reactive power output of all the 3 generators and Figure 5.35 demonstrates the terminal voltage output variation of all generators for a fault at bus 9. Figure 5.36 illustrates the frequency output variation of bus 9 and Figure 5.37 shows the voltage output variation of bus 9 for fault at bus 9.

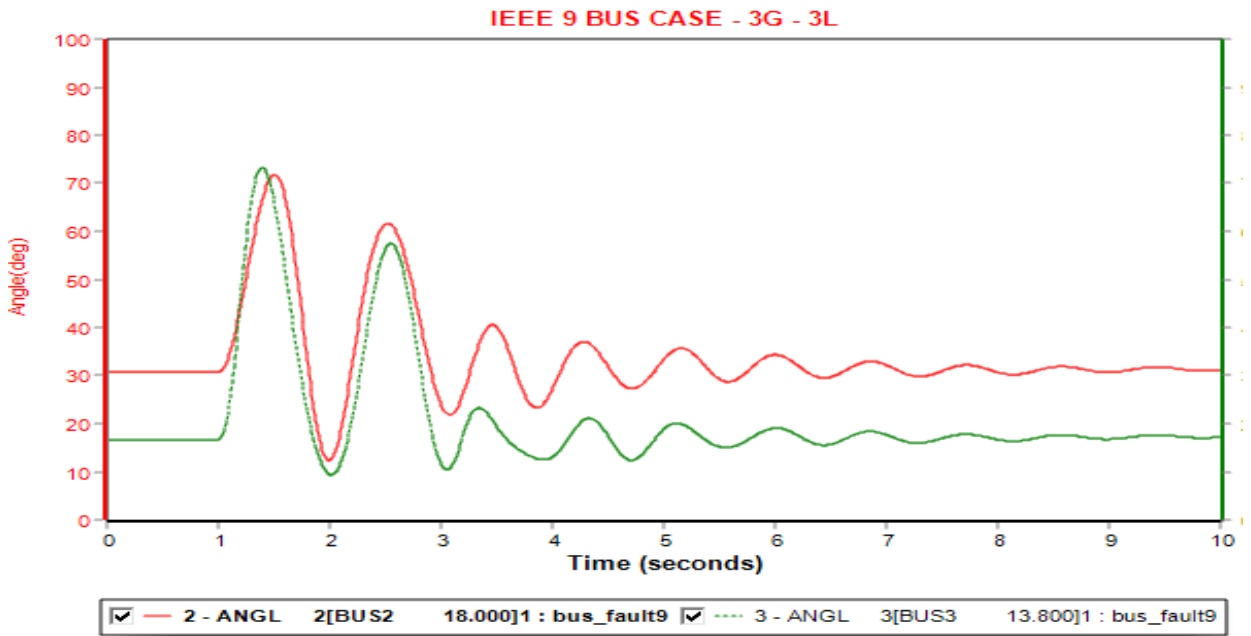


Figure 5.32 - Angle plot of all generators for a fault at bus 9

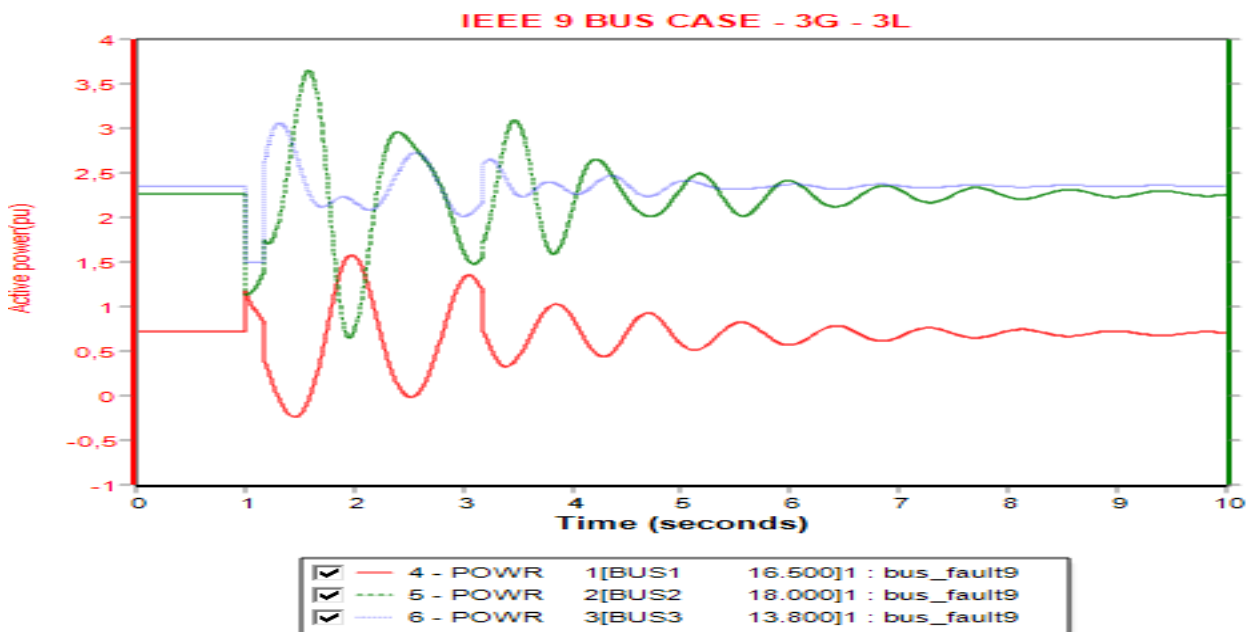


Figure 5.33 - Active power output variation of all generators for fault at bus 9



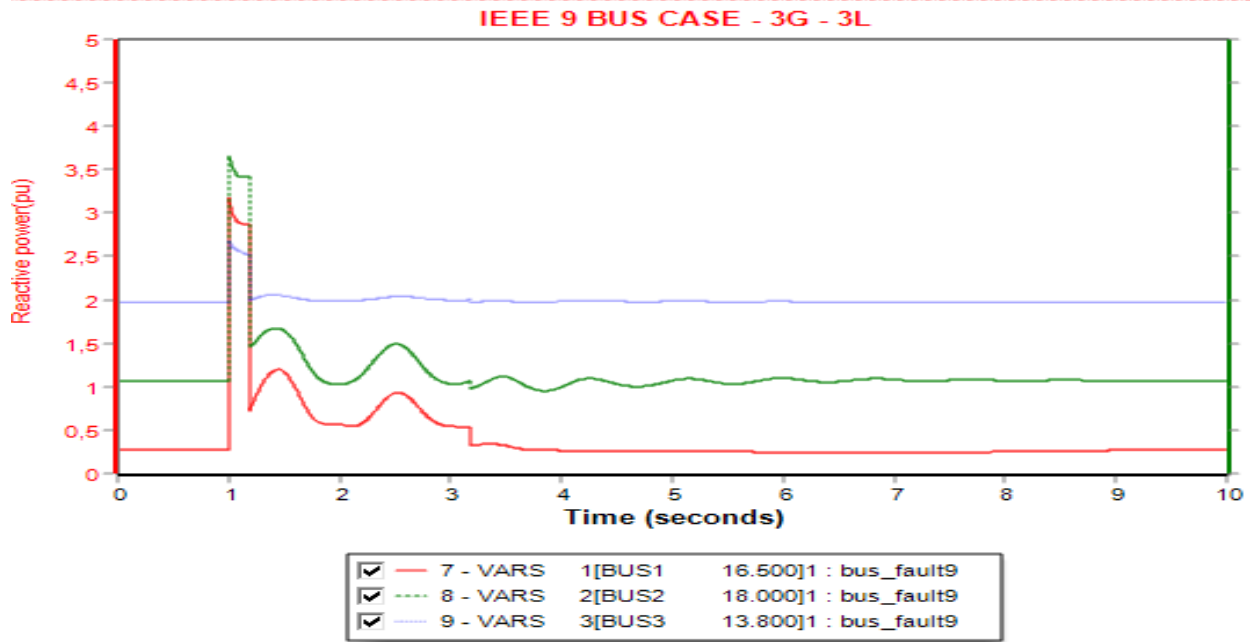


Figure 5.34 - Reactive power output variation of all generators for fault at bus 9

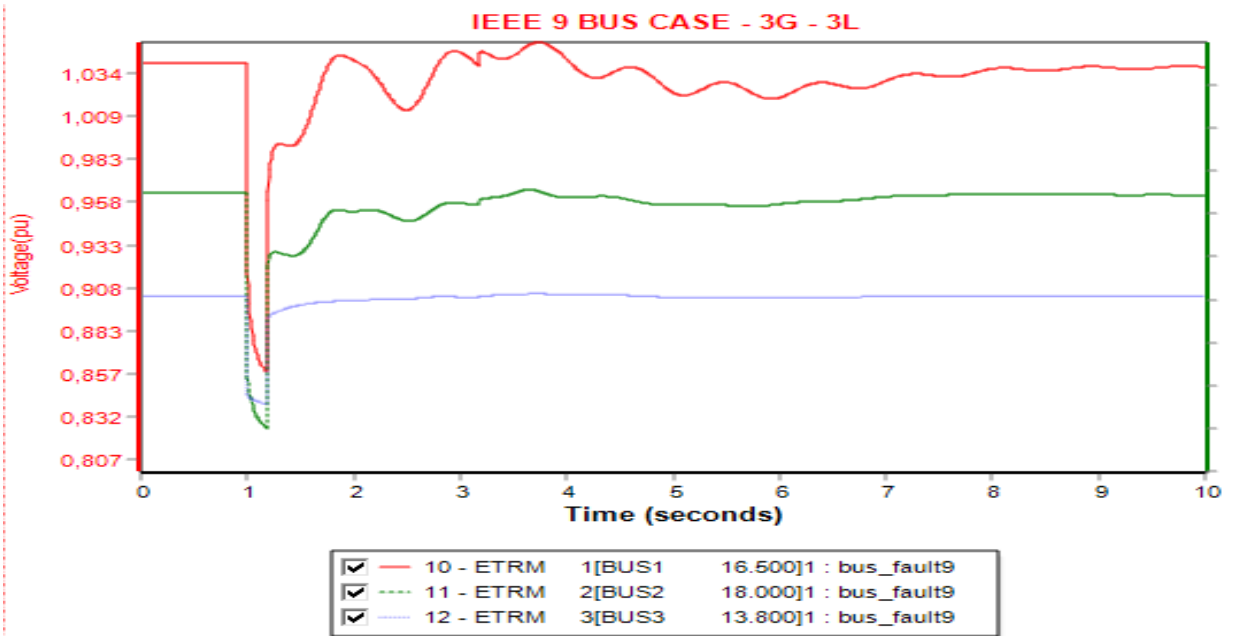


Figure 5.35 - Terminal voltage output variation of all generators for fault at bus 9

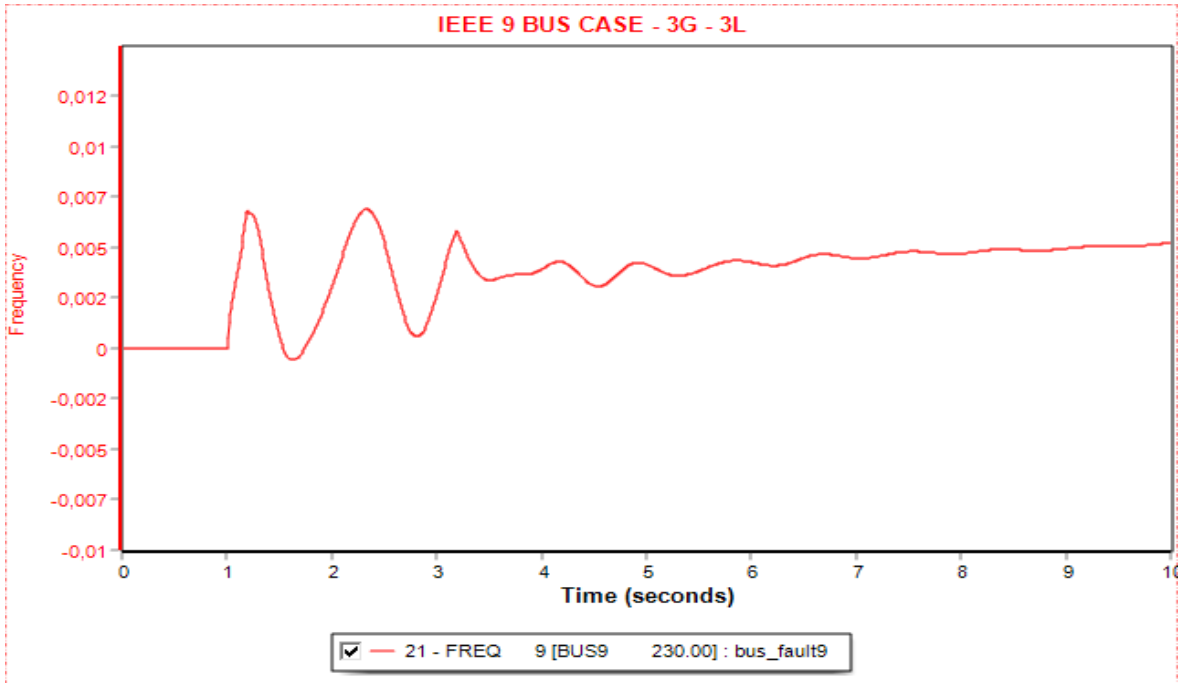


Figure 5.36 - Frequency output variation of bus 9 for fault at bus 9

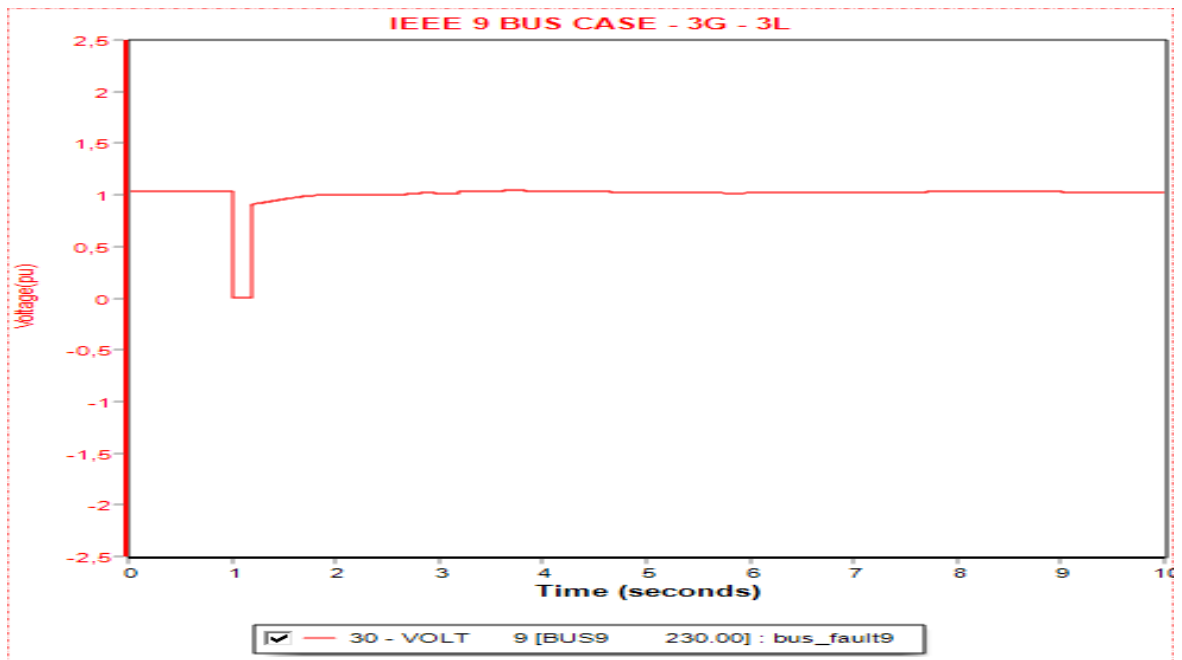


Figure 5.37 – Voltage output variation of bus 9 for fault at bus 9

Table 2 shows the critical clearing time and the maximum angle deviation of generator rotor angles of buses 4,5,6,7,8 and 9.

Table 2 - CCT and maximum angle deviation of generator rotor angles for six case studies in PSS/E.

Bus Fault No	CCT(cycles)	$\Delta\delta_{21}$	$\Delta\delta_{31}$
Bus 4	18	45	35
Bus 5	12	37	42
Bus 6	27	53	57
Bus 7	6	64	55
Bus 8	15	68	71
Bus 9	12	71	72

### 5.2.2 Unstable condition

To fully understand the concept of transient stability, we have to analyze the grid during unstable condition.

The steps followed to examine the unstable cases are:

- 1) The system is initialized.
- 2) One second after the initiation of the system, a bus fault occurs.
- 3) We run the simulation with the fault for a few msec.
- 4) 100 msec after the critical clearing time of each case, the fault is cleared and a line from the faulted bus is tripped.
- 5) The simulation continues for 1000msec after the critical clearing time of each case and then the tripped line closes. The total simulation time is 10 seconds.

#### Unstable Case A: 3-L-G Fault at bus 8

A 3-L-G fault occurs to bus 8 in line 8-9. The rotor angle plot (Figure 5.38) illustrates the complete deflection of generator relative rotor angle which means that the generators are no longer in synchronism. The real and reactive power plot (Figure 5.39 and 5.40) shows undamped variations along with voltage and frequency plots (Figure 5.41, 5.42 and 5.43) which means that the system is now unstable. To avoid such condition, it is important to clear the fault as soon as it gets.

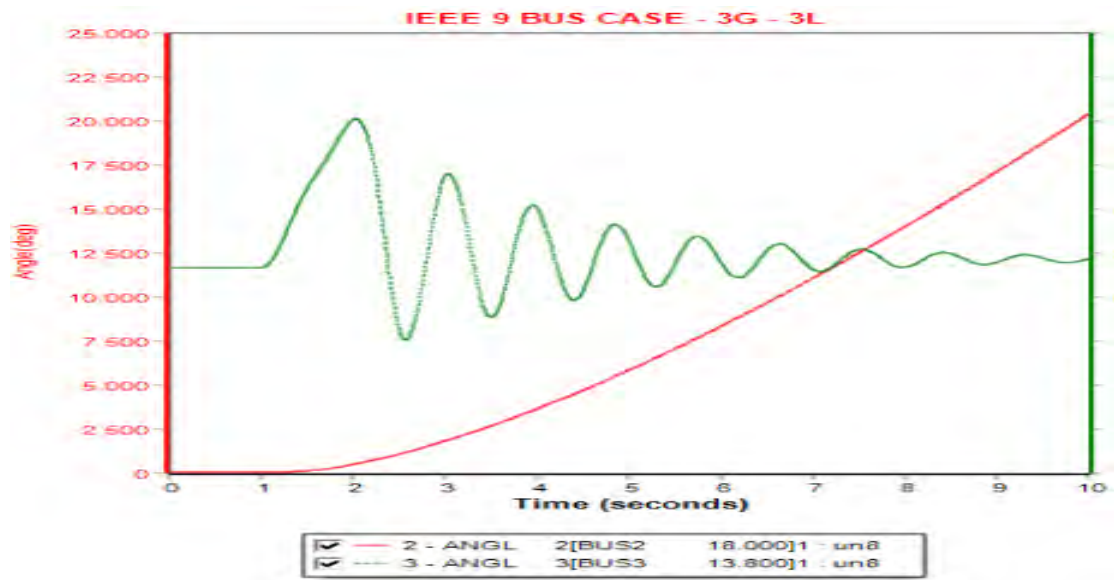


Figure 5.38 - Angle plot of all generators for a fault at bus 8

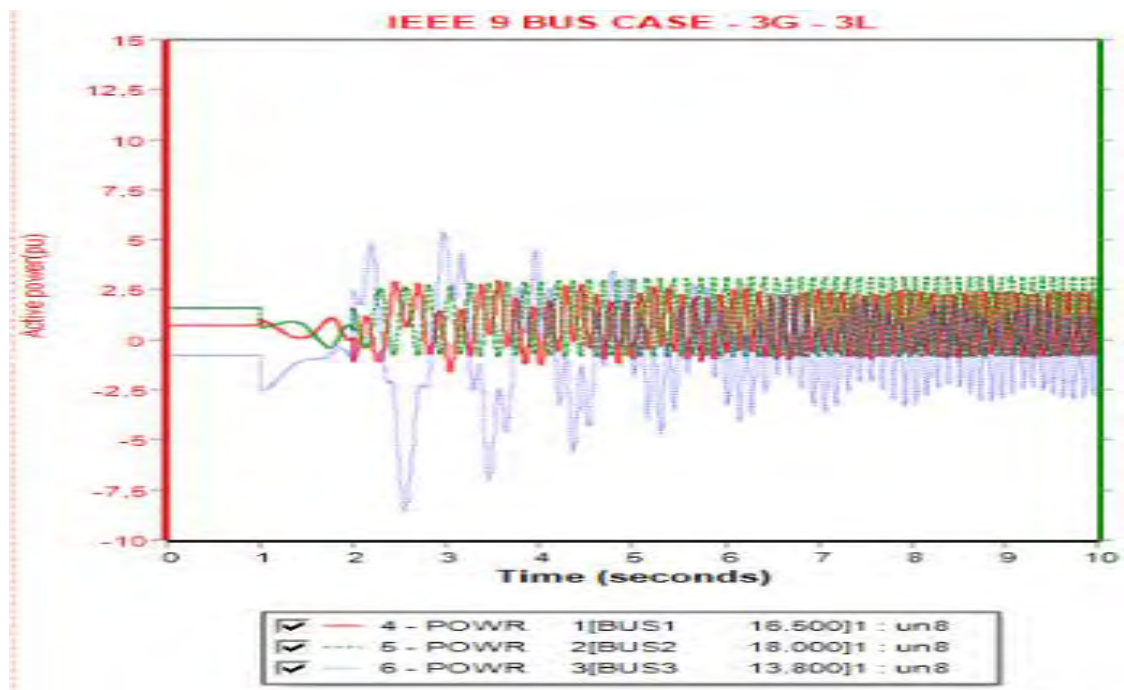


Figure 5.39 - Active power output variation of all generators for fault at bus 8

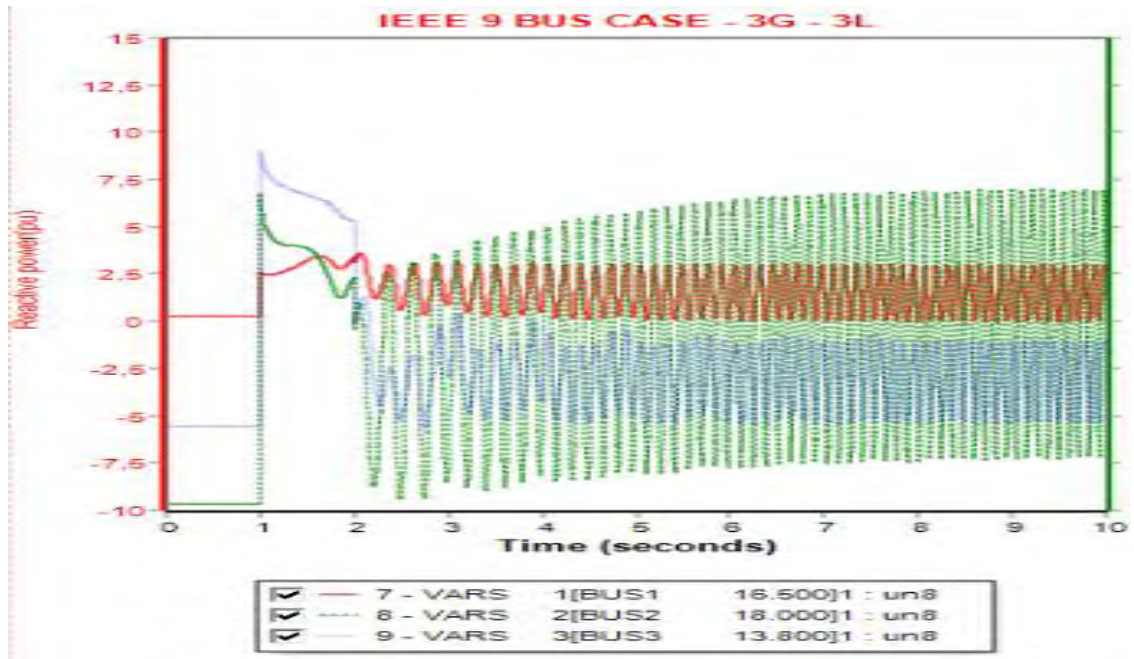


Figure 5.40 - Reactive power output variation of all generators for fault at bus 8

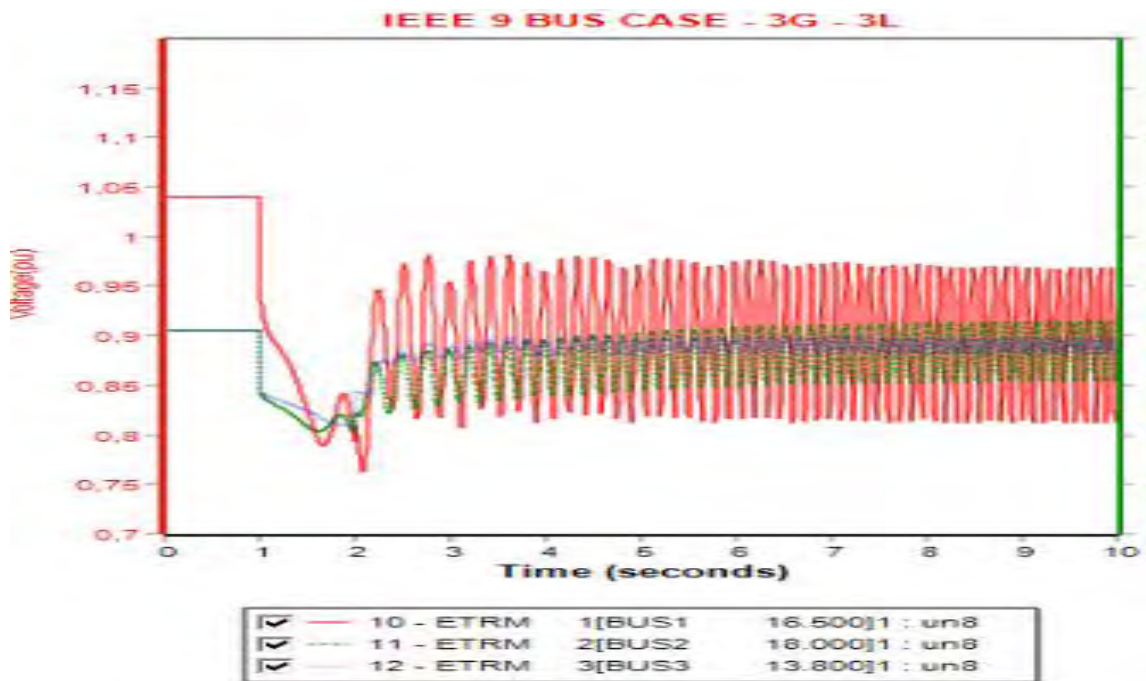


Figure 5.41 - Terminal voltage output variation of all generators for fault at bus 8

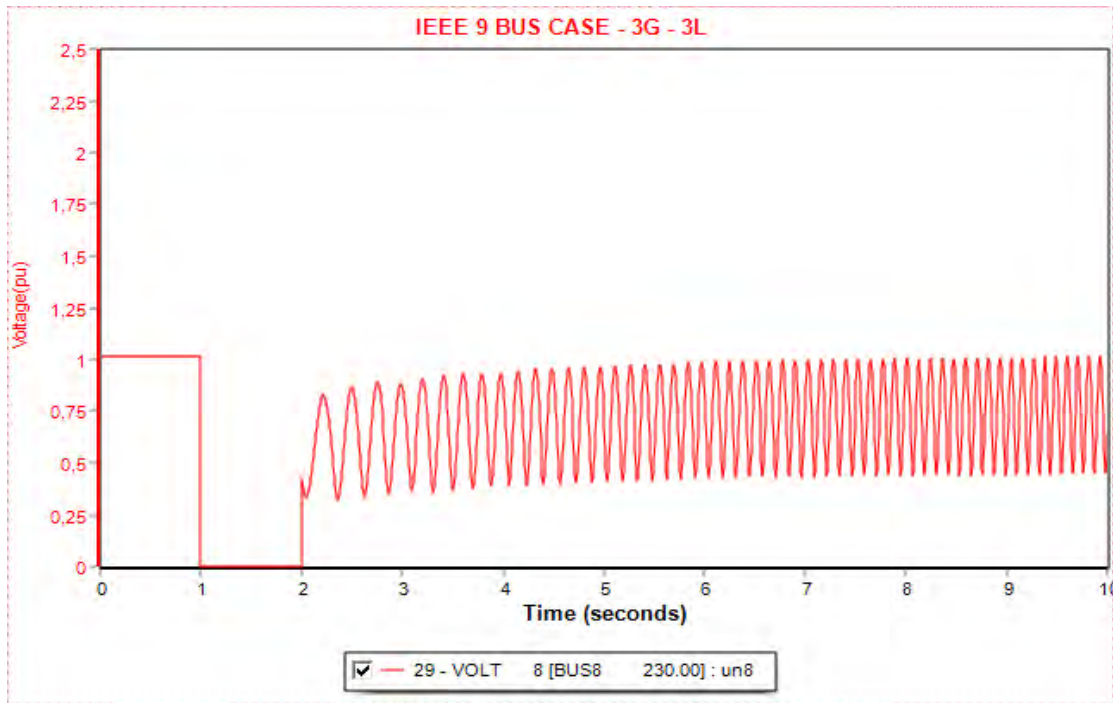


Figure 5.42 - Terminal voltage output variation of bus 8 for fault at bus 8

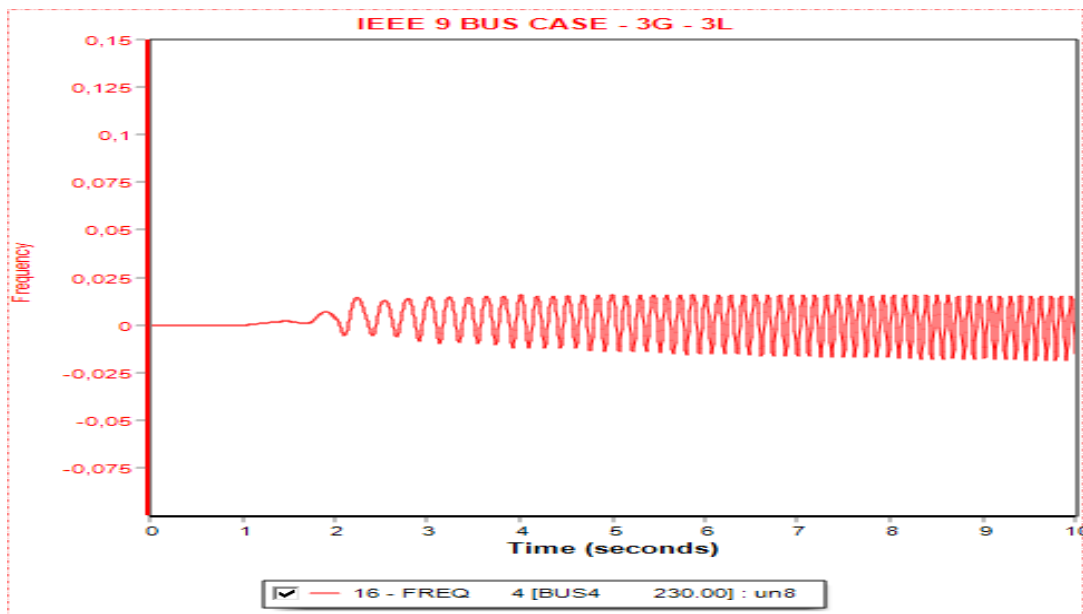


Figure 5.43 – Frequency output variation of bus 8 for fault at bus 8

Unstable Case B: 3-L-G Fault at bus 7

A 3-L-G fault occurs to bus 7 in line 7-8. The rotor angle plot (Figure 5.44) demonstrates the complete deflection of generator relative rotor angle. The real and reactive power plot

(Figure 5.45 and 5.46) illustrates undamped variations along with voltage and frequency plots (Figure 5.47, 5.48 and 5.49).

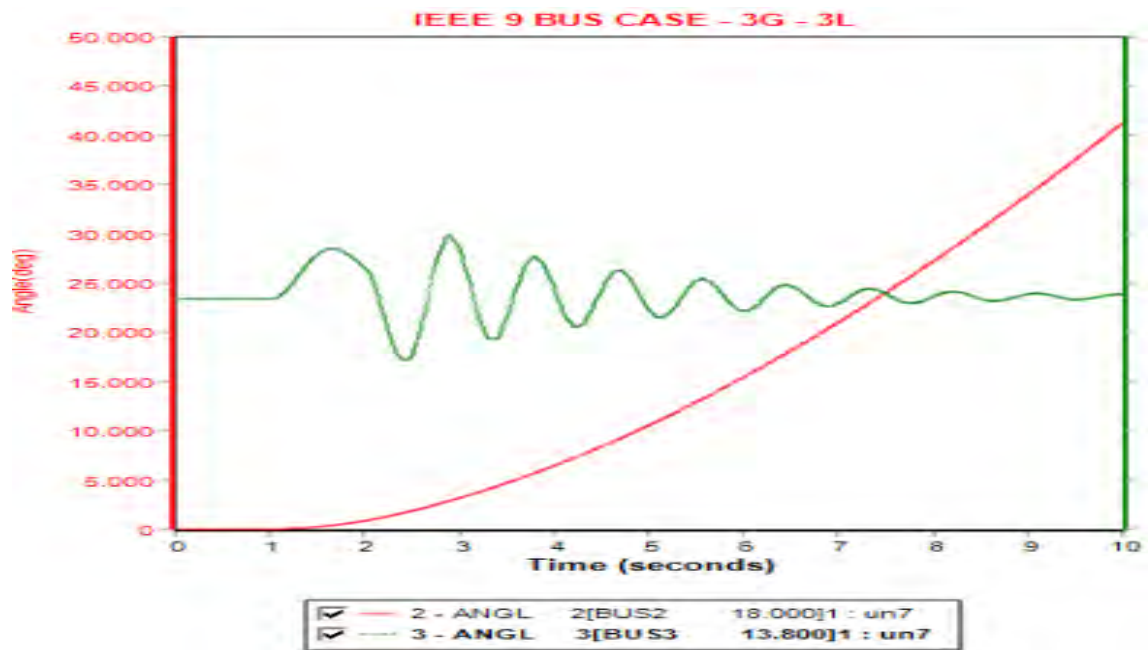


Figure 5.44 - Angle plot of all generators for a fault at bus 7

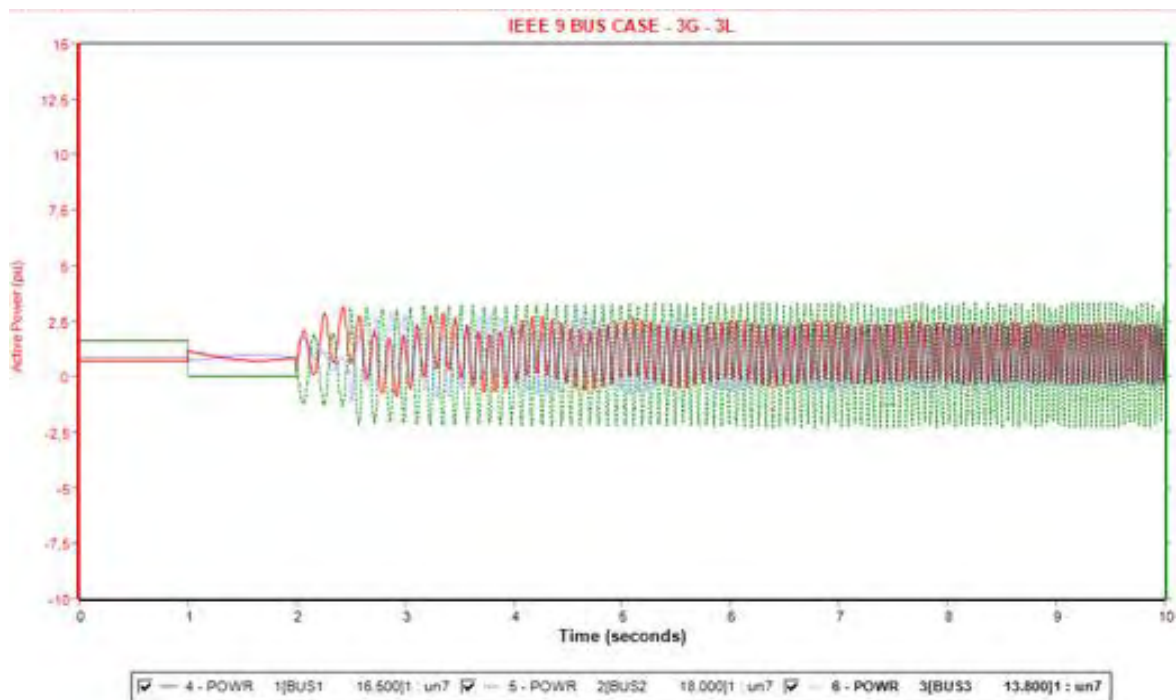


Figure 5.45 - Active power output variation of all generators for fault at bus 7

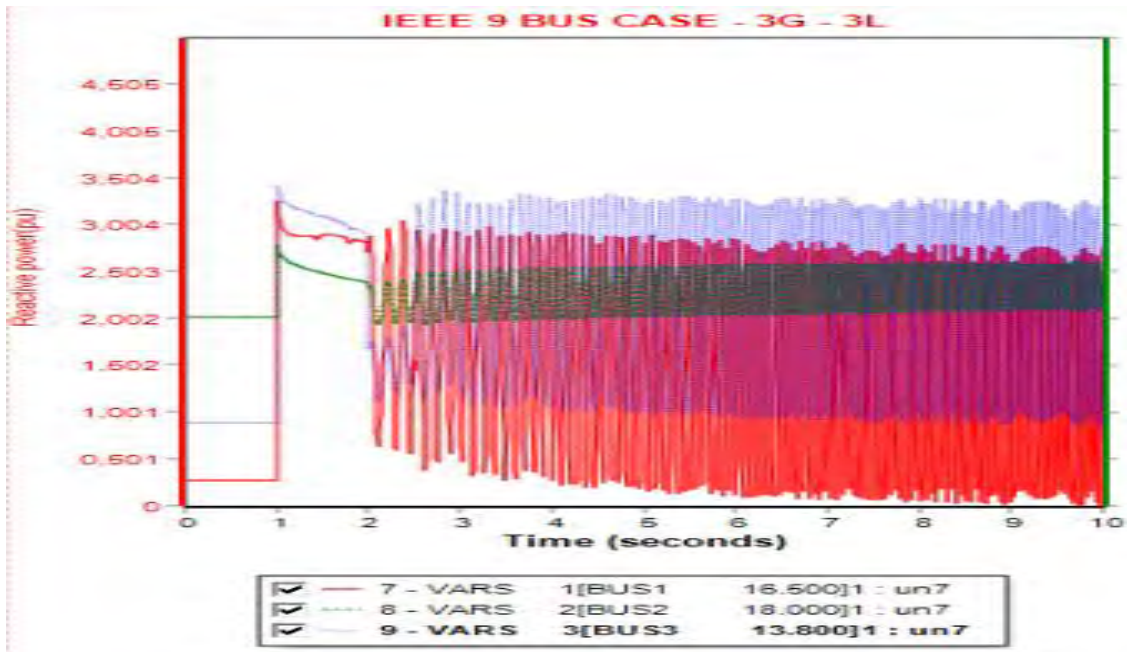


Figure 5.46 - Reactive power output variation of all generators for fault at bus 7

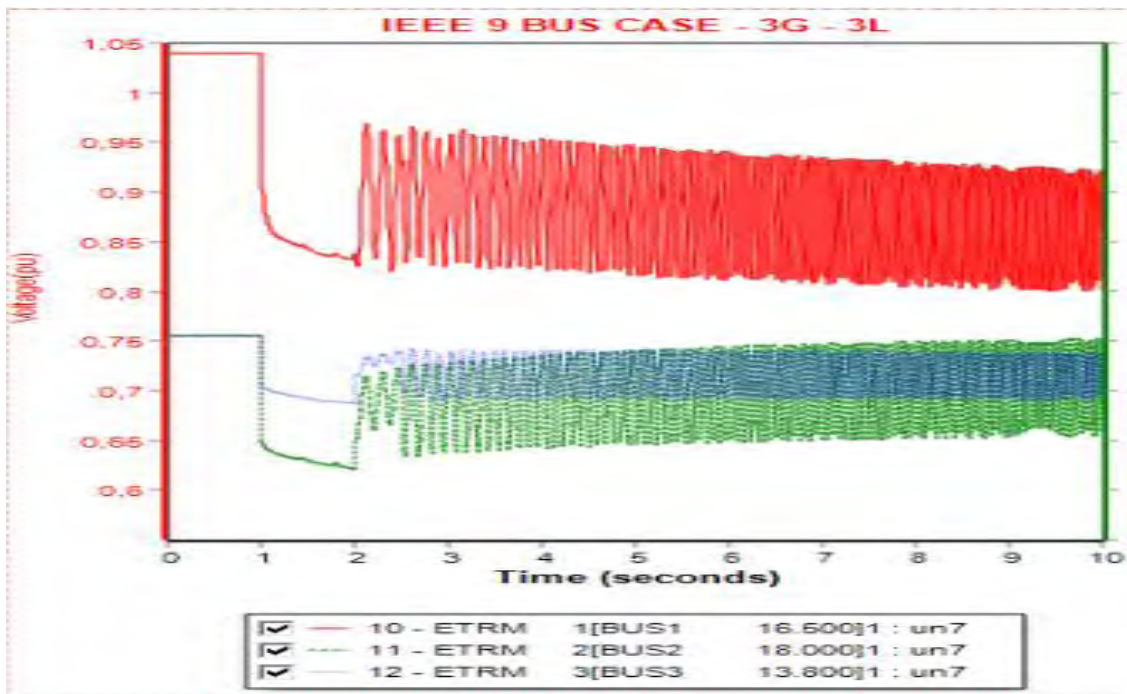


Figure 5.47 - Terminal voltage output variation of all generators for fault at bus 7



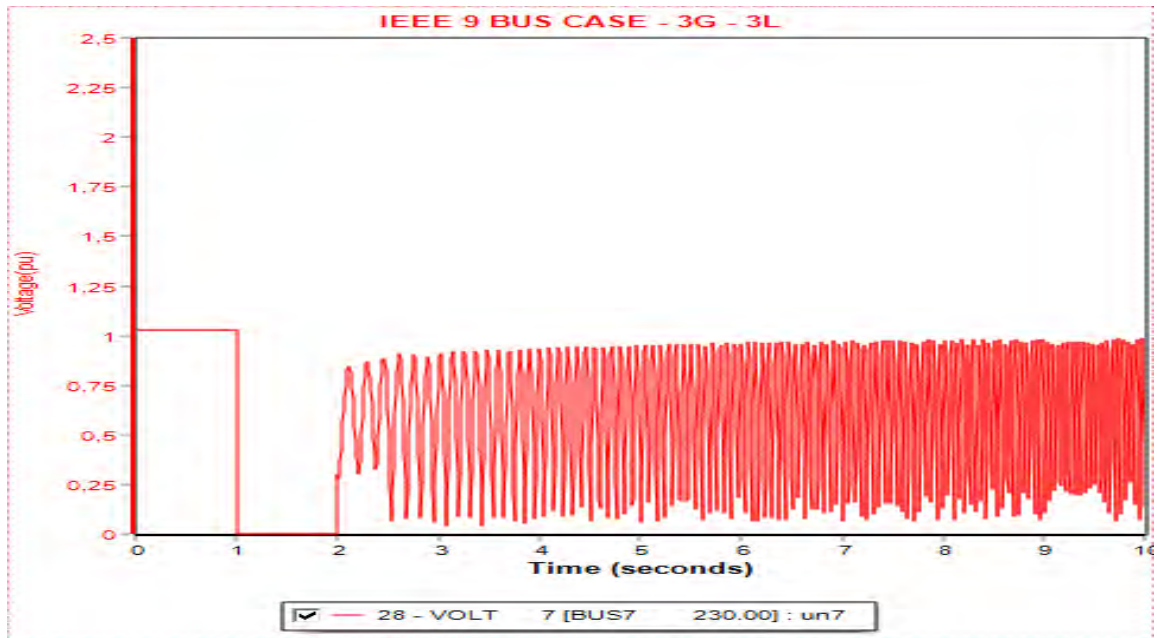


Figure 5.48 - Terminal voltage output variation of bus 7 for fault at bus 7

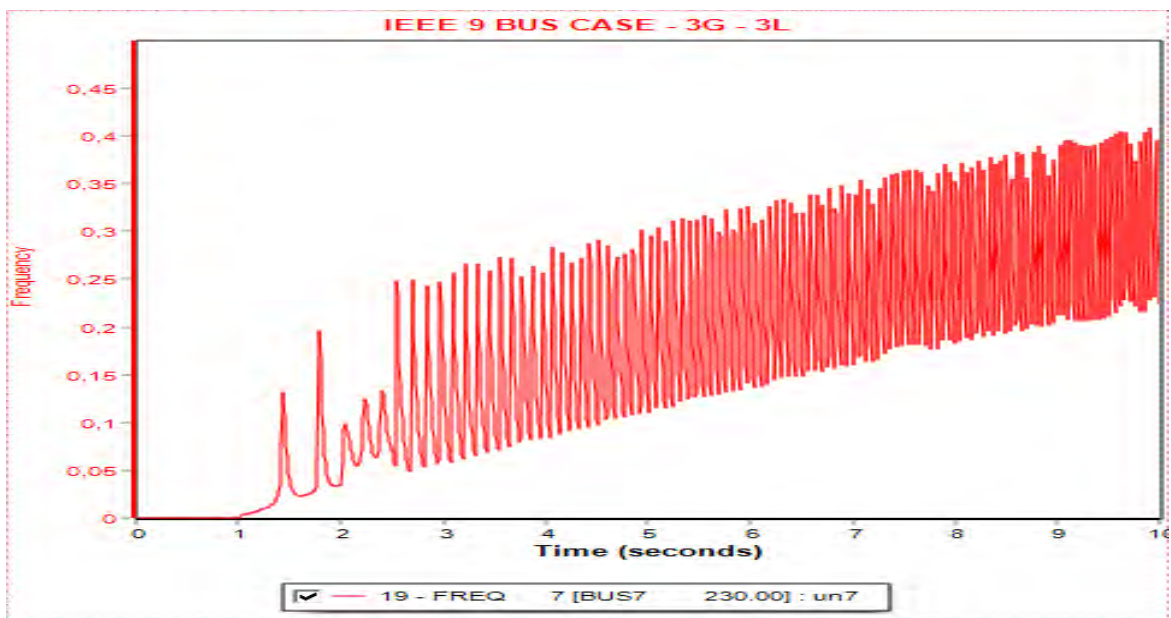


Figure 5.49 – Frequency output variation of bus7 for fault at bus 7

Unstable Case C: 3-L-G Fault at bus 9

A 3-L-G fault occurs to bus 9 in line 9-6. The rotor angle plot (Figure 5.50) reveals complete deflection of generator relative rotor angle. The real and reactive power plot (Figure 5.51 and 5.52) reveals undamped variations along with voltage and frequency plots (Figure 5.53, 5.54 and 5.55).

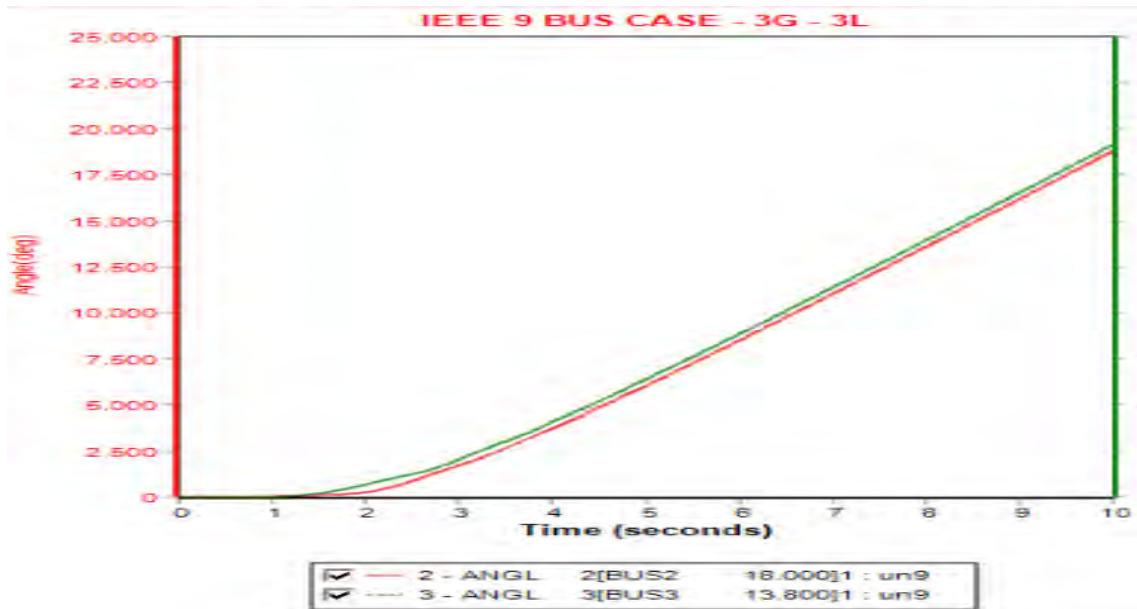


Figure 5.50 - Angle plot of all generators for a fault at bus 9

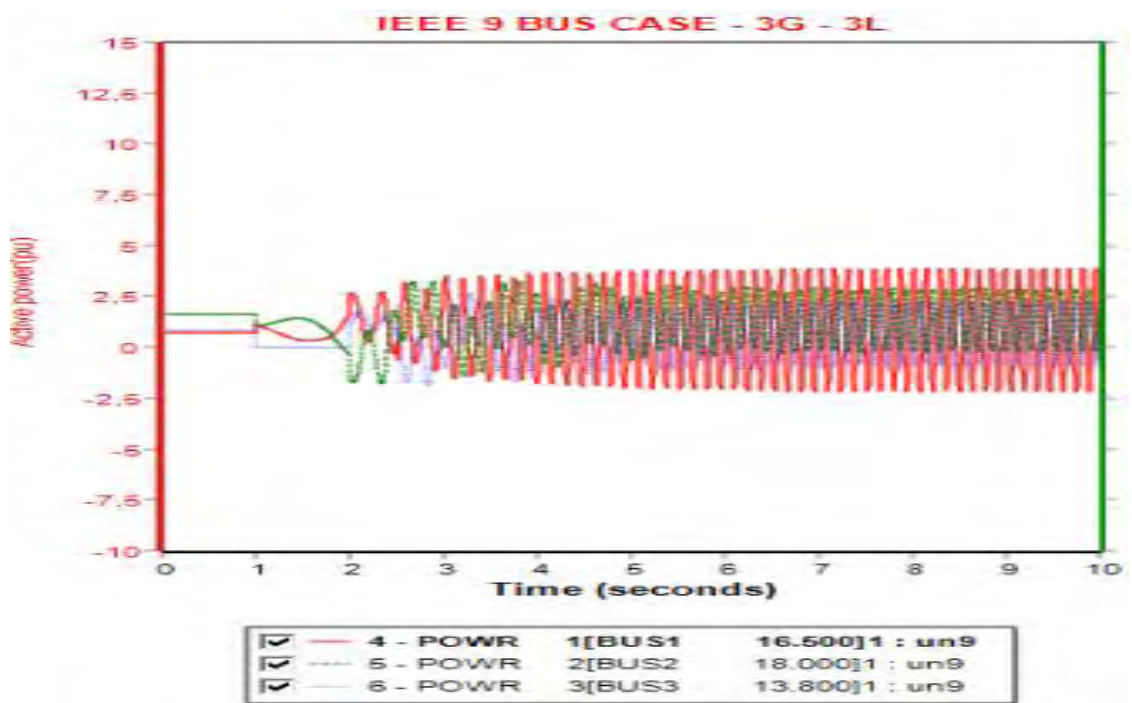


Figure 5.51 - Active power output variation of all generators for fault at bus 9

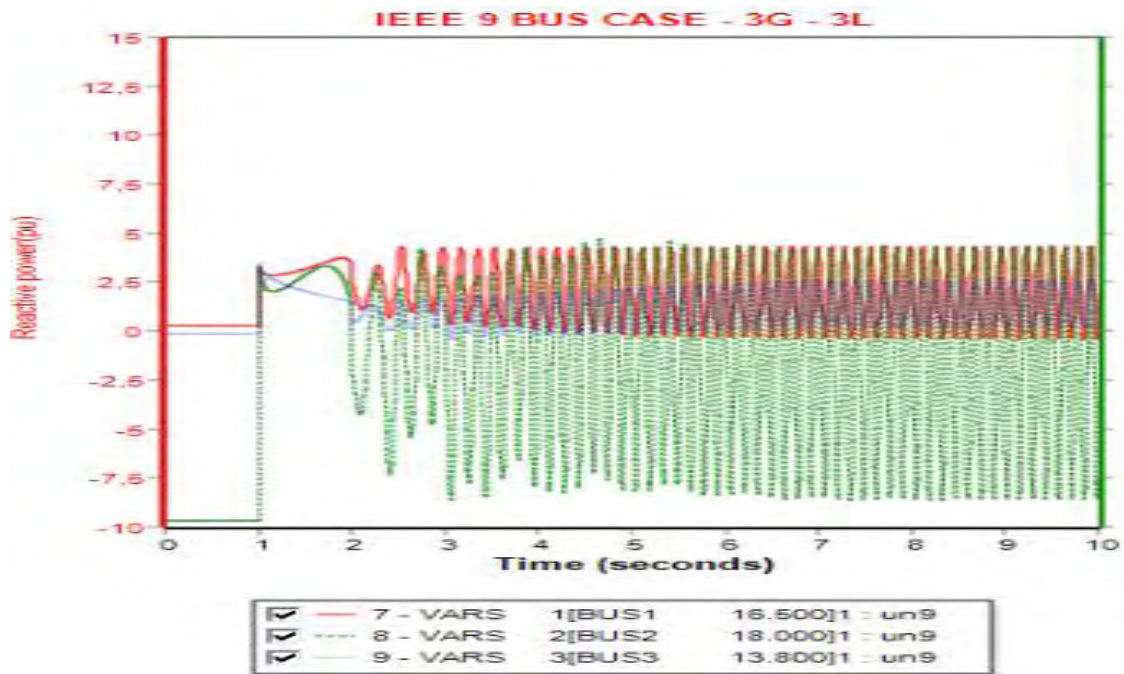


Figure 5.52 - Reactive power output variation of all generators for fault at bus 9

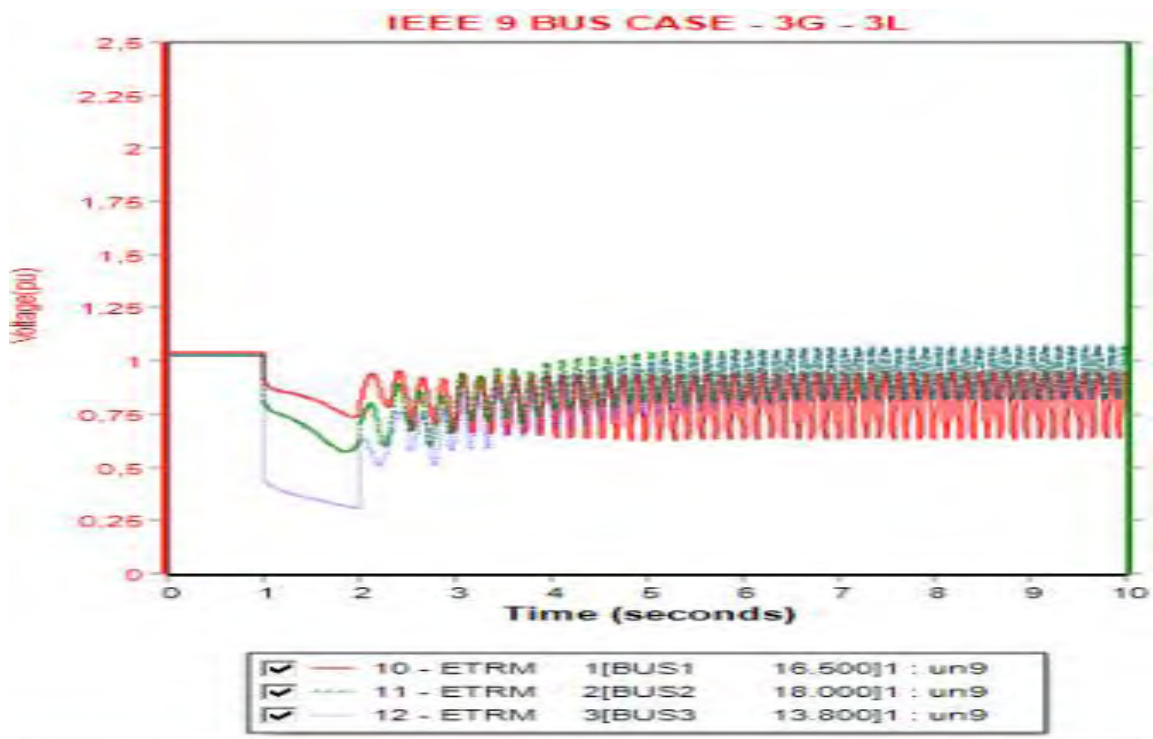


Figure 5.53 - Terminal voltage output variation of all generators for fault at bus 9

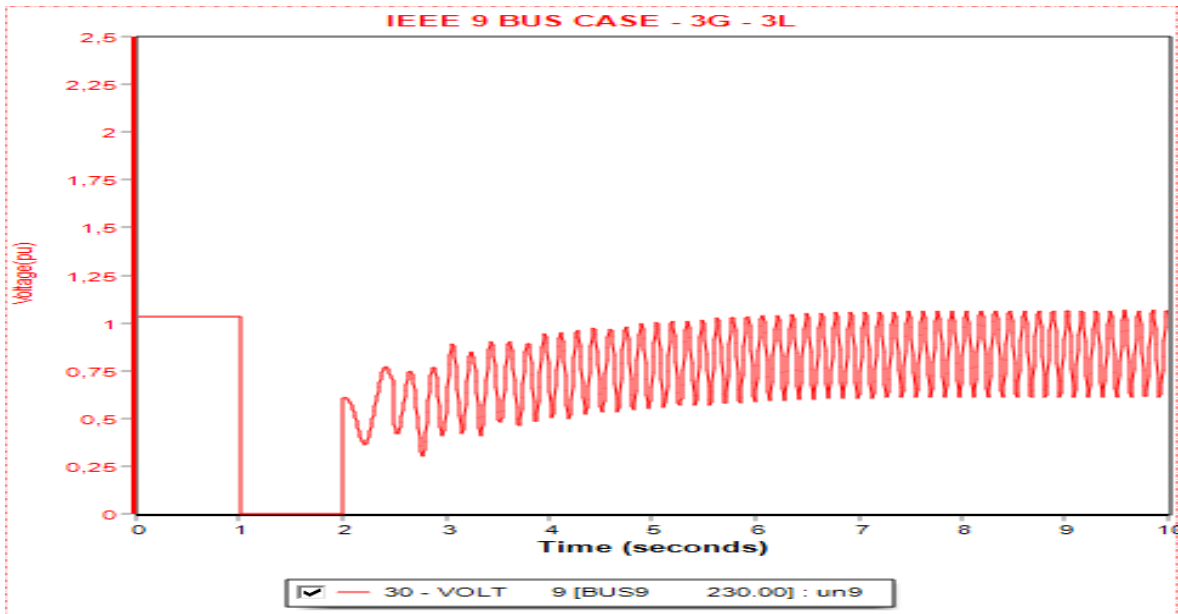


Figure 5.54- Terminal voltage output variation of bus 9 for fault at bus 9

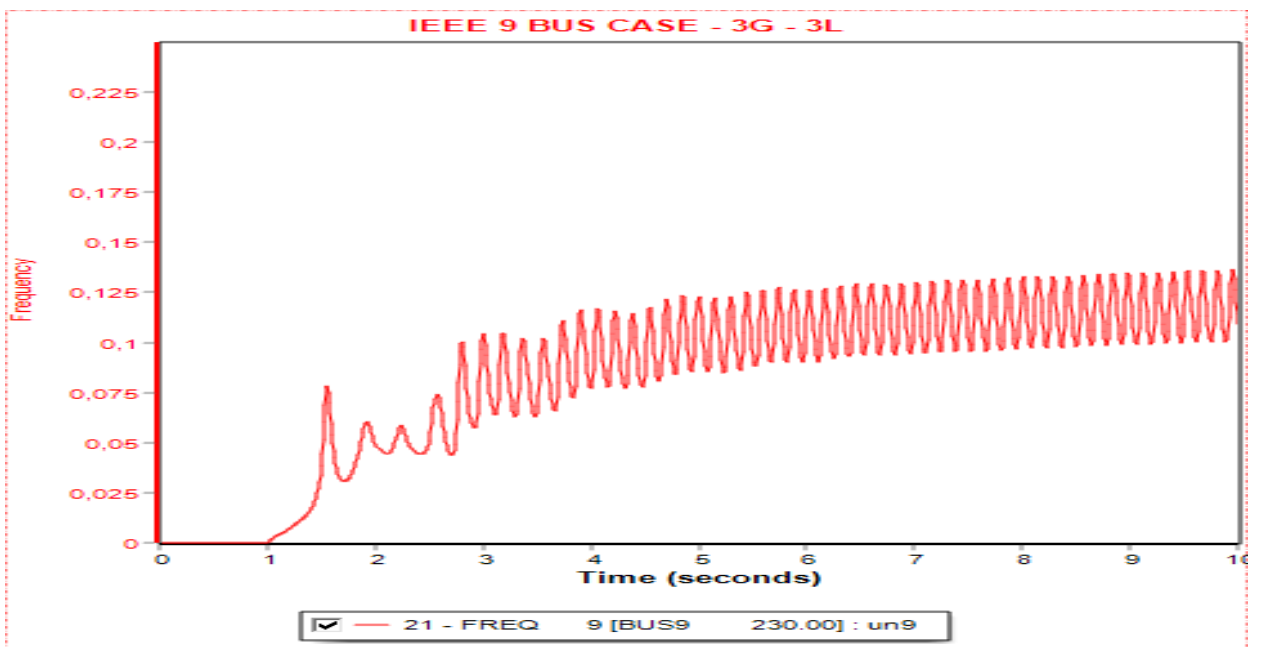


Figure 5.55 – Frequency output variation of bus 9 for fault at bus 9

Unstable Case D: 3-L-G Fault at bus 4

A 3-L-G fault occurs to bus 4 in line 4-5. The rotor angle plot (Figure 5.56) demonstrates complete deflection of generator relative rotor angle. The real and reactive power plot (Figure 5.57 and 5.58) shows undamped variations along with voltage and frequency plots (Figure 5.59, 5.60 and 5.61). The system is now unstable.

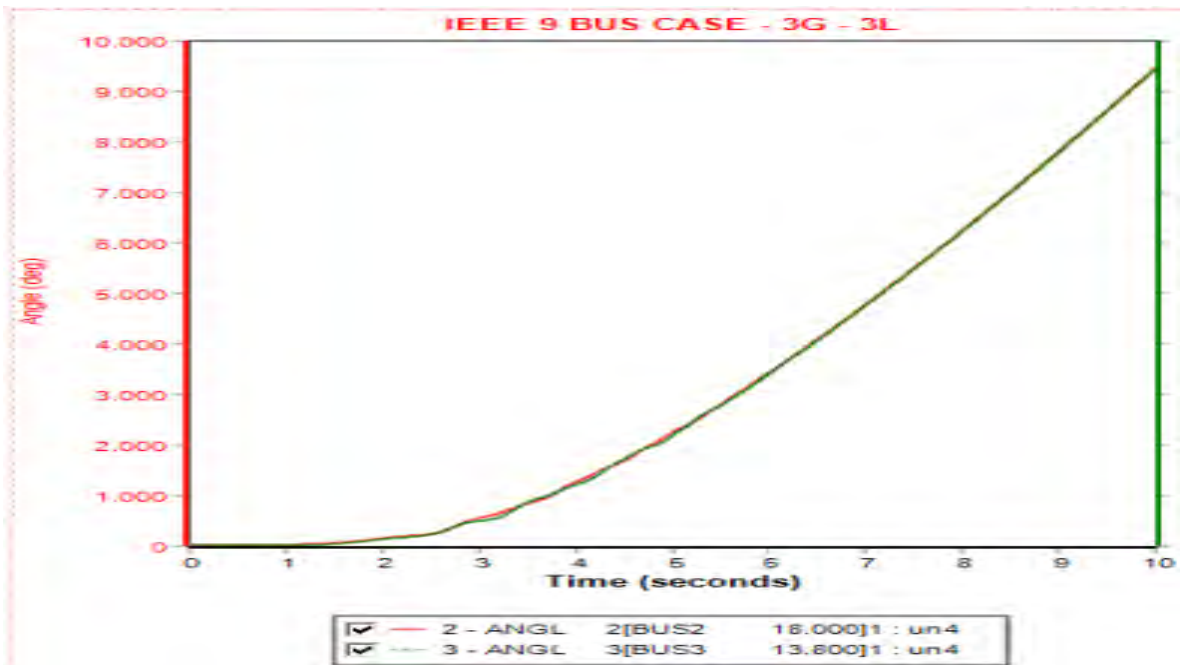


Figure 5.56 - Angle plot of all generators for a fault at bus 4

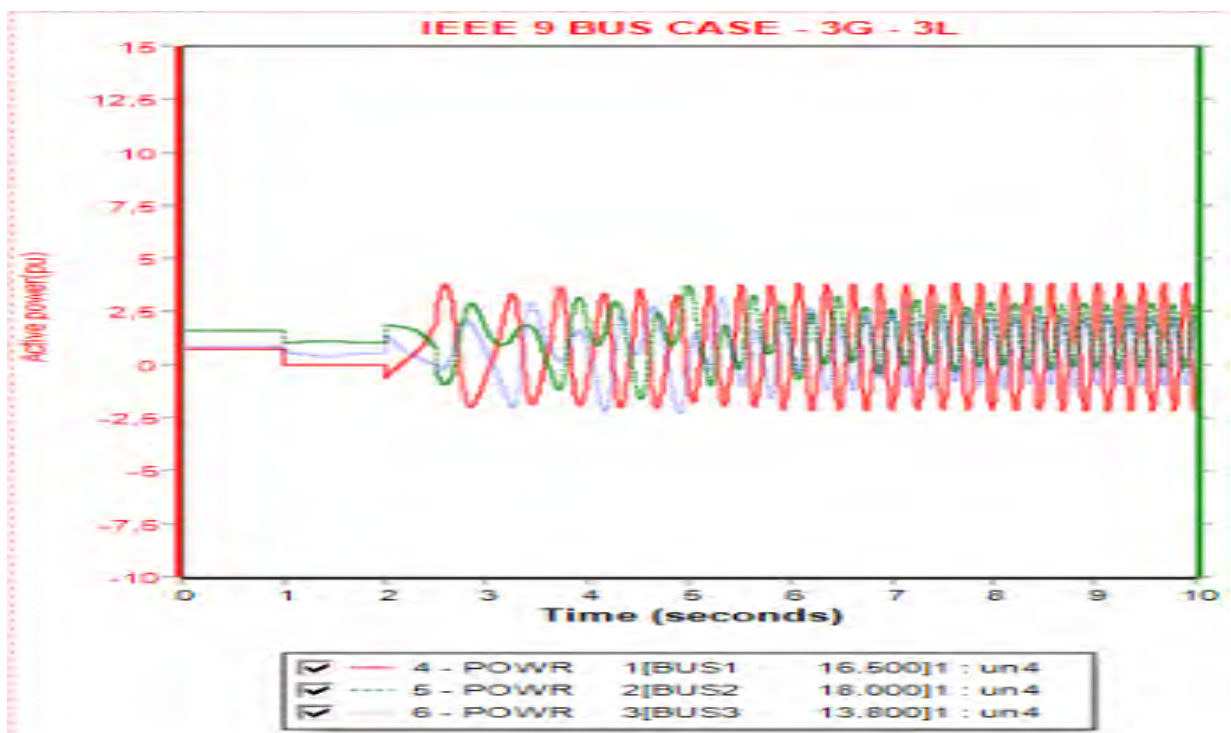


Figure 5.57 - Active power output variation of all generators for fault at bus 4

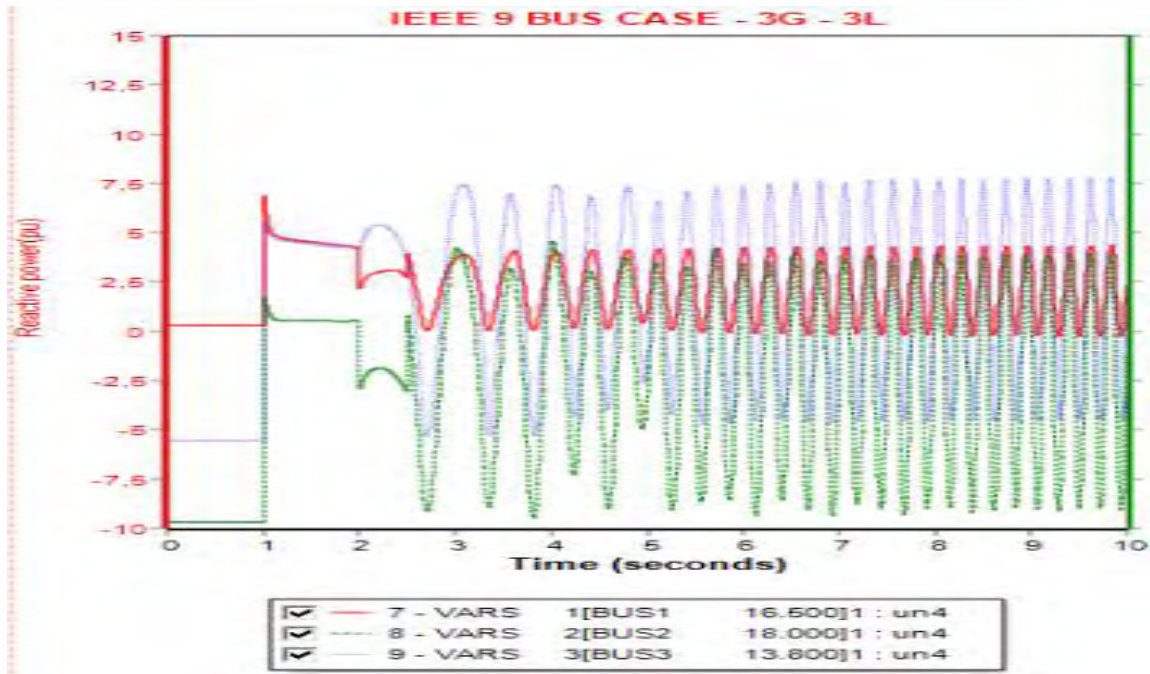


Figure 5.58 - Reactive power output variation of all generators for fault at bus 4

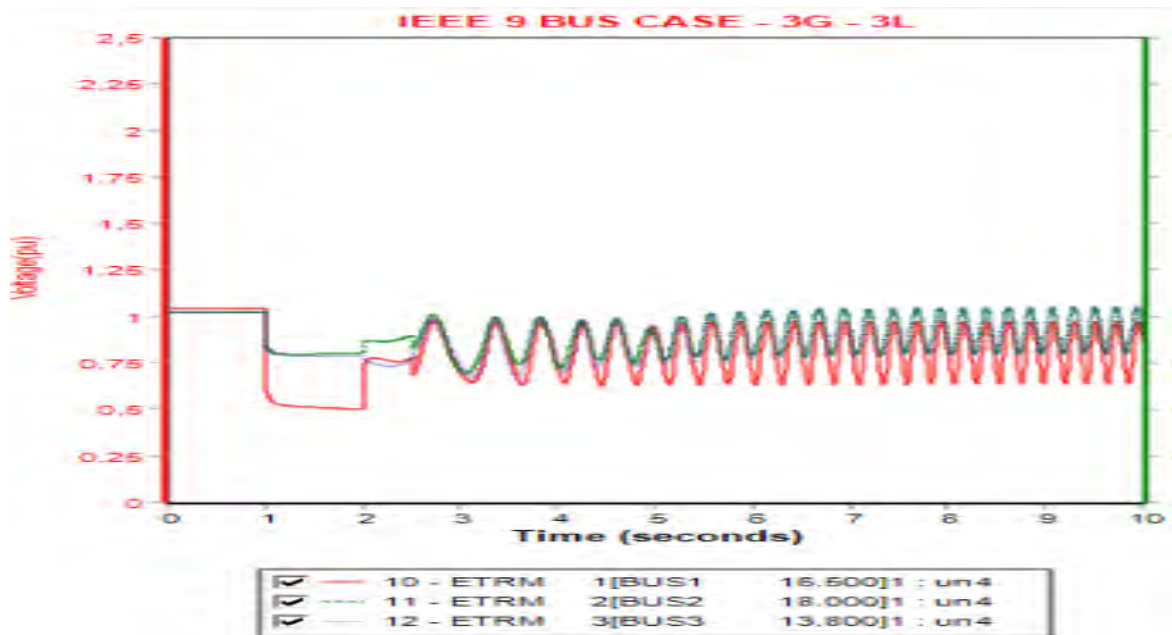


Figure 5.59 - Terminal voltage output variation of all generators for fault at bus 4

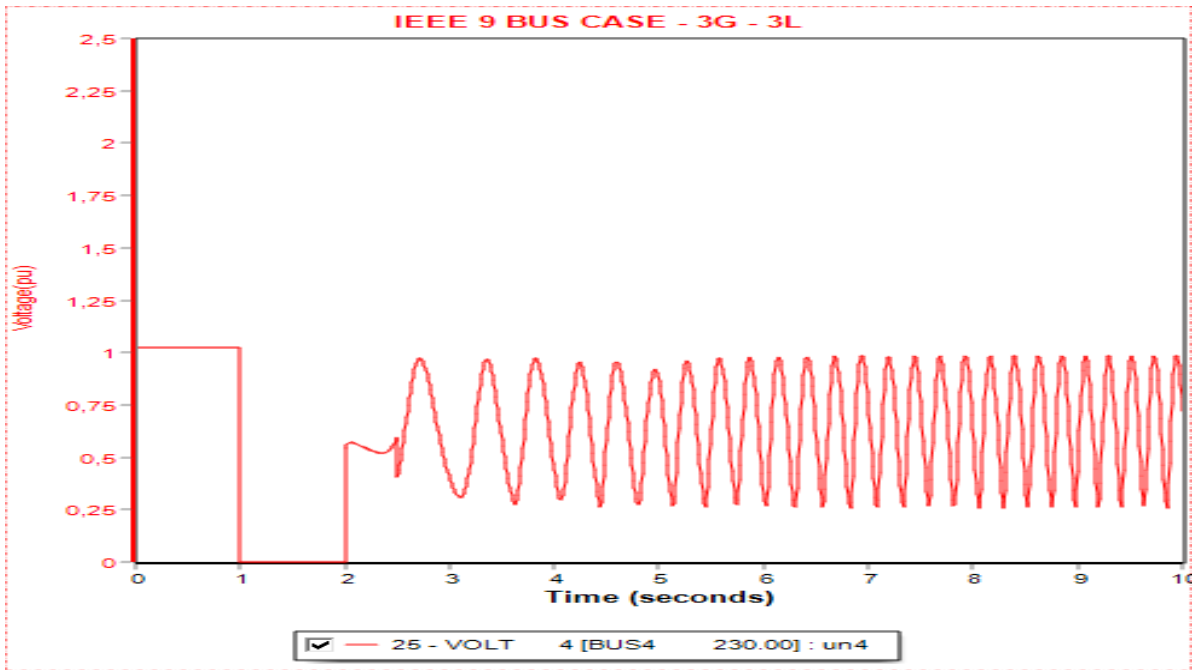


Figure 5.60 - Terminal voltage output variation of bus 4 for fault at bus 4

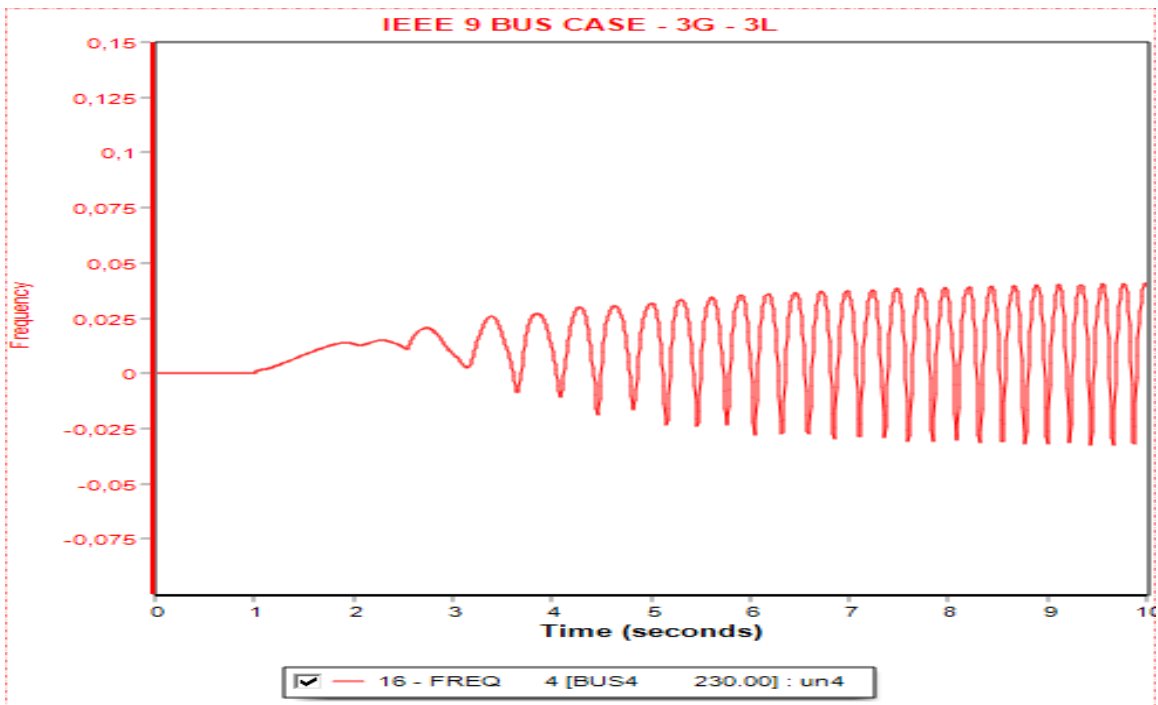


Figure 5.61 – Frequency output variation of bus 4 for fault at bus 4

## **CHAPTER 6**

### **CONCLUSIONS**

In this thesis, transient stability analysis in PSS/E of IEEE 9 bus system has resulted to better understanding of the concept of transient stability and the importance of critical clearing time. This analysis has also highlighted the need of preserving power system's stability by taking protection measures.

A future project could include the study of the effects of other types of faults, except for solid three-phase balanced faults, on transient stability of a power system. In addition, it would be interesting to study different types of stabilities, such as voltage or frequency stability. Finally, the transient stability analysis of a larger system could lead to results for better understanding the behavior of the power systems after major disturbances.



## REFERENCES

- [1] P. Kundur, "Power System Stability and Control". New York: McGraw-Hill, 1994.
- [2] P. Kundur et al., "Definition and classification of power system stability IEEE/CIGRE joint task force on stability terms and definitions," IEEE Transactions on Power Systems, vol. 19, no. 3, Aug. 2004.
- [3] Erik Orum, "Future system inertia," Entso-e.
- [4] B.S.Abdulraheem and C.Kim Gan,"Power System Frequency Stability and Control: Survey",International Journal of Applied Engineering Research,vol.11,no.8 ,pp. 5688-5695, 2016
- [5] I. Kamwa, R. Grondin, and Y. Hebert, "Wide-Area Measurement Based Stabilizing Control of Large Power Systems - A Decentralized/Hierarchical Approach", IEEE Transactions on Power System, pp.136–153, 2001.
- [6] "Voltage Stability Assessment: Concepts, Practices and Tools," in Special Publication, August 2003.
- [7] Renewables Academy (RENAC), 'Frequency and voltage regulation in electrical grids', Federal Ministry for the Environmental, Nature Conservation and Nuclear Safety, Berlin, Germany, 2013.
- [8] Sauer, Peter W. and Pai, M. A. "Power System Dynamics and Stability" New Jersey Prentice Hall, 1998.
- [9] C. Counan, M. Trotignon, E. Corride, G. Bortoni, M. Stubbe, and J. Deuse, "Major incidents on the French electric system- Potentiality and curative measures," IEEE Trans. on Power Systems, vol. 8, pp. 879-886, Aug. 1993.
- [10] "Ανάλυση Κυκλωμάτων Ισχύος", Ν. Α. Βοβός, Γ. Β. Γιαννακόπουλος, Ι. Μήλιας – Αργεΐτης, Εκδόσεις Ζήτη, 2008.
- [11] "Εισαγωγή στα Συστήματα Ηλεκτρικής Ενέργειας", Γ. Β. Γιαννακόπουλος, Ν. Α. Βοβός, Εκδόσεις Ζήτη, 2008.
- [12] "Ανάλυση Συστημάτων Ηλεκτρικής Ενέργειας", Ν. Α. Βοβός, Γ. Β. Γιαννακόπουλος, Εκδόσεις Ζήτη, 2008.
- [13] "Έλεγχος και Ευστάθεια Συστημάτων Ηλεκτρικής Ενέργειας", Ν. Α. Βοβός, Γ. Β. Γιαννακόπουλος, Εκδόσεις Ζήτη, 2008.
- [14] Goran Andersson,"Power System Analysis",Lecture 227-0526-00,Zurich,September 2012

- [15] X.-F. Wang et al., “Modern Power Systems Analysis”, Springer Science and Business Media, LLC 2008
- [16] P. Kessel and H. Glavitsch, “Estimating the voltage stability of a power system,” IEEE Transaction on Power delivery, vol. 1, no. 3, pp. 346-354, Jul. 1986.
- [17] Olukayode A. Afolabi et al., “Analysis of the Load Flow Problem in Power System Planning Studies” ,USA, September 2015
- [18] A.S. Mubarak et al.,”An Analytical Study of Power System under the Fault Conditions using different Methods of Fault Analysis”,Advanced Research in Electrical and Electronic Engineering ,Vol. 2, no. 10, pp. 113-119, April-June (2015)
- [19] <https://www.electronicshub.org>
- [20] E. Larsen and D.A. Swann. Applying Power System Stabilizers: Parts I, II and III. IEEE Transactions on Power Apparatus and Systems, 1981.
- [21] E.V. Larsen, J.J. Sanchez-Gasca, and J.H. Chow. Concepts of Design of FACTS Controllers to Damp Power Swings. IEEE Transactions on Power Systems, pp.948–956, May 1995.
- [22] G.E. Boukarim, S. Wang, J.H. Chow, G.N. Taranto, and N. Martins. A Comparison of Classical, Robust, and Decentralized Control Designs for Multiple Power System Stabilizers. IEEE Transactions on Power System, November 2000.
- [23] Y. Zhang and A. Bose. Design of Wide-Area Damping Controllers for Interarea Oscillations. IEEE Transactions on Power Systems, August 2008.
- [24] Gómez E. et al., “Electric Energy Systems Analysis and Operation”, CRC Press, p. 665,2009
- [25] <https://circuitglobe.com/types-of-faults-in-power-system.html>
- [26] K. M. Amirthalingam and R. P. Ramachandran,”Improvement of Transient Stability of Power System Using Solid State Circuit Breaker”,American Journal of Applied Sciences, no.10,pp.563-569, 2013

## APPENDIX A

### IEEE 9 bus PSSE model

#### • Power flow model

#### Bus data

Bus Number	Base kV	Area Num	Zone Num	Owner Num	Code	Voltage (pu)	Angle (deg)	Normal Vmax (pu)	Normal Vmin (pu)	Emergency Vmax (pu)	Emergency Vmin (pu)
1	16,5	1	1	1	3	1,04	0	1,1	0,9	1,1	0,9
2	18	2	2	1	2	1,025	9,28	1,1	0,9	1,1	0,9
3	13,8	2	3	1	2	1,025	4,66	1,1	0,9	1,1	0,9
4	230	1	1	1	1	1,0258	-2,22	1,1	0,9	1,1	0,9
5	230	1	4	2	1	0,9956	-3,99	1,1	0,9	1,1	0,9
6	230	1	5	2	1	1,0127	-3,69	1,1	0,9	1,1	0,9
7	230	2	2	1	1	1,0258	3,72	1,1	0,9	1,1	0,9
8	230	2	6	2	1	1,0159	0,73	1,1	0,9	1,1	0,9
9	230	2	3	1	1	1,0324	1,97	1,1	0,9	1,1	0,9

#### Load data

Bus Number	Id	Code	Area Num	Zone Num	Owner Num	Pload (MW)	Qload (Mvar)	IPload (MW)	YPload (MW)	YQload (Mvar)	Distributed Gen (MW)
5	1	1	1	1	1	125	50	0	0	0	0
6	1	1	1	1	1	90	30	0	0	0	0
8	1	1	1	1	1	100	35	0	0	0	0

#### Generator data

Bus Number	Area Num	Code	PGen (MW)	QGen (Mvar)	QMax (Mvar)	QMin (Mvar)	VSched (pu)	Voltage (pu)	RMPCT
1	1	3	71,6	27	300	-300	1,04	1,04	100
2	2	2	163	6,7	300	-300	1,025	1,025	100
3	2	2	85	-10,9	300	-300	1,025	1,025	100

## Branch data

From Bus Number	To Bus Number	Id	Line R (pu)	Line X (pu)	Charging B (pu)	Line G From (pu)	Line B From (pu)	Line G To (pu)	Line B To (pu)	RATE1 (I as MVA)	RATE2 (I as MVA)	RATE3 (I as MVA)
4	5	1	0,01	0,085	0,176	0	0	0	0	250	250	250
4	6	1	0,017	0,092	0,158	0	0	0	0	250	250	250
5	7	1	0,032	0,161	0,306	0	0	0	0	250	250	250
6	9	1	0,039	0,17	0,358	0	0	0	0	150	150	150
7	8	1	0,0085	0,072	0,149	0	0	0	0	250	250	250
8	9	1	0,0119	0,1008	0,209	0	0	0	0	150	150	150

## Transformer data

From Bus Number	To Bus Number	Id	Specified R (pu or watts)	Specified X (pu)	RATE1 (MVA)	RATE2 (MVA)	RATE3 (MVA)	Magnetizing G (pu or watts)	Magnetizing B (pu)	Winding MVA Base	Wnd 1 Ratio (pu or kV)
1	4	T1	0	0,0576	0	0	0	0	0	100	1
2	7	T2	0	0,0625	0	0	0	0	0	100	1
3	9	T3	0	0,0586	0	0	0	0	0	100	1

Id	Wnd 1 Nominal kV	Wnd 1 Angle (degrees)	Wnd 2 Ratio (pu or kV)	Wnd 2 Nominal kV	Rmax (pu, kV, deg)	Rmin (pu, kV, deg)	Vmax (pu, Mvar, MW)	Vmin (pu, Mvar, MW)	Wnd Connect Angle (deg)
T1	0	0	1	0	1,1	0,9	1,1	0,9	0
T2	0	0	1	0	1,1	0,9	1,1	0,9	0
T3	0	0	1	0	1,1	0,9	1,1	0,9	0

Id	Load Drop Comp R (pu)	Load Drop Comp X (pu)	R (table corrected pu or watts)	X (table corrected pu)
T1	0	0	0	0,0576
T2	0	0	0	0,0625
T3	0	0	0	0,0586

## • Dynamic data

Bus Number	Id	Mbase (MVA)	Generator	Exciter	Turbine Governor	Stabilizer
1	1	260	GENSAL	IEEET1	IEESGO	PSS2A
2	1	310	GENROU	IEEET1	IEESGO	PSS2A
3	1	280	GENROU	IEEET1	IEESGO	PSS2A